

**POLITECNICO DI TORINO  
TECHNISCHE UNIVERSITEIT DELFT**

Master's Degree in Aerospace Engineering



Master's Thesis

**Megaconstellations: is it possible to achieve  
the same performance using fewer satellites?**

Supervisors

Prof. Ron NOOMEN

Prof. Lorenzo CASALINO

Candidate

Alessandro PELUSO

OCTOBER 2022



# Summary

The new frontier of the Internet will be satellite connections through which it will be possible to provide broadband Internet with global coverage in the coming years. This will be made possible by constructing mega-constellations of satellites operating in low Earth orbit (LEO) or very low Earth orbit (VLEO), ensuring very competitive latency times far shorter than the latency times experienced with current geostationary constellations.

Among the constellations that will be active in the coming decades, Starlink is the one that is currently attracting particular attention as its final configuration has a huge number of satellites and its deployment is already underway. This high number of satellites greatly concerns the scientific community mainly because it dramatically increases the possibility that the Kessler syndrome may be realized, and thus space will become inaccessible for the next decades or centuries. For this very reason, a study aimed at understanding the reasons behind SpaceX's design of this constellation becomes necessary, and it would be interesting also to see if there is a way to lower the number of satellites required.

The following study, therefore, looks at the final configuration of the constellation in which 42,000 satellites distributed over 16 shells capable of communicating via laser technology are involved.

Given the orbital parameters of each shell, it was necessary to propagate their orbits using the Walker pattern. However, the first considerable difficulty was the identification of the F parameter, which is used to determine the phasing between the satellites in the different orbital planes and consequently serves to avoid a collision between satellites. After that, knowing the position of the satellites in time, to estimate the optimal latency times, Dijkstra's algorithm was applied, which allowed the identification of the best path in the network of satellites. This provided insight into the potential of the constellation in terms of coverage, latency and connection stability, and allowed for further investigation by studying the effects of reducing the number of satellites on the performance of the system.

There are few accessible data, and those used in this thesis have been released by the Federal Communications Commission and Starlink itself on its website.

Consequently, it was necessary to do a simplified study in which possible traffic

congestion was not taken into account. However, this gave us interesting results; for example, it was shown how, in the case of the most numerous shells, even a 70% reduction of satellites does not affect coverage and minimum latency times. In general, all the results obtained are interesting and serve as a stimulus to encourage subsequent, more in-depth studies in which other aspects unknown today, such as data traffic, are evaluated.

*To my wonderful family,  
to my grandparents,  
thanks.*



# Table of Contents

List of Tables	X
List of Figures	XII
Acronyms	XVII
<b>1 Introduction</b>	<b>1</b>
<b>2 Starlink constellation</b>	<b>3</b>
2.1 The project . . . . .	3
2.2 Project history . . . . .	5
2.3 Final Configuration . . . . .	7
2.4 Satellite characteristics . . . . .	8
2.5 Reliable and demisable satellites . . . . .	9
2.6 Extremely low orbit insertion . . . . .	10
2.7 Transparency and data sharing . . . . .	11
2.8 Collision avoidance system . . . . .	11
2.9 Impact on astronomy . . . . .	12
2.10 Network architecture . . . . .	14
2.11 User terminals . . . . .	17
2.12 Ground Stations . . . . .	18
2.13 Laser Inter-satellite link (LISL) . . . . .	19
2.14 Frequencies Range . . . . .	20
<b>3 Starlink competitors</b>	<b>23</b>
3.1 Kuiper LEO system . . . . .	24
3.1.1 Orbital characteristics . . . . .	24
3.1.2 System infrastructure . . . . .	24
3.2 OneWeb LEO system . . . . .	26
3.2.1 Orbital characteristics . . . . .	27
3.2.2 System infrastructure . . . . .	28

3.3	Telesat LEO system . . . . .	29
3.3.1	Orbital characteristics . . . . .	29
3.3.2	System infrastructure . . . . .	29
<b>4</b>	<b>Constellation analysis</b>	<b>33</b>
4.1	Explanation of conducted work . . . . .	34
4.2	Constellation geometry . . . . .	36
4.2.1	Walker constellation and propagation . . . . .	36
4.2.2	Transformation from orbital elements to rectangular coordinates	38
4.2.3	F parameter . . . . .	39
4.2.4	Satellites ID code . . . . .	46
4.2.5	Python code . . . . .	47
<b>5</b>	<b>Starlink performance: evaluation techniques</b>	<b>49</b>
5.1	Earth - satellite communication . . . . .	49
5.1.1	Ground station position over time . . . . .	50
5.1.2	Elevation angle . . . . .	50
5.1.3	Python code . . . . .	53
5.2	Communication link between two cities . . . . .	53
5.2.1	Constraints in satellites communication . . . . .	54
5.2.2	Dijkstra algorithm . . . . .	55
5.2.3	Python code . . . . .	56
5.3	Connection stability . . . . .	60
<b>6</b>	<b>Starlink performance: results</b>	<b>61</b>
6.1	Coverage . . . . .	61
6.2	Latency . . . . .	62
6.2.1	Torino - San Francisco . . . . .	64
6.2.2	Torino - Cape Town . . . . .	66
6.2.3	Torino - Buenos Aires . . . . .	68
6.3	Connection stability . . . . .	74
6.4	Critical analysis of each shell . . . . .	78
6.4.1	Shell $A_A$ . . . . .	78
6.4.2	Shell $A_B$ . . . . .	78
6.4.3	Shell $A_{CD}$ . . . . .	78
6.4.4	Shell $A_E$ . . . . .	79
6.4.5	Shell $B_A$ . . . . .	79
6.4.6	Shell $B_B$ . . . . .	79
6.4.7	Shell $B_C$ . . . . .	80
6.4.8	Shell $II_A$ . . . . .	80
6.4.9	Shell $II_B$ . . . . .	80

6.4.10	Shell $II_C$	81
6.4.11	Shell $II_D$	81
6.4.12	Shell $II_E$	81
6.4.13	Shell $II_F$	81
6.4.14	Shell $II_G$	82
6.4.15	Shell $II_H$	82
6.4.16	Shell $II_I$	82
<b>7</b>	<b>Alternative proposals to current constellation</b>	<b>83</b>
7.1	Shell $A_A$	84
7.1.1	Torino $\rightarrow$ San Francisco	86
7.1.2	Torino $\rightarrow$ Cape Town	87
7.1.3	Torino $\rightarrow$ Buenos Aires	87
7.2	Shell $II_C$	90
<b>8</b>	<b>Conclusions and recommendations</b>	<b>93</b>
8.1	Conclusions	93
8.2	Recommendations	94
<b>A</b>	<b>Tables</b>	<b>97</b>
A.1	F parameter	97
A.1.1	F that guarantees the maximum minimum distance	97
A.1.2	Best F evaluation	103
<b>B</b>	<b>Python codes</b>	<b>107</b>
B.1	Walker constellation	107
B.2	Communication link between two cities	109
B.3	Latency calculation along the best path	112
<b>C</b>	<b>Alternative proposals</b>	<b>117</b>
C.1	F parameter evaluation of $A_A$ alternatives	117
C.2	Switches available for $A_A$ alternatives	117
C.3	F parameter evaluation of $II_C$ alternatives	117

# List of Tables

2.1	Starlink Gen1 Constellation Characteristics. . . . .	7
2.2	Starlink Gen2 Constellation Characteristics (Configuration 1). . . . .	7
2.3	Starlink Gen2 Constellation Characteristics (Configuration 2). . . . .	8
2.4	Frequency range and different uses. . . . .	20
3.1	Orbital characteristics of Kuiper system [39] . . . . .	24
3.2	Kuiper system components and characteristics [39]. . . . .	26
3.3	Orbital characteristics of OneWeb system. . . . .	27
3.4	Oneweb system components and characteristics. . . . .	28
3.5	Orbital characteristics of Telesat system . . . . .	29
3.6	Telesat system components and characteristics [43]. . . . .	31
4.1	Classification of the different shells. . . . .	36
4.2	Distance results obtained for $\Delta t=1$ s and $\Delta t=0.1$ s in the $A_E$ shell. . . . .	41
4.3	Evaluation of the best F parameter based on the minimum guaranteed distance between satellites. The full table is available in Appendix A. . . . .	42
4.4	Coverage for each shell with the F parameter that guarantees the maximum minimum distance (the average was calculated only in the latitude zone that the shells cover). . . . .	44
4.5	Coverage per latitude for each F parameter of the $A_B$ shell. . . . .	45
4.6	Coverage for each shell with the F parameter that guarantees the best trade-off between coverage and distance. . . . .	46
4.7	List of F parameter values used. . . . .	46
6.1	Coverage of the higher latitudes settlements on Earth and the number of satellites in view every second for 30 minutes. . . . .	63
6.2	Percentage of coverage guaranteed over 1800 s. . . . .	65
6.3	Percentage of coverage guaranteed over 1800 s. . . . .	67
6.4	Comparison of best performing shells in terms of number of satellites and average latency. . . . .	68

6.5	Percentage of coverage guaranteed over 1800 s. . . . .	69
6.6	Satellites in view of Torino and San Francisco in $t = 300s$ . . . . .	74
7.1	Original $A_A$ shell and different alternatives. . . . .	84
7.2	Coverage and latency of $A_A$ 's alternatives for Torino - San Francisco. . . . .	86
7.3	Coverage and latency of $A_A$ 's alternatives for Torino - Cape Town. . . . .	87
7.4	Coverage and latency of $A_A$ 's alternatives for Torino - Buenos Aires. . . . .	88
7.5	Number of available paths of each shell over 1800 s. . . . .	90
7.6	Original $II_C$ shell and different alternatives. . . . .	91
A.1	Evaluation of the best F parameter based on the minimum guaranteed distance between satellites. . . . .	103

# List of Figures

2.1	Starlink satellites currently in orbit (black dots). Active ground stations (red dots). Users (green areas). . . . .	6
2.2	Orbital lifetime for a satellite with a mass-to-area ratio of $40 \text{ kg/m}^2$ at various starting altitudes and average solar cycle [23]. . . . .	10
2.3	Debris per 1-km altitude shell as a function of orbital altitude [23].	11
2.4	Number and classification of SpaceX maneuvers in July-Dec 2021 (total was 3300) [23]. . . . .	12
2.5	SpaceX’s “duck” maneuver (right) minimizing area in potential collision direction compared with worst-case orientation (left) [23]. .	13
2.6	On Nov. 20, 2019, the Blanco Telescope of the Cerro Tololo Inter-American Observatory (CTIO) recorded a heavy loss of signal and the appearance of 19 white lines on a DECam shot. This was caused by the transit of a Starlink satellite train, launched a week earlier. [29]. . . . .	14
2.7	Starlink Network Architecture [30]. . . . .	15
2.8	Phased array scheme [31]. . . . .	16
2.9	Radiation pattern of a phased array. The dark area is the beam or main lobe, while the light lines fanning out around it are sidelobes [31]. . . . .	16
2.10	Correct way to install user antenna. . . . .	17
2.11	User antenna. . . . .	17
2.12	An array of user terminals (bottom left) and ground stations (right) that SpaceX may be using to test Starlink. . . . .	18
2.13	LISL architecture system [35]. . . . .	19
3.1	Kuiper system ground track visualization (side view) [40]. . . . .	25
3.2	Kuiper system ground track visualization (polar view) [40]. . . . .	25
3.3	Telesat system ground track visualization (side view) [40]. . . . .	30
3.4	Telesat system ground track visualization (polar view) [40]. . . . .	30
4.1	Scheme of conducted work. . . . .	34

4.2	Orbital parameters [48]. . . . .	37
4.3	Mean anomaly ( $M$ ), true anomaly ( $\theta$ ) and eccentric anomaly ( $E$ ) [49].	37
4.4	Parameters of a satellite constellation [46]. . . . .	40
4.5	Side view (left) and top view (right) of the shell $A_{CD}$ where blue dots belong to $A_C$ while red dots belong to $A_D$ .The axes are expressed in km. . . . .	41
4.6	Plot of $A_E$ shell with $F=37$ where the red dots are the satellites in the first orbital plane. . . . .	43
4.7	Plot of $A_E$ shell with $F=65$ where the red dots are the satellites in the first orbital plane. . . . .	43
5.1	Necessary values to know in order to determine the satellites in view. Here $h$ is the altitude of the orbit, $R$ is the Earth's radius, $L$ is the slant range and $\alpha$ is the elevation angle. . . . .	51
5.2	Geometry for maximum inter-satellite distance calculation. In this figure, the Earth is shown in blue, the atmospheric layer in gray and the satellites in yellow [51]. . . . .	54
5.3	Example of a graph representation. . . . .	55
5.4	Output of the code: best possible paths between the two ground stations. . . . .	57
5.5	The figure shows, over a 3 minute range, the communication between Torino and San Francisco through the $A_E$ shell. Among all the possible paths that may be established over time, those characterized by maximum latency and minimum latency have been shown. Average latency will later be considered as a reference. . . . .	57
5.6	Analysis of the route between Torino and San Francisco: on the left is the area considered in the original code; on the right is the area considered in the modified code. . . . .	58
5.7	Latency for the Torino - San Francisco path, with two codes . . . . .	59
5.8	Latency for the Torino - Cape Town path, with two codes . . . . .	59
5.9	Latency for the Torino - Buenos Aires path, with two codes . . . . .	59
6.1	Population density per latitude [53]. . . . .	62
6.2	Average latency of the $m \cdot n$ best paths for each instant of time over 1800 s between Torino and San Francisco. . . . .	64
6.3	Average latency of the $m \cdot n$ best paths for each instant of time over 1800 s between Torino and Cape Town. . . . .	66
6.4	Average latency of the $m \cdot n$ best paths for each instant of time over 1800 s between Torino and Buenos Aires. . . . .	68
6.5	Average latency of the $m \cdot n$ best paths between <b>Torino</b> and <b>San Francisco</b> for each instant of time. . . . .	71

6.6	Average latency of the $m \cdot n$ best paths between <b>Torino</b> and <b>Cape Town</b> for each instant of time. . . . .	72
6.7	Average latency of the $m \cdot n$ best paths between <b>Torino</b> and <b>Buenos Aires</b> for each instant of time. . . . .	73
6.8	Latency over time of all the 24 possible paths. . . . .	76
6.9	Pareto front which relates the number of switches and latency. . . . .	77
6.10	Link of the most persistent paths at $t = 300s$ . . . . .	77
7.1	Coverage as a function of latitude for different $A_A$ alternative shells. . . . .	85
7.2	Coverage as a function of number of satellites for $A_A$ 's alternatives. . . . .	85
7.3	Average latency of $A_A$ 's alternatives in Torino - San Francisco. . . . .	86
7.4	Average latency of $A_A$ 's alternatives in Torino - Cape Town. . . . .	87
7.5	Average latency of $A_A$ 's alternatives in Torino - Buenos Aires. . . . .	87
7.6	Latency over time of all the 16 possible paths (shell $A_{A2}$ ). . . . .	89
7.7	Latency over time of all the 3 possible paths (shell $A_{A7}$ ). . . . .	89
7.8	Coverage as a function of latitude for different $II_C$ alternative shells. . . . .	91
7.9	Coverage as a function of number of satellites for $II_C$ 's alternatives. . . . .	92
A.1	Best F evaluation for shell $II_E$ . . . . .	103
A.2	Best F evaluation for shell $A_E$ . . . . .	104
A.3	Best F evaluation for shell $II_H$ . . . . .	104
A.4	Best F evaluation for shell $II_I$ . . . . .	105
C.1	Best F evaluation for shell $A_{A1}$ . . . . .	118
C.2	Best F evaluation for shell $A_{A2}$ . . . . .	119
C.3	Best F evaluation for shell $A_{A3}$ . . . . .	120
C.4	Best F evaluation for shell $A_{A4}$ . . . . .	121
C.5	Best F evaluation for shell $A_{A5}$ . . . . .	122
C.6	Best F evaluation for shell $A_{A6}$ . . . . .	123
C.7	Best F evaluation for shell $A_{A1}$ . . . . .	124
C.8	Best F evaluation for shell $A_{A7}$ . . . . .	125
C.9	Latency over time of all the 15 possible paths (shell $A_{A1}$ ). . . . .	126
C.10	Latency over time of all the 16 possible paths (shell $A_{A2}$ ). . . . .	126
C.11	Latency over time of all the 15 possible paths (shell $A_{A3}$ ). . . . .	126
C.12	Latency over time of all the 9 possible paths (shell $A_{A4}$ ). . . . .	127
C.13	Latency over time of all the 15 possible paths (shell $A_{A5}$ ). . . . .	127
C.14	Latency over time of all the 6 possible paths (shell $A_{A6}$ ). . . . .	127
C.15	Latency over time of all the 3 possible paths (shell $A_{A7}$ ). . . . .	128
C.16	Best F evaluation for shell $II_{C1}$ . . . . .	128
C.17	Best F evaluation for shell $II_{C2}$ . . . . .	129
C.18	Best F evaluation for shell $II_{C3}$ . . . . .	129
C.19	Best F evaluation for shell $II_{C4}$ . . . . .	130

C.20 Best F evaluation for shell $II_{C5}$ .	130
C.21 Best F evaluation for shell $II_{C6}$ .	131
C.22 Best F evaluation for shell $II_{C7}$ .	131
C.23 Best F evaluation for shell $II_{C8}$ .	132
C.24 Best F evaluation for shell $II_{C9}$ .	132



# Acronyms

**AOS** Acquisition of the Satellite

**CDM** conjunction data messages

**FCC** Federal Communications Commission

**Gen1** Generation I

**Gen2** Generation II

**GEO** Geostationary Earth Orbit

**ITU** International Telecommunication Union

**ISS** International Space Station

**LEO** Low Earth Orbit

**LISL** Laser Inter-Satellite Link

**LOS** Loss of the Satellite

**RAAN** Right ascension of the ascending node

**R&D** Research and Development

**TT&C** Telemetry, Tracking and Command

**VLEO** Very Low Earth Orbit

# Nomenclature

$\alpha$	Elevation angle [deg]
$\mu$	Gravitational parameter of the Earth [ $\text{km}^3/\text{s}^2$ ]
$\Omega$	Right ascension of the ascending node or RAAN [deg]
$\theta$	True anomaly [deg]
$a$	Semi-major axis [km]
$c$	Speed of light in vacuum [m/s]
$E$	Eccentric anomaly [deg]
$e$	Eccentricity
$F$	Phasing parameter
$i$	Inclination of the orbital plane [deg]
$L$	Slant range [km]
$lat$	Latitude [deg]
$lon$	Longitude [deg]
$M$	Mean anomaly [deg]
$N$	Total number of satellites
$n$	Mean angular motion [deg/s]
$P$	Number of equally spaced orbital planes
$R$	Earth radius [km]
$t$	Time [s]



# Chapter 1

## Introduction

Nowadays, being connected to the Internet corresponds to a basic necessity, and it would seem impossible to think of a world without it. And yet everything that we know today and governs our daily routines did not exist until a few years ago.

From the very beginning, Internet has emerged as a potent tool that can connect people around the world, and, over the years, more and more potential uses are being discovered. Consequently, the technologies required to distribute that service worldwide have made huge strides, moving from connection via copper cables to ultra-broadband connection via fiber optics or satellite connection. Now, the new challenge is to deliver broadband Internet with global coverage in the coming few years.

To date, fiber optics has been the preferred way to distribute broadband Internet due to its characteristics: material flexibility and passivity to electromagnetic fields, weather events or extreme temperatures. However, it also has significant limitations. One physical limitation is due to the fact that light in optical fiber travels at speed generally 47% lower than in vacuum [1]. Another significant limitation is the impossibility of connecting remote areas of the globe such as deserts, mountains or some islands. It also often happens that even easily accessible territories are not served because they lack the financial resources to build the infrastructure. So, some remote areas are served using high-frequency radio systems, using radio signals that bounce off the ionosphere to provide a long distance, but limited bandwidth service.

All these coverage problems can be solved by using a satellite infrastructure. Currently, most satellite Internet traffic passes through satellites in geostationary orbit (GEO) that can offer high bandwidth but have significantly high latency as the satellite is orbiting at 35,786 km above the Earth in order to synchronize the orbital period with the planet's revolution. For these very reasons, the solution that has been taking hold in recent years is to build megaconstellations in low Earth orbit (LEO) because they can provide both high bandwidth and low latency. But even in

this case, a number of advantages correspond to a number of cons, such as the very large number of satellites involved in these megaconstellations and the increasing risk of collision.

Giving a precise answer to which technology is the best is difficult as there are so many parameters to take into account, and there is no correct answer that is valid everywhere. Certainly, compromises have to be made and a broader view that takes into account all the indirect issues has to be taken. However, there are more choices that could be made and there are many projects underway that are worth billions of dollars.

As the megaconstellation industry is developing, there are no strict restrictions yet limiting access to space; consequently, analyzing the various proposed solutions to find out how correct a choice made by a particular company is can be crucial to avoid facing severe problems in the future such as Kessler's syndrome, that is, the impossibility of access to space in the coming decades or centuries. This would lead to a huge technological crisis since in-orbit services would no longer be available but more importantly it would stop the race for space exploration.

Thus, the goal of this thesis is to examine the most prominent megacostellation which is Starlink and understand why SpaceX made its design decisions and especially try to understand why the project plans an exorbitant number of satellites.

# Chapter 2

## Starlink constellation

### 2.1 The project

Starlink is a satellite Internet constellation designed and operated by SpaceX, Elon Musk's aerospace company, aiming to provide high-speed, low-latency and competitively-priced broadband internet connections across every corner of the planet by way of a network of private satellites orbiting overhead.

While most satellite Internet services today use single geostationary satellites that orbit the planet at an altitude of about 36,000 km, Starlink is a constellation of numerous satellites that orbit the planet much closer to Earth. As such, the round-trip data time between the user, the satellite and the target, also known as end-to-end latency, is much lower than when using satellites in geostationary orbit. In fact, the theoretical round-trip latency between the user and the ground gateway through a geostationary satellite is at least 477 ms, but current satellites have latencies of up to 600 ms. Thus, to provide a lower earth-sat latency of about 25-35 ms, Starlink satellites orbit at an altitude between 1/105 and 1/30 that of geostationary orbits [2]. With high download speeds of 100 to 200 Mb/s and a latency of only 20 ms in most locations [3], Starlink can provide services such as video calling, online gaming, streaming, and other high data rate activities that are usually not possible with other satellite broadband systems. However, Starlink's noblest purpose is undoubtedly worldwide coverage. Indeed, without the limitations imposed by traditional terrestrial infrastructure, Starlink can provide high-speed broadband Internet in places where access has been difficult or completely unavailable. In addition, the service can be enabled in vehicles, ships, and aircraft. To reach its objective, Starlink needs an enormous number of satellites. The constellation consists of thousands of mass-produced small satellites communicating with designated ground transceivers. Until March 2022, more than 2200 have been launched and the beta Internet service offering is already available in 29 countries.

However, the first part of the constellation may be considered completed only when about 12,000 satellites will be operative in orbit. Then 30,000 additional Starlink satellites will have to be launched in order to reinforce constellation performance. This is something never seen before; in fact, according to the United Nations Office of Outer Space Affairs (UNOOSA), the number of satellites orbiting the Earth as of December 2021 is about 8,100, of which only 4,852 are still operational.

Hence, in a few years, Starlink will literally have control of our skies with dozens of thousands of satellites orbiting in LEO. This fact worries the scientific community because it dramatically increases the possibility of collisions between satellites and the fateful Kessler syndrome could become a real problem.

On the other hand, Starlink satellites are equipped with the best technology available. They autonomously maneuver to avoid collisions with orbital debris and other spacecraft by reducing human error and proving exceptional reliability, exceeding the industry standard by an order of magnitude. The satellite's custom-built navigation sensors survey the stars to determine each satellite's location, altitude, and orientation, enabling precise placement of broadband throughput. Moreover, satellites use an efficient ion thruster, powered by krypton, that enables them to raise orbit, maneuver in space and deorbit at the end of their operational life [3].

Some small satellite operators have expressed concerns that SpaceX's operations would make it more difficult for them to deploy non-propulsive systems near SpaceX's orbits, given their own limited capability. However, SpaceX has repeatedly made clear that it intends to conduct active maneuvers to avoid collisions with both debris and other spacecraft throughout the life of its satellites.

While SpaceX will use its propulsive capabilities to avoid non-propulsive systems, it also expects other systems to take reasonable steps to avoid collision as well. To help in this effort, SpaceX also provides all of its ephemeris data to other operators and it is the first operator to optimize the usefulness of this data by supplementing it with co-variance data, which allows other operators to predict the trajectories of SpaceX satellites better [4].

Launches are also optimized; in fact, SpaceX uses its Falcon 9 rocket to launch Starlink satellites, which have a compact, flat design that minimizes volume, allowing a dense launch stack to take full advantage of SpaceX's rocket launch capabilities.

Finally, some members of the optical astronomer community have expressed concern that reflected light from these satellites could interfere with their space observations. Although the Commission does not have jurisdiction over the visibility of satellites, SpaceX is committed to promoting all forms of space exploration, so it has already taken several proactive measures to ensure that it will not have a tangible impact on optical astronomy. SpaceX is working with the U.S. and international astronomical organizations and observatories to measure and reduce the actual impact of its

satellites scientifically.

Starlink is, therefore, a very ambitious, complex and expensive, but very profitable project; in particular, SpaceX expects the global satellite Internet business to bring in up to \$30 billion in revenue annually by 2025, while revenue from its launch business is expected to reach \$5 billion in the same year. The company said that a positive cash flow from the sale of satellite Internet services will be needed to fund its plans for exploring and colonizing Mars. There are many pros and cons, most of which are due to the number of satellites required. So questions arise:

- Why did SpaceX engineers choose this complex, expensive, questionable configuration?
- Is it possible to achieve the same results using fewer satellites?

The primary purpose of this Thesis is to answer these questions critically, advancing a detailed study of the constellation to fully understand its potential, and then propose alternatives.

## 2.2 Project history

As early as the 1980s several low-orbit megaconstellations such as Celestri, Teledesic, Iridium and Globalstar had been planned, but they went bankrupt with the bursting of the dot-com bubble, partly due to excessive launch costs at the time [5][6]. SpaceX's interest in satellite Internet has been evident since its founding in 2004, but only in 2014 we were able to see a first draft of the project, when Elon Musk and Greg Wyler, future founder of OneWeb, jointly planned a constellation of about 700 satellites called WorldVu. However, these plans fell apart later in the same year, when SpaceX "stealthily" submitted an International Telecommunication Union (ITU) application through the Norwegian Telecommunications Regulatory Authority under the name STEAM [7]. During the unveiling, Elon Musk stated that Starlink would meet the significant unmet demand for low-cost broadband capacity worldwide and that the constellation would be partially operational as early as 2020 [8].

Megaconstellation projects are ambiguous and constantly evolving, and the Starlink project, in particular, has evolved by often changing its configuration several times. The first project submitted to the Federal Communications Commission (FCC) between 2016 and 2017 included a shell of 7,518 satellites in Very-Low Earth Orbit (VLEO) at an altitude of only 340 km and another smaller shell of 4,425 satellites at an altitude of 1,200 km [9]. After some bureaucratic issues were resolved, in 2019 Starlink submitted a new application to FCC requesting to be allowed to modify the constellation by increasing the number of satellites involved and placing

them in three different shells: 7,500 satellites at 340 km, 1,440 satellites at 550 km and 2,825 satellites at 1,110 km [10] [11]. Still, new modifications were requested in the same year to optimize coverage over U.S. territory.

Again in April 2020, SpaceX asked FCC for a lower altitude for higher shells [12]. This is to provide low-latency broadband to Americans located in remote areas of the planet not served by high-performance services. The lower orbits will also help ensure that the satellites re-enter the atmosphere more quickly in the event of failure and will allow them to transmit signals at reduced power levels because they are closer to Earth.

Also in 2020, SpaceX filed an application to request authority to deploy and operate a "next-generation" constellation of low-Earth orbit satellites. SpaceX proposed two alternative configurations depending on the availability of launch vehicles. The first configuration consists of 29,988 satellites at altitudes ranging from 340 km to 614 km, and the second consists of 29,996 satellites at altitudes ranging from 328 km to 614 km [13].

Currently, nearly 12,000 satellites are planned to be launched, with a possible future extension to 42,000. Meanwhile, constellation construction is already underway and more than 2,000 satellites have been launched. To date, SpaceX continues to produce and launch about 120 satellites per month [14] to complete the 'Generation 1' constellation by the end of 2027. Due to ITU regulations, although the Starlink network has a nearly global reach at latitudes below about  $60^\circ$ , broadband services are currently provided in 29 countries where the service reaches speeds between 150 and 500 Mbps [15].

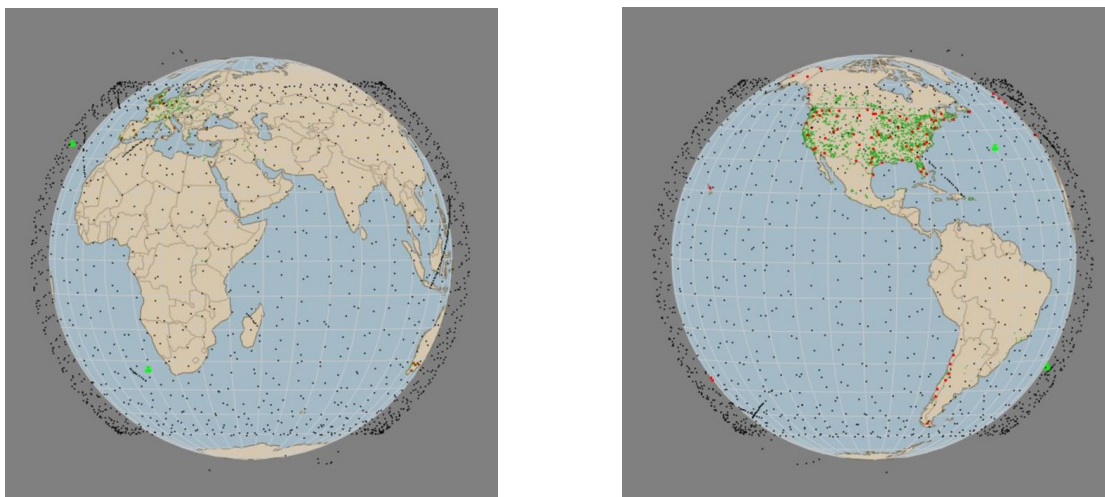


**Figure 2.1:** Starlink satellites currently in orbit (black dots). Active ground stations (red dots). Users (green areas).

## 2.3 Final Configuration

As mentioned above, the final constellation architecture has about 42,000 satellites. While Gen1 has a design that is supposed to be the final one with 11,941 satellites, Gen2 is still under the decision phase, and there are two proposed alternatives with 29,988 or 29,996 satellites. The satellites launched so far are those of shells A with the shell  $A_E$  being almost completed.

Constellation	No. of Sats	No. of Planes	Sats per Plane	Inclination [°]	Interplane Spacing [°]	Altitude [km]
Shell A						
SpaceX $A_A$	1584	72	22	53.2	5	540
SpaceX $A_B$	720	36	20	70	10	570
SpaceX $A_C$	348	6	58	97.6	60	560
SpaceX $A_D$	172	4	43	97.6	90	560
SpaceX $A_E$	1584	72	22	53	5	550
Shell B						
SpaceX $B_A$	2493	2493	1	42	0.144	335.9
SpaceX $B_B$	2493	2493	1	48	0.144	340.8
SpaceX $B_C$	2547	2547	1	53	0.141	345.6

**Table 2.1:** Starlink Gen1 Constellation Characteristics.

Constellation	No. of Sats	No. of Planes	Sats per Plane	Inclination [°]	Interplane Spacing [°]	Altitude [km]
Shell II						
SpaceX $II_{A'}$	5280	48	110	53	3.27	340
SpaceX $II_{B'}$	5280	48	110	46	3.27	345
SpaceX $II_{C'}$	5280	48	110	38	3.27	350
SpaceX $II_{D'}$	3600	30	120	96.9	3	360
SpaceX $II_{E'}$	3360	28	120	53	3	525
SpaceX $II_{F'}$	3360	28	120	43	3	530
SpaceX $II_{G'}$	3360	28	120	33	3	535
SpaceX $II_{H'}$	144	12	12	148	30	604
SpaceX $II_{I'}$	324	18	18	115.7	18	614

**Table 2.2:** Starlink Gen2 Constellation Characteristics (Configuration 1).

Constellation	No. of Sats	No. of Planes	Sats per Plane	Inclination [°]	Interplane Spacing [°]	Altitude [km]
Shell II						
SpaceX II <sub>A</sub> ''	5816	5816	1	30	0	328
SpaceX II <sub>B</sub> ''	5816	5816	1	40	0	334
SpaceX II <sub>C</sub> ''	5816	5816	1	53	0	346
SpaceX II <sub>D</sub> ''	2000	40	50	96.6	7.2	360
SpaceX II <sub>E</sub> ''	1656	72	23	14	15.65	510
SpaceX II <sub>F</sub> ''	1656	72	23	22	15.65	515
SpaceX II <sub>G</sub> ''	1656	72	23	30	15.65	520
SpaceX II <sub>H</sub> ''	1656	72	23	53	15.65	525
SpaceX II <sub>I</sub> ''	1728	72	24	45	15	530
SpaceX II <sub>L</sub> ''	1728	72	24	38	15	535
SpaceX II <sub>M</sub> ''	144	12	12	148	30	604
SpaceX II <sub>N</sub> ''	324	18	18	115.7	20	614

**Table 2.3:** Starlink Gen2 Constellation Characteristics (Configuration 2).

## 2.4 Satellite characteristics

SpaceX satellites are designed and built for high reliability and redundancy so that they can successfully complete their missions. They have an expected lifetime of five years, and the design of newly launched satellites is improved with each subsequent launch. This way, Starlink will be in its third or fourth generation and the entire fleet will be renewed every five years whilst its competitors are still in their first generations. By so doing, the Starlink service will always operate with the latest technology.

Currently, only the features of four versions are public, of which v0.9 was used in the testing phase, v1.0 and v1.5 are currently operational while v2.0 is in the design phase.

- **v0.9 (test)**

There are only 60 v0.9 Starlink satellites which were launched in 2019 [16].

They weigh 227 kg and feature flat-panel designs with multiple high-performance antennas and a single solar array.

For orbit position maneuvers, altitude maintenance and deorbit, Hall Effect Thrusters using krypton as reaction mass are used. They are also able to use debris data provided by the Department of Defense to autonomously avoid collisions [17]. 95% percent of all components in this project burn up in Earth's atmosphere during the reentry of each satellite.

- **v1.0 (operational)**

Starlink v1.0 satellites have been launched since late 2019.

Compared to their predecessors, they weigh 260 kg, have added Ka-band [18] and are equipped with Sun visors to block sunlight reflecting off parts of the satellite to further reduce its albedo [19]. During the reentry phase, 100% of all components burn up in the atmosphere [20].

- **v1.5 (operational)**

Launched from 2021 in polar orbits, they weigh 295 kg. They are equipped with lasers for inter-satellite communication [21].

- **v2.0 (planned)**

There are not many details on this yet, but they are expected to be deployed as of 2022. According to a tweet by Elon Musk, Starlink v2.0 satellites will be almost an order of magnitude more capable than the v1.0 satellites. However, it is known that they will weigh 1,250 kg and have a length of 7 meters [22].

## 2.5 Reliable and demisable satellites

Based on the satellites launched so far, the demonstrated reliability is more than 99%. In fact, less than 1% have failed after deployment and have been deorbited to prevent dead satellites from accumulating in orbit. Typically, SpaceX satellites are propulsively deorbited with maneuvers that last roughly four weeks. Once the right altitude is reached, the satellites arrange themselves in a way that increases aerodynamic drag and then in a way that reduces the satellite's energy to the point of causing deorbiting. Starting from these low altitudes, satellites deorbit rapidly, depending on atmospheric density. In addition, satellites use several strategies to prevent debris generation in space, such as proper deorbiting design, applications of on-board collision avoidance system, use of Whipple shields to protect key components, and failure modes that do not create secondary debris. SpaceX claims that it is the only commercial operator to have developed the necessary skills to orbit in a controlled manner in this low-altitude, high-drag environment, which is incredibly difficult and requires significant investments [23].

## 2.6 Extremely low orbit insertion

Compared to industry standards, the use of extremely low orbits further mitigates the problem associated with the generation of new space debris. This also allows for rapid reentry when a just deployed satellite does not respond appropriately to initial system checks. The orbits chosen by SpaceX are all (except the two with fewer satellites) within 600 km and are called "self-cleaning," because unmaneuverable satellites and debris deorbit due to atmospheric drag within 5-6 years. This greatly reduces the risk of persistent orbital debris and far exceeds the international standard of 25 years. In contrast, Starlink's competitors operate in orbits greater than 1,000 km, where satellites require hundreds of years for natural deorbiting. As can be seen from Figure 2.2 the trend of the curve is exponential, and to deorbit as soon as possible it is convenient to settle at low altitudes.

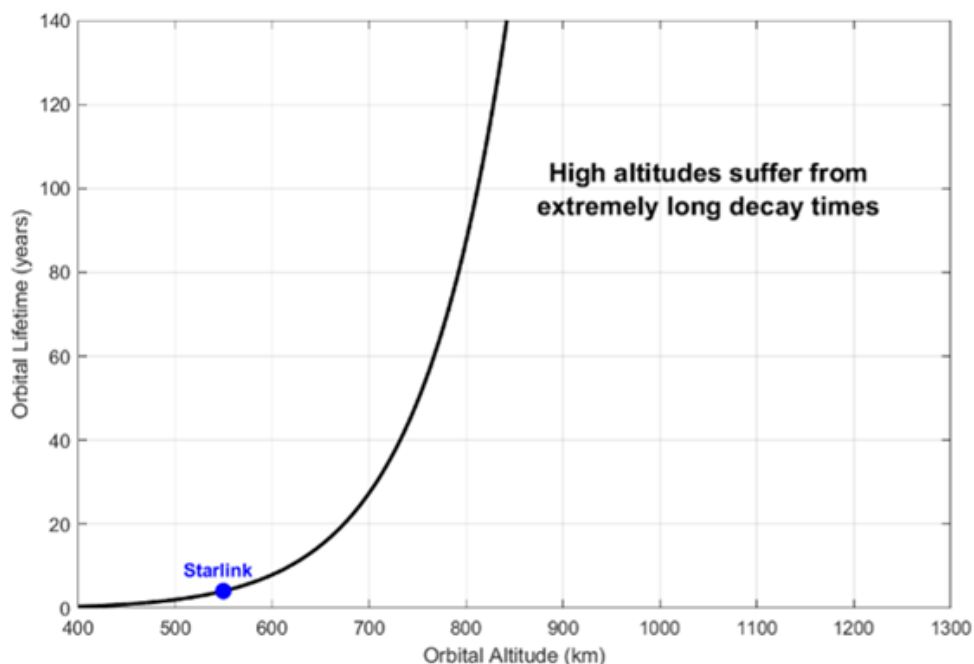


**Figure 2.2:** Orbital lifetime for a satellite with a mass-to-area ratio of  $40 \text{ kg/m}^2$  at various starting altitudes and average solar cycle [23].

Figure 2.3 shows the amount of debris as a function of altitude. Debris generated by collision events of satellites orbiting at altitudes above 600 km will remain in orbit for decades and create a hazard for those who want to transit through those orbits.

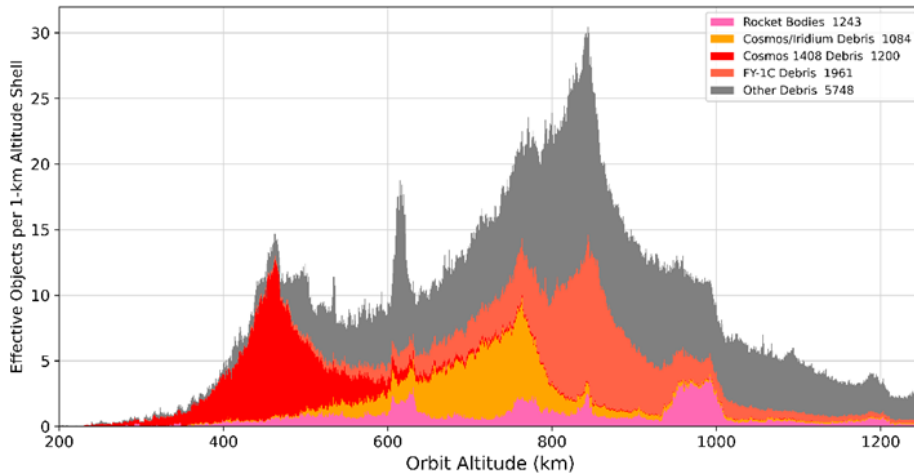


**Figure 2.3:** Debris per 1-km altitude shell as a function of orbital altitude [23].

## 2.7 Transparency and data sharing

In order to ensure a safe environment, SpaceX continuously shares the Starlink network’s accurate orbital information from the onboard GPS and the ephemeris of each satellite with both governments and other satellite operators. All data are available at Space-Track.org upon permission. This ensures greater safety control by anyone operating in orbit or wanting to access space. Also, unlike other companies, SpaceX provides periodic constellation health reports to the FCC. From one of these reports, one can see (Figure 2.4) the number of maneuvers performed to reduce the probability of collision with other objects compared to that of other systems [23].

## 2.8 Collision avoidance system

Data published by Starlink and other systems and debris data are analyzed by the U.S. Space Force’s Space Control Squadron and LeoLabs to predict possible conjunctions. These conjunctions are then communicated to the various satellite operators in the form of conjunction data messages (CDMs). When a Starlink satellite receives a high probability of conjunction with another maneuverable satellite, SpaceX coordinates with the other operator. To achieve safe space operations, SpaceX has equipped each satellite with an autonomous onboard collision avoidance system, ensuring it can maneuver to avoid collisions with other objects. The satellites plan avoidance maneuvers if the collision probability is

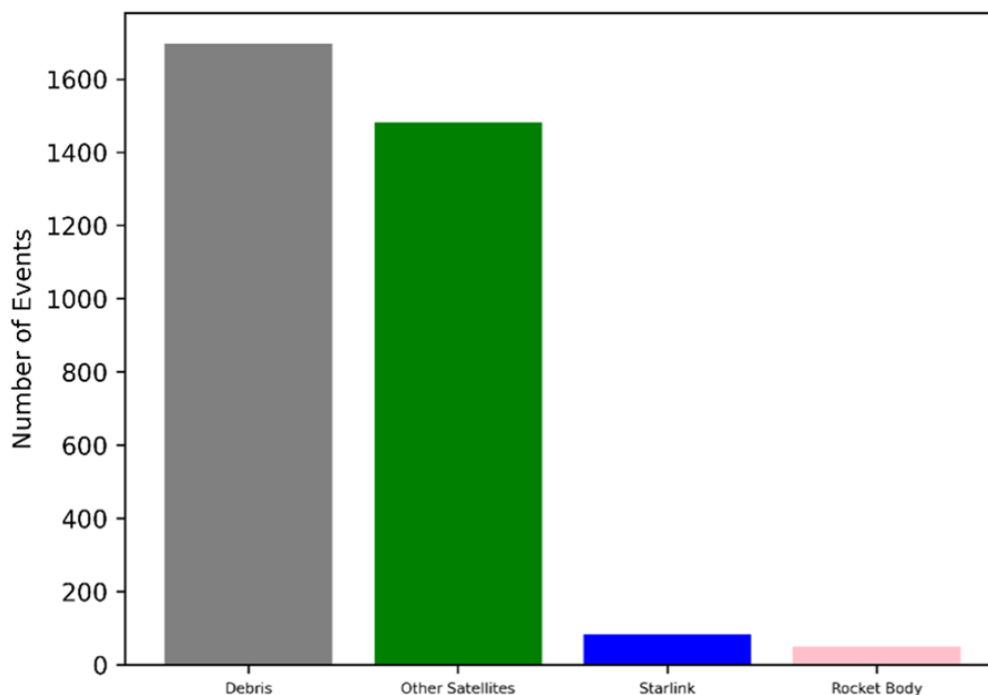


**Figure 2.4:** Number and classification of SpaceX maneuvers in July-Dec 2021 (total was 3300) [23].

greater than  $1/100,000$  (10 times less than the industry standard of  $1/10,000$ ) for a conjunction. In addition, when a maneuver is planned, a check takes place to ensure that the risk for other conjunctions above the same threshold is not inadvertently increased. In addition to maneuvers, Starlink satellites can change their attitude in the event of an expected conjunction by orienting themselves to have the smallest possible cross section in the direction of the potential conjunction, reducing the probability of collision by another factor 4-10 (Figure 2.5) [23]. Among other things, the trajectories used by SpaceX satellites are designed to avoid inhabited space stations such as the International Space Station (ISS) and China’s Tiangong space station by a wide margin.

## 2.9 Impact on astronomy

The astronomical community expressed concern about the light pollution caused by the large number of satellites expected. In fact, they argue that soon the number of visible satellites will exceed the number of visible stars, and their brightness will have a major impact on scientific observations [24][25][26]. In addition, since Starlink satellites orbit at low altitudes, they move with very high speeds and

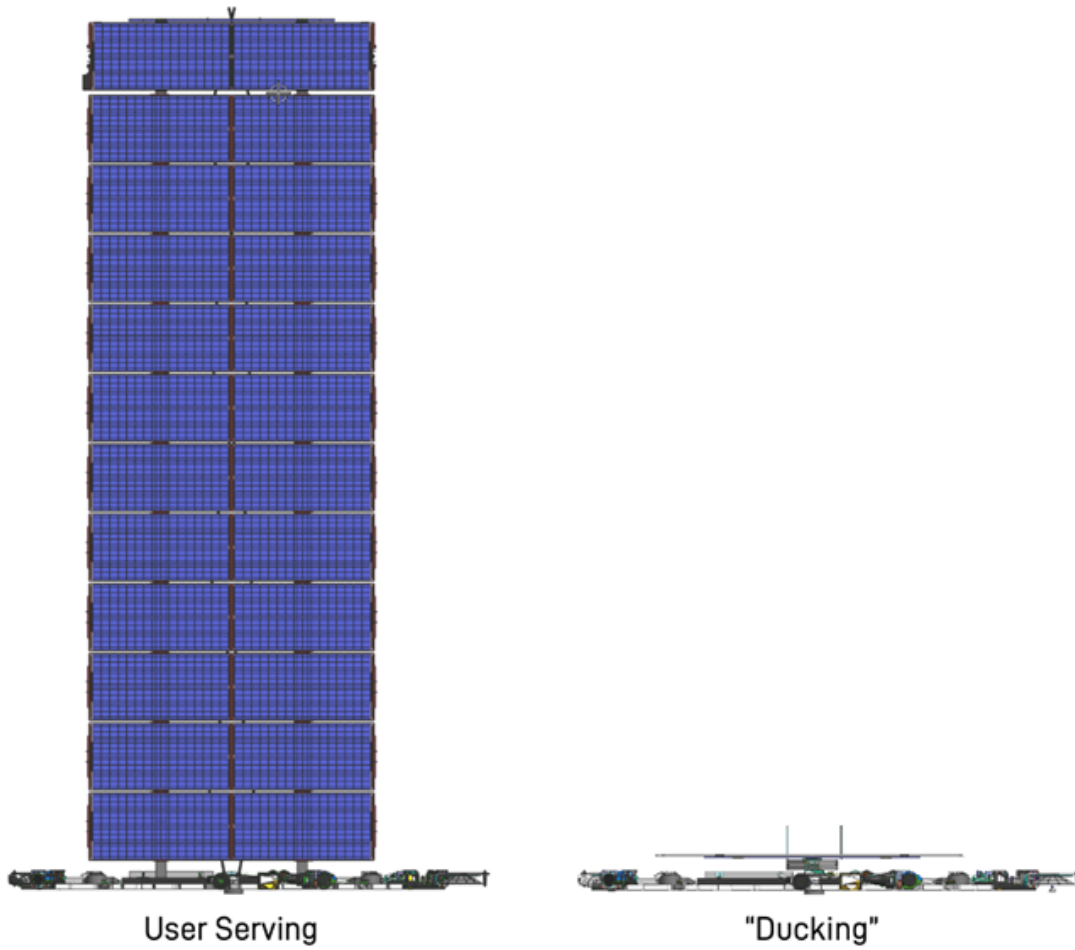


**Figure 2.5:** SpaceX’s “duck” maneuver (right) minimizing area in potential collision direction compared with worst-case orientation (left) [23].

consequently the impact on observations will be more significant (Figure 2.6). Although observations can be scheduled to avoid pointing where the satellites orbit, this will become increasingly difficult as more satellites are activated. For this reason, Starlink is currently working to reduce satellite albedo. Despite several attempts, such as the Starlink 1130 / DarkSat test satellite, which was launched with an experimental coating to reduce albedo, astronomers complained that the satellites were still too bright. A new attempt involved the introduction of a new sunshade designed to reduce the brightness of the Starlink satellites, but the end result was only slightly better than DarkSat [27]. However, real-time sharing of the position of Starlink satellites is expected to be of enormous help in partially solving the problem, as astronomers would proactively avoid the satellites. In 2022, the

International Astronomical Union (IAU) established a center to help astronomers solve satellite constellation problems. The work will be based on developing new software tools to help astronomers, community outreach campaigns, and advancing national and international policies [28].

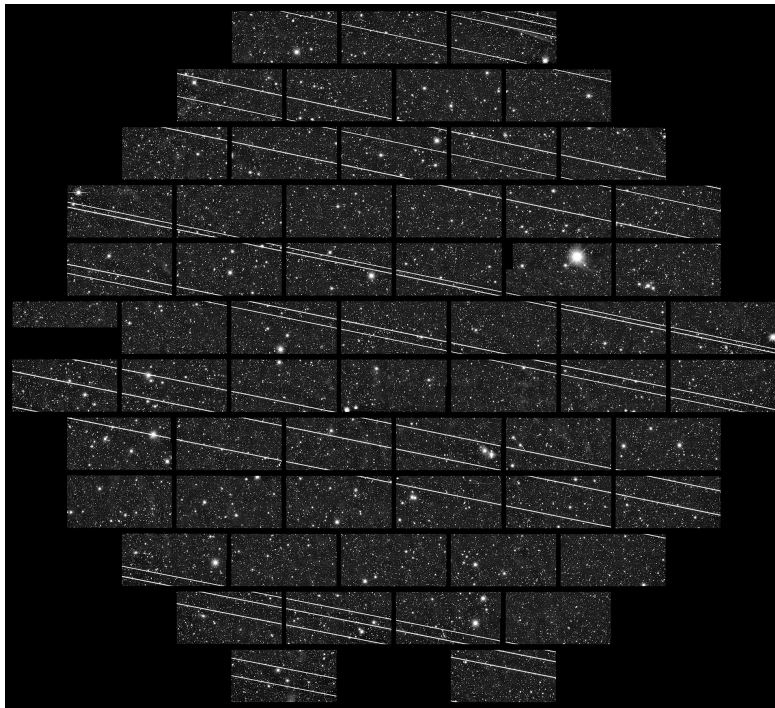


**Figure 2.6:** On Nov. 20, 2019, the Blanco Telescope of the Cerro Tololo Inter-American Observatory (CTIO) recorded a heavy loss of signal and the appearance of 19 white lines on a DECam shot. This was caused by the transit of a Starlink satellite train, launched a week earlier. [29].

## 2.10 Network architecture

The current constellation bases its operation on three components: user antenna, satellites and gateways, which are connected by fiber throughout the country. The operation diagram is shown in Figure 2.7 and provides communication in Ka-band between gateway and satellites and communication in Ku-band between satellites and user antennas. In this case, the signal path is optimized and a latency time of just 30 ms is guaranteed. However, the users' antenna must have a ground station within approximately 800 km of their location to get the service. Since the Starlink satellites are in constant motion, the network schedules these connections at intervals of 15 seconds and regenerates itself continuously. To perform all these

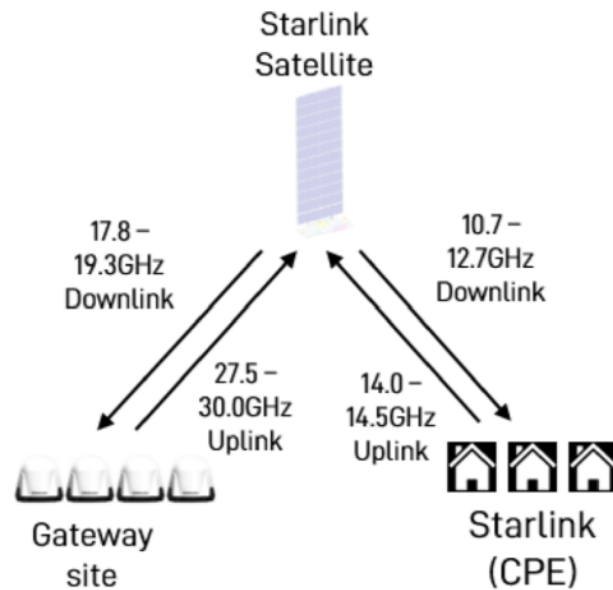


**Figure 2.7:** Starlink Network Architecture [30].

hand-offs, Starlink uses advanced phased-array technology for both the satellite and the customer’s device in the Ku and Ka-bands. Phased-array technologies enable efficient spectrum sharing by allowing the satellite and user antennas to adjust the direction of the beams simply by adjusting the signal of the single antenna.

As can be seen from Figure 2.8 both the user terminal and the satellite phased array are made up of hundreds of antenna elements (A) powered by a transmitter (TX), individually controlled by a phase shifter ( $\phi$ ) in turn controlled by a computer (C) that SpaceX designed for dynamic hand-offs [31]. The spherical wavefronts of the emitted waves (the red lines) can rotate thanks to the phase shifters that delay the generation of radio waves so that each antenna emits its wavefront later than the one below; in this way they combine in front of the antenna to create a plane wave that travels in a specific direction directed at an angle  $\theta$  with respect to the antenna axis. The ability to control hand-offs in the software with extreme precision allows SpaceX to transform the constant movement of the constellation into an advantage for the Starlink network. These micro-adjustments improve the reliability of Starlink and allow for more efficient capacity management on real time.

Things will totally change in the near future; in fact the next generation of Starlink satellites will be equipped with lasers that will allow inter-satellite communication. Instead of connecting people to the nearest ground station, the laser communication system would allow satellites to communicate with each other directly at the speed

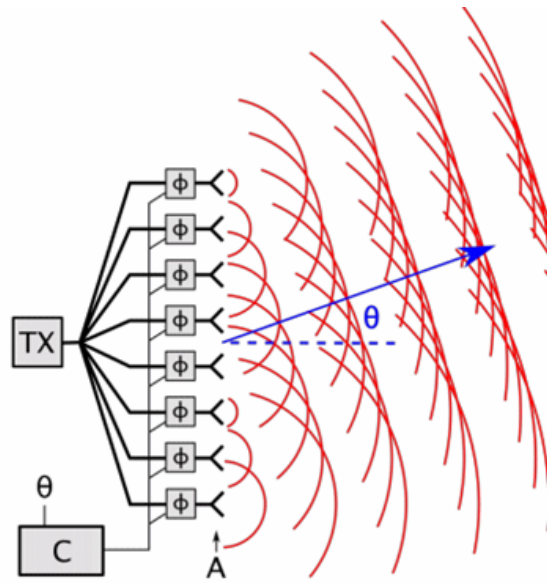


**Figure 2.8:** Phased array scheme [31].

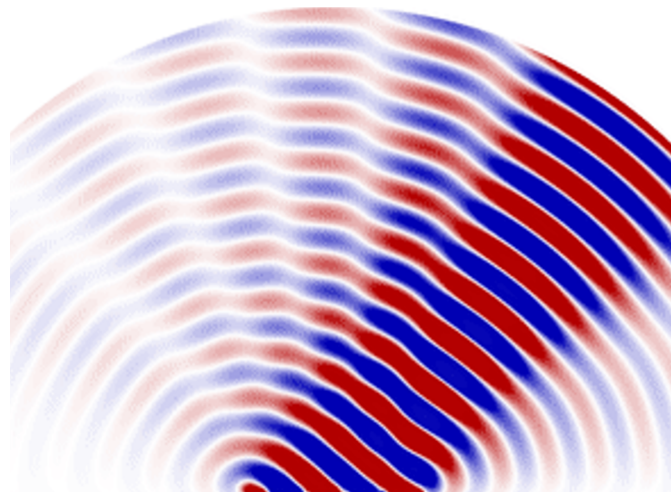


**Figure 2.9:** Radiation pattern of a phased array. The dark area is the beam or main lobe, while the light lines fanning out around it are sidelobes [31].

of light (which is faster in the vacuum of space 300'000 km/s than fiber-optic cables -200'000 km/s). Furthermore, SpaceX is currently working with the US Air Force's research arm with the goal of establishing connectivity without the need for ground stations between ground sites, aircraft and satellites.

## 2.11 User terminals

Users must be equipped with a special antenna to use the Starlink service, as their devices (smartphones, computers, tablets, etc.) use these antennas to connect to satellites. The antenna is small in size and is designed to handle a wide range of temperatures and bad weather conditions. It is very easy to install but it requires to be mounted where it can track satellites with a clear view of the sky, in fact, every object that obstructs the connection between Starlink and the satellite causes service interruptions [32].

For these reasons, it could be applied in fast-moving objects like trains or cars. In a while, SpaceX is testing them on the ship in order to enter the maritime market in the future [33].

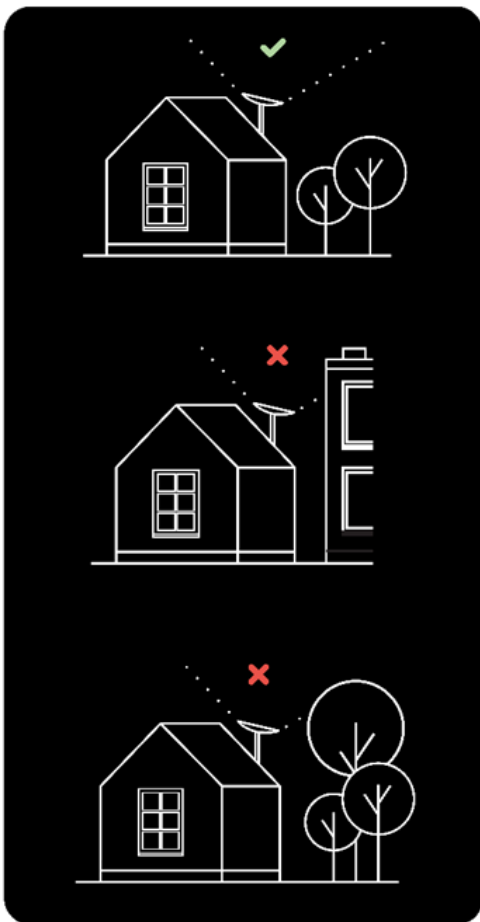


**Figure 2.10:** Correct way to install user antenna.



**Figure 2.11:** User antenna.

## 2.12 Ground Stations

Although the initial idea was to connect the various satellites by laser, the first generation of launched satellites did not adopt this technology and hundreds of ground stations had to be built around the world. So, until the new version of satellites has been launched, the service will be based on a system of ground stations called a gateway connected with Starlink satellites through Ka-band parabolic antennas. Starlink Gateway ground stations constitute another essential piece of the constellation infrastructure since they allow connection between the satellites in space and the internet data centers on Earth that connect to existing fiber-optic infrastructure which connects to the world wide web. Nowadays there are licensed gateways that are strategically located to optimize service in the United States while in other parts of the world the service is weakened [2]. According to the tracking site [34], SpaceX has 14 permanent ground stations in Europe and Turkey, more than 40 in North America, 14 in Latin America, 25 in Australasia, and others on islands including Guam and Puerto Rico. It has none yet in Asia or Africa.



**Figure 2.12:** An array of user terminals (bottom left) and ground stations (right) that SpaceX may be using to test Starlink.

## 2.13 Laser Inter-satellite link (LISL)

All satellites of the Starlink constellation, starting from generation v1.5, will be equipped with inter-satellite laser links (LISL). The main benefit of using laser communications is the higher bandwidth, which allows to transfer more data in less time. LISL terminals are expected to offer capacities up to 10 Gbps and can be easily integrated into the satellite due to their small size, low weight and low power requirements. According to a recent research it has been shown that a LISL type communication has superior performance, in terms of latency, to any other terrestrial fiber optic network for communications over a distance greater than about 3,000 km [1]. The current satellite configuration includes four LISLs per satellite of which two are used for communication in the same orbital plane and two are used in different orbital planes. Originally a fifth LISL was also planned to be used for connecting to a satellite in an orbital plane of crossing, but due to the difficulty in developing this fifth LISL, the configuration with only four LISLs was adopted [35].

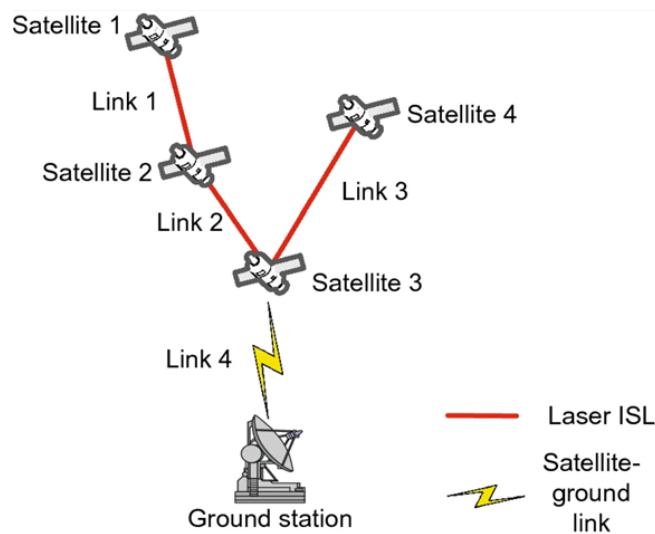


**Figure 2.13:** LISL architecture system [35].

## 2.14 Frequencies Range

On March 29, 2018, the FCC authorized SpaceX to provide broadband satellite internet services using the Ka-band and Ku-band. The Ka-band is the range from 27-40 GHz and the Ku-band covers 12-18 GHz. Starlink also uses the V-band, which is the range of 40-75 GHz, as well as dipping into the X-band and K-band, which are the ranges of 8-12 GHz and 18-27 GHz, respectively. In Table 2.4 it can be seen how FCC has authorized the various frequencies to be used.

Frequencies	
Range [GHz]	Use
10.70-12.70	Data from Starlink satellites to the customer's terminal on the ground;
12.15-12.25	TT&C downlink communications
13.85-14.00	TT&C uplink communications
14.00-14.50	Transmissions from the customer's terminal back up to the satellites in orbit
17.80-18.60	Satellite to gateway transmissions
18.55-18.60	TT&C downlink communications
18.80-19.30	Satellite to gateway transmissions
27.50-29.10	Send information from the gateways back up to the satellites
29.50-30.00	Send information from the gateways back up to the satellites
37.50-37.75	TT&C downlink communications
37.50-42.50	Transmission of data from Starlink satellites to the customer's terminal on the ground and from satellite to gateway transmissions
47.20-47.45	TT&C uplink communications
47.20-50.20	Transmissions from the customer's terminal back up to the satellites in orbit and from the gateways back up to the satellites
50.40-51.40	Transmissions from the customer's terminal back up to the satellites in orbit and from the gateways back up to the satellites

**Table 2.4:** Frequency range and different uses.

Starlink is thus a satellite constellation with very ambitious goals and seems to anticipate some of the future needs. However, the final design involves a very high number of satellites, and this worries a significant part of the scientific community. The problems associated with a high number of satellites are many; first among them is the risk of a collision with the consequent risk of creating the Kessler syndrome and thus the inaccessibility of space for decades to come. Starlink, from its side, plans to resolve any disputes without compromising safety.

Although the company and the official institutions approving such projects are to be trusted, it is interesting to understand the motivations behind SpaceX's plan to design this mega-constellation, and it would be interesting to undertake a study to see if this design can be improved by decreasing the number of satellites and thus the risk of a potential collision.

This thesis will analyze all the features that can be extrapolated from the available data focusing on the final configuration of the constellation in which 42,000 satellites equipped with LISLs will be used.



# Chapter 3

## Starlink competitors

SpaceX is not the only company whose goal is to provide high-speed low-latency broadband Internet connections worldwide through a constellation of LEO or VLEO satellites. There are currently many private companies that are planning to build their own mega-constellation in order to sell their high-performance Internet service. Among all the existing constellations, the following three constellations have been specifically taken into account in this research:

- Kuiper LEO system (Amazon)
- OneWeb LEO system (OneWeb)
- Telesat LEO system (Telesat)

These three constellations were chosen as they also have a large number of satellites (although significantly fewer than those used by Starlink) and have almost the same ambitious goals as the SpaceX constellation. A comparison between the various constellations is helpful to understand how each of them tries to achieve a similar objective. Certainly their performances are not identical but they all pursue the same goal and it is interesting to understand how they have compromised with the various design challenges to achieve it.

It must be said that although some of these projects have already taken shape, the architecture of the constellations is constantly evolving due to opposition from both other competitors and the authorities. Although all data has been taken from official documents, they may be out of date.

Due to the rapid changes in the orbital characteristics of each constellation, a 'data freeze' has been set for March 14th, 2022. Therefore the following analyses will be based on official data prior to the aforementioned date.

## 3.1 Kuiper LEO system

In April 2019, Amazon announced that within the following decade it would build a large constellation of broadband satellite Internet called Project Kuiper to provide the Internet to tens of millions of people without basic broadband Internet access [36]. The constellation foresees 3,236 satellites and, although the deployment of the entire constellation takes about ten years, Amazon plans to start selling its service as early as 2023 after the deployment of the first 578 satellites [37].

To unfold its constellation, Amazon will be "launch agnostic" and will not only entrust the launch capability to Jeff Bezos' company Blue Origin, but also to any other potential customers [38].

### 3.1.1 Orbital characteristics

With its 3,236 satellites in 98 orbital planes distributed over three orbital shells at altitudes of 590, 610 and 630 km, Kuiper is the only constellation, among those analyzed, that does not guarantee global coverage. In fact, the maximum orbital inclination in the system is  $51.9^\circ$  so the satellites cover all latitudes between  $56^\circ\text{N}$  -  $56^\circ\text{S}$ ; this means a coverage of 83% of the Earth's surface [39].

Table 3.1 and the following images summarize the architecture of the constellation.

Constellation Shell(s)	No. of Sats	No. of Planes	Sats per Plane	Inclination [ $^\circ$ ]	Interplane Spacing [ $^\circ$ ]	Altitude [km]
Kuiper A	1156	34	34	51.9	10.6	630
Kuiper B	1296	36	36	42	10	610
Kuiper C	784	28	28	33	12.9	590

**Table 3.1:** Orbital characteristics of Kuiper system [39]

### 3.1.2 System infrastructure

The system's performance is determined by the characteristics of the three components: satellites, gateway terminals and user terminals. The Kuiper satellites will be equipped with laser terminals for inter-satellite links in order to communicate with the other satellites in both the same plane and adjacent planes or in different shells. All the features are summarized in Table 3.2.

Amazon has not yet released details on the location of the gateways, however their location depends on the elevation angle to initiate a communication.



**Figure 3.1:** Kuiper system ground track visualization (side view) [40].

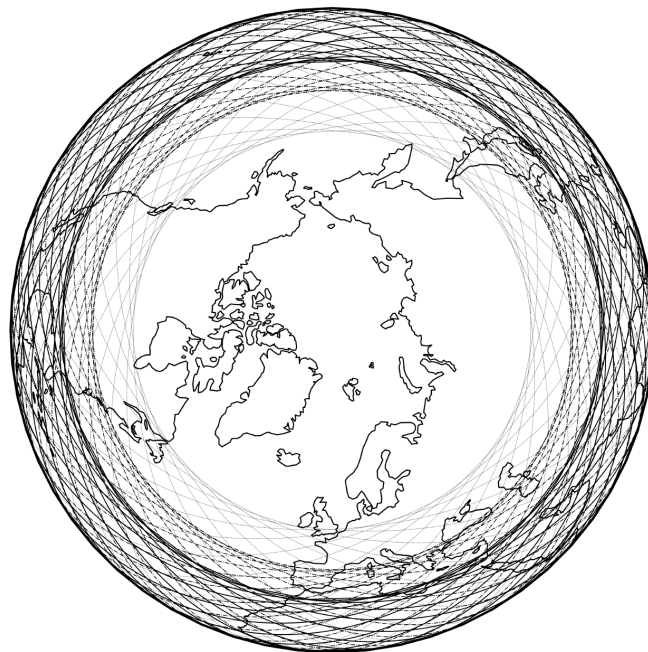


**Figure 3.2:** Kuiper system ground track visualization (polar view) [40].

Component	Characteristics
<b>Satellite</b>	
Number	3236
Mass	-
Capacity	11 Gbps
Antenna(s)	2 steerable GW antenna
Beams	8-12 steerable and shapeable user beams 14-16 steerable gateway spot beams
Intersatellite links	Yes
<b>Gateway Terminal</b>	
Number	92
Antenna(s) per site	4
Antenna Diameter	1.47 m
Frequency Band(s)	Ka-band
Min. elevation angle	20°
Sat. view angle	58.8°
<b>User Terminal</b>	
Compatible Antenna(s)	Mechanically steerable/electronically steerable
Antenna Diameter	0.48 m
Frequency Band(s)	Ka-band
Min. elevation angle	35°
Sat. view angle	48.2°

**Table 3.2:** Kuiper system components and characteristics [39].

## 3.2 OneWeb LEO system

OneWeb, formerly known as WorldVu Satellites Ltd, is a communications company founded in 2012 that aims to build its own constellation of satellites to sell its broadband satellite Internet service focusing on previously under-served fields, including aviation and maritime industries. After a series of financial problems that led the company to bankruptcy, from 2020 on the company has a new group of owners led by the UK government willing to carry on the project already started. The OneWeb satellite constellation aims to provide broadband satellite Internet services with global coverage.

Although the constellation has not yet been completed, as of 2021 the service has been made available to regions north of 50 ° latitude (UK, Alaska, Northern Europe, Greenland, Iceland, Arctic Ocean and Canada).

The first part of the constellation, involving 648 satellites, is expected to be completed by the end of 2022 and OneWeb will make global Internet services

available at that time. The second part will involve a much higher number of satellites but this is still in the definition phase [41].

Until February 2022 OneWeb was using Russian launchers but due to tensions caused by the current war between Russia and Ukraine, the company announced that it has signed a launch agreement with its competitor SpaceX to launch the remaining satellites on Falcon 9 rockets [42].

### 3.2.1 Orbital characteristics

OneWeb’s first phase initial operational satellite network includes 648 satellites distributed in a circular orbit at 1,200 km altitude. The spacecraft are expected to be deployed in 18 orbital planes with 36 satellites in each plane. As global demand for its services grows, the constellation will grow to more than 900 first-generation satellites operating simultaneously.

The second phase requires many more satellites and has undergone many changes over the years. The original proposal filed with the FCC called for a system of 47,844 satellites in orbits 1,200 km high arranged in 32 planes of 720 satellites each with an inclination of 40 degrees, 32 planes with 720 satellites each with an inclination of 55 degrees and 36 planes with 49 satellites each with an inclination of 87.9 degrees.

The latest revised system, which has 6,372 satellites, maintains the same arrangement of the orbital planes, but reduces the number of satellites in each of the 40-degree and 55-degree planes from 720 to 72 while the satellites in the orbital planes to 87.9 degrees are unchanged [43].

However, it is not yet certain that this will be the final configuration.

Constellation	No. of Sats	No. of Planes	Sats per Plane	Inclination [°]	Interplane Spacing [°]	Altitude [km]
Phase I						
OneWeb I	648	18	36	86.4	10	1200
Phase II						
OneWeb IIA	2304	32	72	40	5	1200
OneWeb IIB	2304	32	72	55	5	1200
OneWeb IIC	1764	36	49	87.9	7.3	1200

**Table 3.3:** Orbital characteristics of OneWeb system.

### 3.2.2 System infrastructure

The system's performance is determined by the characteristics of the three components: satellites, gateway terminals and user terminals. First-generation satellites do not have inter-satellite data links, so they will only work when they are within range of a gateway ground station.

Typically a site hosts ten or more gateway ground station antennas in order to access several OneWeb satellites visible at the same time from that location. The exact number of gateway ground station sites will depend on markets and services in various parts of the world; in the initial phase of the project only 50 were estimated but they will tend to increase.

Component	Characteristics
<b>Satellite</b>	
Number	648 (I) + 6372 (II)
Mass	175–200 kg
Capacity	9.97 Gbps
Antenna(s)	1 steerable GW antenna
Beams	16 highly elliptical user beams 2 steerable gateway spot beams
Intersatellite links	Yes (only phase II)
<b>Gateway Terminal</b>	
Number	50-70
Antenna(s) per site	$\geq 10$
Antenna Diameter	2.4 m
Frequency band(s)	Ka-Band
Min. elevation angle	15 °
Sat. view angle	40 °
<b>User Terminal</b>	
Frequency band(s)	Ku-Band
Compatible Antenna(s)	Mechanically or electronically steerable
Antenna Diameter	30-75 cm
Min. elevation angle	55 °
Sat. view angle	25 °

**Table 3.4:** Oneweb system components and characteristics.

### 3.3 Telesat LEO system

Telesat, a Canadian satellite communications company, announced in 2016 that it would launch a constellation of 120 LEO satellites with the aim of bridging the digital divide in remote environments and improving performance for mobility and for government uses. The company went on to say that Telesat's core businesses will be the aviation and maritime cellular data markets.

#### 3.3.1 Orbital characteristics

In 2020, after some changes were made to the initial project, Telesat delivered the final project for its constellation to FCC, defining two deployment phases: "Phase I" which consists of 298 satellites and "Phase II" which consists of 1373 satellites for a total of 1671 satellites in the final constellation. The final constellation will be characterized by two shells, one of which will have polar orbits with an inclination of  $98.98^\circ$  while the second will point to the lower latitudes with an inclination of  $50.88^\circ$  [44]. The displays of the terrestrial traces for shell and final constellation can be seen in Figures 3.3 and 3.4 respectively.

Constellation	No. of Sats	No. of Planes	Sats per Plane	Inclination [°]	Interplane Spacing [°]	Altitude [km]
Phase I						
Telesat IA	78	06	13	98.98	31.6	1015
Telesat IA	220	20	11	50.88	36	1325
Phase II						
Telesat IIA	351	27	13	98.98	31.6	1015
Telesat IIB	1320	40	33	50.88	36	1325

**Table 3.5:** Orbital characteristics of Telesat system

#### 3.3.2 System infrastructure

The performance of the system is determined by the characteristics of the three components: satellites, gateway terminals and user terminals. Telesat satellites will be equipped with laser terminals for inter-satellite links in order to communicate with the other satellites in both the same plane and adjacent planes or in different shells. Table 3.6 lists the characteristics of the Telesat components:



**Figure 3.3:** Telesat system ground track visualization (side view) [40].

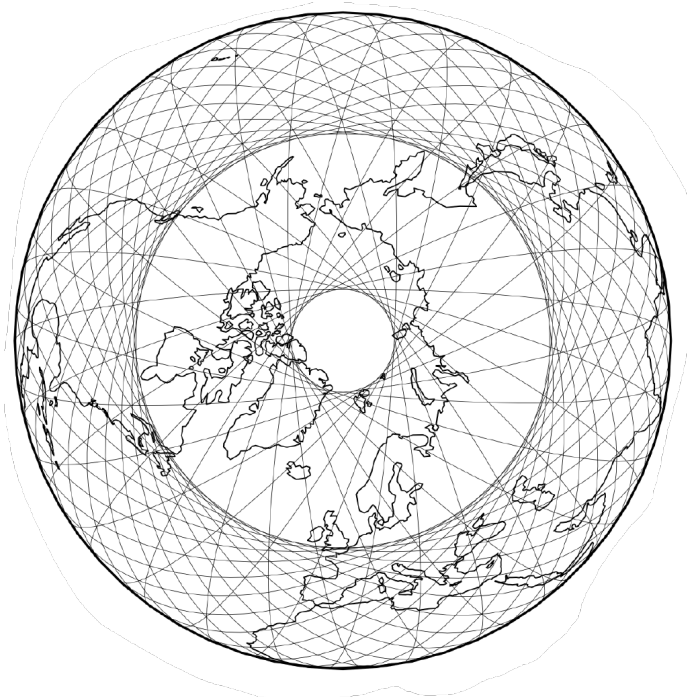


**Figure 3.4:** Telesat system ground track visualization (polar view) [40].

<b>Component</b>	<b>Characteristics</b>
<b>Satellite</b>	
Number	1671
Mass	700 kg
Capacity	38.68 Gbps
Antenna(s)	2 steerable GW antenna
Beams	16-18 highly elliptical user beams 2 steerable gateway spot beams
Intersatellite links	Yes
<b>Gateway Terminal</b>	
Number	56-60
Antenna(s) per site	5-6
Antenna Diameter	3-5 m
Frequency band(s)	Ka-Band
Min. elevation angle	10 °
Sat. view angle	-
<b>User Terminal</b>	
Frequency band(s)	Ka-Band
Compatible Antenna(s)	Mechanically or electronically steerable
Antenna Diameter	100 cm
Min. elevation angle	20 °
Sat. view angle	-

**Table 3.6:** Telesat system components and characteristics [43].



# Chapter 4

## Constellation analysis

Compared to its competitors, Starlink raised the bar. Although the goals of all these companies are similar, SpaceX's planned constellation looks much more complex, much more ambitious and much more challenging. Consequently, some doubts arise. In addition, despite the best technologies implemented by SpaceX, the large number of satellites involved worries many experts.

Before the entire constellation is deployed, it would be interesting to conduct a detailed study of it to fully understand its functionality and potential, and at the same time to see if any action can be taken to try to improve it. No previous work with this purpose is currently available in literature, and this thesis aims to pave the way for a more thorough study. However, this is not straightforward.

The major limitations to be taken into account are:

- the limited amount of information related to the constellation; many data are unavailable to the public and consequently many assumptions must be made;
- the large number of data involved and the high computational power required.

Some assumptions have been made in the case of this thesis that should reflect an ideal case. The lack of data concerning the details of the satellites and the subsystems used inevitably led to a partial study. In addition, in order to be able to fit within the required deadline, the data obtained are approximative although the computational power provided by Politecnico di Torino [45] and Delft University of Technology was used simultaneously.

Despite the limitations, the present study succeeds in giving a clear idea of how the constellation works and therefore gives interesting insights to those who would like to continue this project.

## 4.1 Explanation of conducted work

The following study considers the completed Starlink constellation. Therefore, Gen1 and Gen2 are analyzed at the same time (since the goal is to reduce the number of satellites, the first proposal of Gen2 (Table 2.2) which is less numerous, was considered). According to what is stated in the FCC documents, all satellites will communicate with each other via LILSs while communication between satellites and ground stations will be via radio frequencies.

In particular, each shell contributing to the whole constellation will be analyzed individually. The reason why each shell will work independently of the others is attributable to the laser technology implemented. In fact, it has been shown how the difference in orbital speed between the various shells makes effective laser communication difficult, and even with more advanced technologies, it would require too much time and thus more latency [1]. This is the reason why there has been a shift from five laser transceivers on each satellite to four.

The only exception are the  $A_C$  and  $A_D$  shells which, having the same altitude and inclination, were analyzed as if they were a single shell:  $A_{CD}$ .

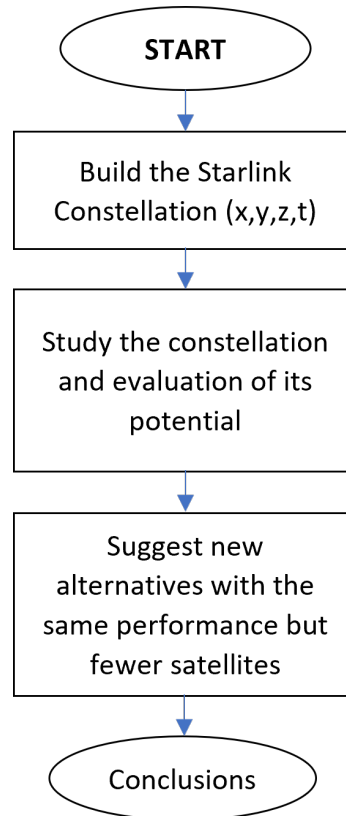


Figure 4.1: Scheme of conducted work.

In order to conduct a proper study, it was necessary to propagate the constellation over time so as to know the position of the various satellites over time. Walker's model was selected as the propagator while a time range of 30 min and a stepsize time resolution of  $\Delta t = 1$  s were chosen. Thus in total 1800 instants of time were taken into analysis. Whereas this range is equivalent to about one-third of the orbital period of the satellites in the various shells, it manages, in acceptable computational times, to give a clear idea of what happens.

Once the constellation has been propagated over time, some aspects that enable understanding its potential have been analyzed. The aspects that have been analyzed are: the coverage that each shell provides, the latency taken by a signal to reach a ground station from another ground station, the number of switches between satellites that must be made to ensure the most stable connection over time. These analyses allowed an understanding of what is the alleged use and performance of each shell.

Finally, two shells have been selected and appropriately modified by reducing the number of satellites. The analyses done previously were repeated so that they could be compared with the original ones. Despite the many limitations and the consequent study of an ideal case in which real data traffic is ignored, interesting results were obtained.

For each type of analysis performed no specific software was used, rather codes were written in Python or Matlab language.

## 4.2 Constellation geometry

### 4.2.1 Walker constellation and propagation

In order to represent each shell in the constellation, Walker’s model was selected because it fits well with a symmetrical distribution of satellites over orbital planes and with circular constellations composed of many satellites aiming for global coverage. It is very likely that SpaceX engineers used such a pattern, although in no FCC document is it explicitly stated, also because some articles [46] suggest how the Walker pattern might suit Starlink.

A constellation described by this model uses a notation proposed by John Walker[47]:

$$i : N/P/F$$

where:

- $i$  is the inclination of the orbital plane;
- $N$  is the total number of satellites;
- $P$  is the number of equally spaced orbital planes;
- $F$  is the parameter that describes the relative spacing between satellites in adjacent planes.

Each shell will be analyzed individually and will be characterized by its own parameters. While  $i$ ,  $N$ , and  $P$  are known, the parameter  $F$  is unknown and must be calculated. Special attention should be paid to the  $i$  parameter because the values of  $\Omega$  and thus the exact Walker model to be used between Delta or Star configuration will depend on it.

The Walker Star model describes nearly polar orbits with inclinations close to  $90^\circ$  and with the planes being uniformly spaced within  $180^\circ$ . As such, the angle between neighboring orbital planes is  $180/P$ . In this way, potential head-on collision are avoided.

The Walker Delta model describes orbits with typical inclinations of  $<70^\circ$  and with the planes being uniformly spaced within  $360^\circ$ . As such, the angle between neighboring orbital planes is  $360/P$ .

Walker Star	$A_{CD}, II_D$
Walker Delta	$A_A, A_B, A_E, B_A, B_B, B_C, II_A, II_B, II_C, II_E, II_F, II_G, II_H, II_I$

**Table 4.1:** Classification of the different shells.

As a consequence, the various shells were appropriately classified as shown in Table 4.1.

Satellites in a Walker constellation are uniformly distributed in space so, for each  $j$ -th satellite on each  $i$ -th plane, there are specific values of the right ascension of the ascending nodes (RAAN or  $\Omega$ ) and the initial mean anomaly (M).

While RAAN represents the longitude of the point at which the spacecraft crosses the equatorial plane moving from south to north, the initial mean anomaly corresponds to the angle between the periapsis point and the imagined position of an object for the same elapsed time since periapsis for a circular orbit around the same body with the same orbital period.

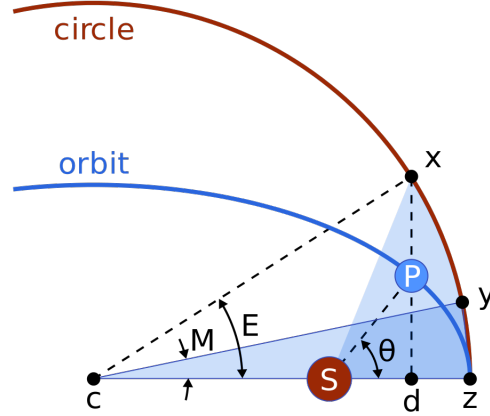
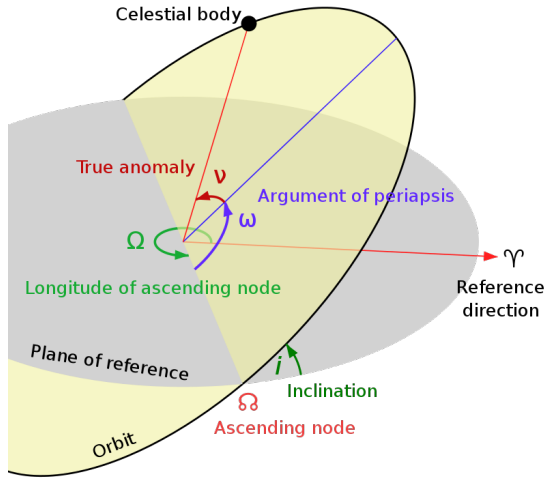


**Figure 4.2:** Orbital parameters [48]. **Figure 4.3:** Mean anomaly ( $M$ ), true anomaly ( $\theta$ ) and eccentric anomaly ( $E$ ) [49].

The Walker pattern provides the following formulas:

$$\Omega_{ij} = \frac{2\pi}{P}(i - 1) \quad (4.1)$$

$$M_{0ij} = \frac{2\pi}{N}P(j - 1) + \frac{2\pi}{N}F(1 - i) \quad (4.2)$$

where Equation 4.1 refers to the Walker Delta model but if divided by two the Walker Star formula is obtained; Equation 4.2 refers to the mean anomaly at  $t=0$ .

### 4.2.2 Transformation from orbital elements to rectangular coordinates

In order to obtain the x, y, z coordinates of the satellites, it is necessary to know the value of the true anomaly so the following calculations are to be performed [50]:

$$E - e \sin(E) = n(t - \tau) \quad (4.3)$$

$$n = \sqrt{\frac{\mu}{a^3}}$$

where:

- $e$  is the eccentricity and in these cases it is always 0 because all orbits are circular;
- $n$  is the mean angular motion;
- $\mu$  is the gravitational parameter of the Earth;
- $a$  is the semi-major axis and it is equivalent to the altitude of each shell added to the Earth radius  $R$ ;
- $\tau$  is a constant that comes from an integration and can be assumed to be zero.

At this point Equation 4.3 can be rewritten as:

$$E = n \cdot t \quad (4.4)$$

The right-hand side of Equation 4.4 is the product of the mean angular motion of body  $i$  and the time elapsed since the last pericenter passage. This product is called mean anomaly (M) and it has the dimension of an angle.

$$E = n \cdot t = M \quad (4.5)$$

$$M = M_{0ij} + n \cdot t \quad (4.6)$$

The combination of Equations 4.5 and 4.6 yields:

$$E = M_{0ij} + n \cdot t \quad (4.7)$$

Once the value of the eccentric anomaly is known, it is possible to determine the value of the true anomaly by the following formula:

$$\tan\left(\frac{\theta}{2}\right) = \sqrt{\frac{1+e}{1-e}} \tan\left(\frac{E}{2}\right) \quad (4.8)$$

by which, in the case analyzed, the following is obtained:

$$\theta = E \quad (4.9)$$

With the true anomaly obtained, it is finally possible to apply the transformation from orbital elements to rectangular coordinates formulas.

$$\begin{cases} x = r(l_1 \cos \theta + l_2 \sin \theta) \\ y = r(m_1 \cos \theta + m_2 \sin \theta) \\ z = r(n_1 \cos \theta + n_2 \sin \theta) \end{cases} \quad (4.10)$$

where:

$$r = \frac{a(1 - e^2)}{1 + e \cos \theta} = a$$

$$l_1 = \cos \omega \cos \Omega - \sin \omega \sin \Omega \cos i$$

$$m_1 = \cos \omega \sin \Omega + \sin \omega \cos \Omega \cos i$$

$$n_1 = \sin \omega \sin i$$

$$l_2 = -\sin \omega \cos \Omega - \cos \omega \sin \Omega \cos i$$

$$m_2 = -\sin \omega \sin \Omega + \cos \omega \cos \Omega \cos i$$

$$n_2 = \cos \omega \sin i$$

in which  $\omega$  is the argument of periapsis and in these cases it is irrelevant because of circular orbits so it is put to zero.

### 4.2.3 F parameter

Differently from the other parameters that are known a priori or can be calculated, the parameter F is unknown and there is no official paper that provides this value. According to Walker's model it corresponds to an integer in the range between 0 and P-1 and therefore, in order to best estimate it, it is necessary to check out every possible value of F. This is a very important parameter because it determines the phasing of the satellites contained in each orbital plane of the constellation and consequently avoids collisions when the orbital planes cross. The risk of collision can be avoided by choosing an F parameter that ensures a maximum value of the minimum distance between the various satellites over time.

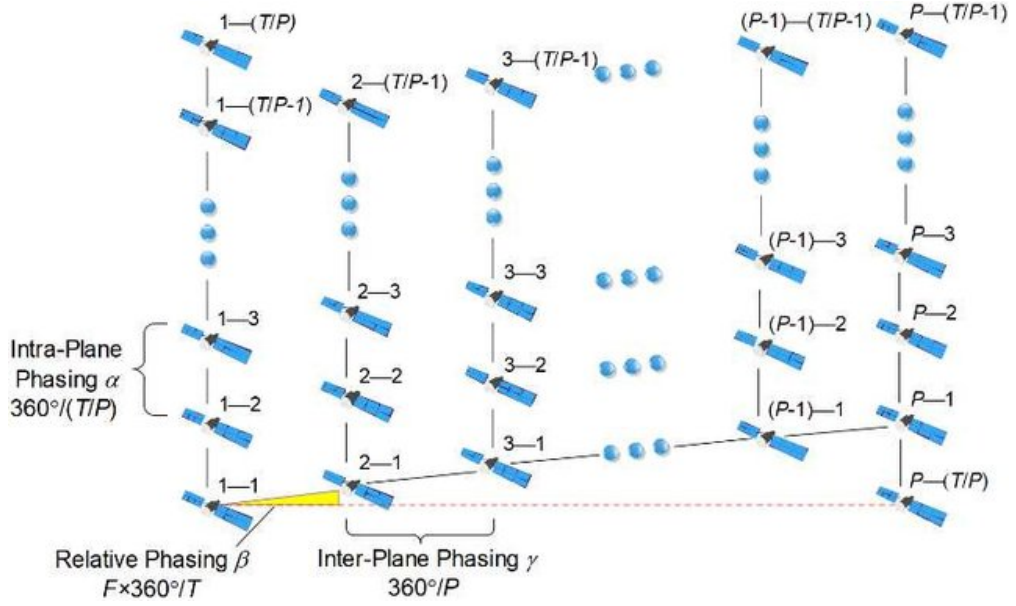


**Figure 4.4:** Parameters of a satellite constellation [46].

Once  $F$  is known, it will be possible to calculate  $\beta$  that corresponds to the phase between satellites in adjacent orbital planes.

$$\beta = F \cdot 2\pi/N$$

As Figure 4.4 shows, the greater the value of  $F$ , the greater the angle  $\beta$ .

A method that can describe the quality of the parameter entails calculating, for each possible  $F$  within its range of variability, the maximum value of the minimum distance that each satellite has from all the remaining ones in the constellation. This calculation has been iterated over a period of time equivalent to each shell's own orbital period, and for each of them the value that provides the greatest minimum distance and thus greater safety has been taken.

Also in this case, a  $\Delta t=1$  s was selected. The choice was forced because a lower  $\Delta t$  would have required too much computational power and time. However, although, in a second each satellite moves more than 7 km, results similar to those obtained with a  $\Delta t=0.1$  s were obtained in some test simulations (Table 4.2, made for the  $A_E$  shell). Therefore, it is reasonable to assume that the following data are affected by negligible error.

All results obtained for each shell have been represented in Table 4.3.

The table shows what the  $F$  parameters are that guarantee greater distances and thus greater safety, because by selecting these values the risk of collision between satellites should be zero. In addition, it can be seen that, tendentially, a shell with many satellites and placed in lower orbits can guarantee, at most, minimum

$\Delta t=1$ s		$\Delta t=0.1$ s	
F	Min distance [km]	F	Min distance [km]
1	3.37	1	3.37
3	58.23	3	58.23
5	35.50	5	35.50
15	1.48	15	1.38
21	13.33	21	13.31
43	21.00	43	21.00

**Table 4.2:** Distance results obtained for  $\Delta t=1$  s and  $\Delta t=0.1$  s in the  $A_E$  shell.

distances on the order of 10-20 km, while a less dense shell placed in higher orbits guarantees greater safety. Currently there are no laws that force the minimum distance that should occur between satellites in space but it is easy to imagine that the smaller this distance the higher the probability of collision. For this reason, in order to adopt a safer solution, all those that guarantee the minimum distance between satellites were selected as F parameters.

Another aspect that can be seen when looking at the table is that all the shells analyzed by the Walker Delta method that have even F parameters lead to collision and must necessarily be avoided.

For the  $A_{CD}$  shell, it has been shown how the union of the two separate shells, each taken with its own best F, continues to provide a sufficiently high distance between satellites even though it is reduced compared to that of the individual shells

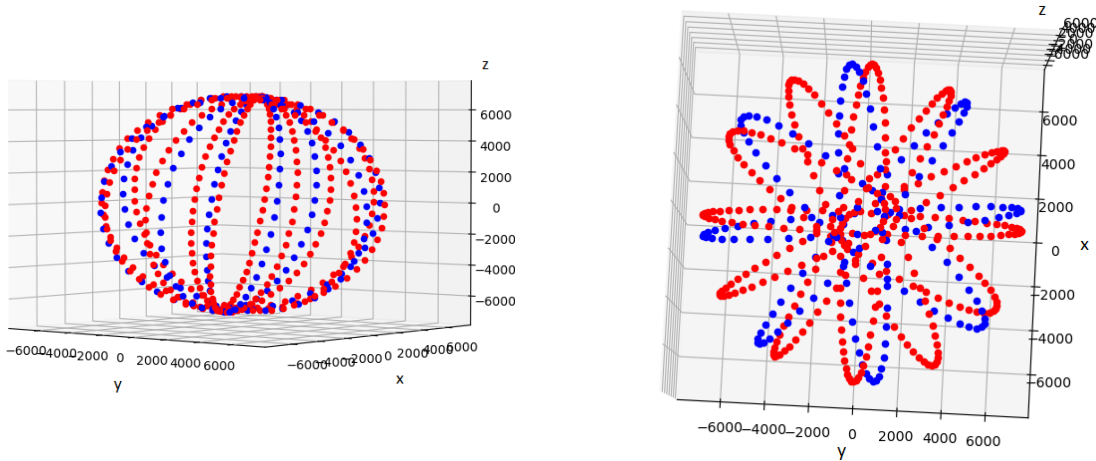


**Figure 4.5:** Side view (left) and top view (right) of the shell  $A_{CD}$  where blue dots belong to  $A_C$  while red dots belong to  $A_D$ . The axes are expressed in km.

Shell	Best F	Max min dist.	Graph
$A_A$	13	47.94 km	
...	...	...	
$B_B$	1509	76.66 km	
...	...	...	
$II_C$	35	29.83 km	

**Table 4.3:** Evaluation of the best F parameter based on the minimum guaranteed distance between satellites. The full table is available in Appendix A.

However, this methodology is not sufficient for assessing the correctness of the F parameter. Although it is extremely necessary that satellites stay as far apart as possible, it is also important, for proper constellation operation, that they be well

placed so as to ensure as homogeneous coverage as possible. Unfortunately, it is not known whether these found parameters are coverage efficient.

In fact, as Figures 4.6 and 4.7 show, it can be seen how different the shell configuration is as the parameter  $F$  changes. In particular, the parameter  $F$  affects the coverage over time of a given area and so directly affects the performance of the constellation. Choosing the correct  $F$  is, therefore, the first important step to take in order to approach the actual Starlink configuration (assuming indeed that it has been optimized from these points of view, as it logically should be).

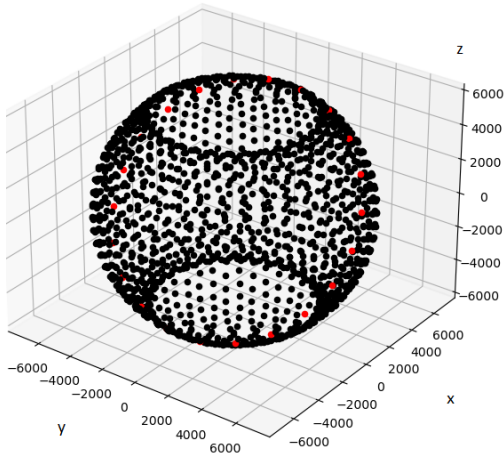


**Figure 4.6:** Plot of  $A_E$  shell with  $F=37$  where the red dots are the satellites in the first orbital plane.

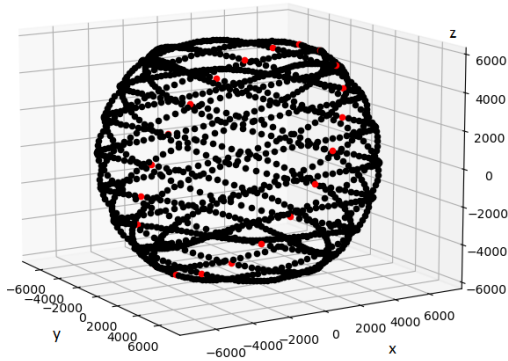


**Figure 4.7:** Plot of  $A_E$  shell with  $F=65$  where the red dots are the satellites in the first orbital plane.

Without doing any calculations, just looking at the images, it can be seen that the coverage provided by the  $F=37$  parameter (randomly chosen) seems to be more homogeneous and definitely better than that provided by  $F=65$ , which is the parameter that provides the maximum distance between satellites.

For this very reason, it was necessary to understand how each previously identified  $F$  value affects the performance of its own shell. Coverage was calculated (using a procedure described below) at latitude intervals of  $5^\circ$  taking the Greenwich Meridian as the reference longitude. Again a time range of 1800 s and a stepsize of  $\Delta t=1$  s were used.

In doing so, we obtained Table 4.4 which clearly shows that the assumption made earlier was correct. However, there are luckily some shells, the more numerous ones, where the parameter that provides the greatest minimum distance is also the one that provides continuous coverage.

	0°	5°	10°	15°	20°	25°	30°	35°	40°	45°	50°	55°	60°	65°	70°	75°	80°	85°	90°	average	
	%	%	%	%	%	%	%	%	%	%	%	%	%	%	%	%	%	%	%	%	%
<b>AA</b>	100	100	100	100	100	100	100	100	100	100	100	100	0	0	0	0	0	0	0	0	<b>100.00</b>
<b>AB</b>	91.7	57.9	96	59.4	94.7	63.9	85.7	78.5	78.8	97.1	60.6	95.6	100	100	100	36.4	0	0	0	0	<b>81.02</b>
<b>ACD</b>	65.6	57.5	49.4	40.4	38.4	42.4	48.4	56.7	70.6	90.6	99.6	100	100	100	100	100	100	100	0	0	<b>75.53</b>
<b>AE</b>	100	77.7	90.9	100	69.1	100	91.8	82.1	100	100	100	100	0	0	0	0	0	0	0	0	<b>92.63</b>
<b>BA</b>	73.4	57.6	48.7	74.2	69.7	44.9	46.4	60.6	62.1	19.8	0	0	0	0	0	0	0	0	0	0	<b>55.74</b>
<b>BB</b>	100	96.8	100	95.7	100	100	100	100	100	100	100	0	0	0	0	0	0	0	0	0	<b>99.32</b>
<b>BC</b>	100	98.1	83	99.8	100	92.9	100	100	100	100	100	100	0	0	0	0	0	0	0	0	<b>97.82</b>
<b>IIA</b>	100	100	100	100	100	100	100	100	100	100	100	100	0	0	0	0	0	0	0	0	<b>100.00</b>
<b>IIB</b>	100	100	100	100	100	100	100	100	100	100	0	0	0	0	0	0	0	0	0	0	<b>100.00</b>
<b>IIC</b>	100	100	100	100	100	100	100	100	100	0	0	0	0	0	0	0	0	0	0	0	<b>100.00</b>
<b>IID</b>	100	100	100	100	100	100	100	100	100	100	100	100	100	100	100	100	100	100	0	0	<b>100.00</b>
<b>IIE</b>	93.3	100	100	100	100	100	100	100	100	100	100	100	0	0	0	0	0	0	0	0	<b>99.44</b>
<b>IIF</b>	100	100	100	100	100	100	100	100	100	100	0	0	0	0	0	0	0	0	0	0	<b>100.00</b>
<b>IIG</b>	96.9	100	100	100	100	100	100	100	0	0	0	0	0	0	0	0	0	0	0	0	<b>99.61</b>
<b>IIH</b>	66.9	41.5	19	62.5	60.4	67.7	80.6	38.4	0	0	0	0	0	0	0	0	0	0	0	0	<b>54.63</b>
<b>III</b>	71.2	54.2	56.4	40.7	38.4	49.2	53.4	82	65.8	83	79.1	86.3	100	100	0	0	0	0	0	0	<b>68.55</b>

**Table 4.4:** Coverage for each shell with the F parameter that guarantees the maximum minimum distance (the average was calculated only in the latitude zone that the shells cover).

Thus for the  $A_A$ ,  $II_A$ ,  $II_B$ ,  $II_C$ ,  $II_D$  and  $II_F$  shells it can be assumed that the selected F parameter is the correct one, while for the other shells it will be necessary to go ahead with the analysis and study the behavior of each possible F. Specifically, the coverage by each shell for each F was calculated and then a rate was assigned through a formula that appropriately weighs the minimum guaranteed distance and the percentage of coverage. Table 4.5 was obtained for each shell (the other tables are available in Appendix A). However, such tables were calculated only for shells  $A_B$ ,  $A_{CD}$ ,  $A_E$ ,  $II_E$ ,  $II_G$ ,  $II_I$  and  $II_H$  while for shells  $B_A$ ,  $B_B$  and  $B_C$  it was impossible because of the time required by the computational operations.

Specifically in Table 4.5 an example has been represented that refers to shell  $A_B$ . As can be seen for this particular shell, there is no F parameter that guarantees total coverage however there are some parameters that guarantee better coverage than that identified by F=25 (which guarantees maximum minimum distance between satellites) even though with smaller maximum guaranteed distances. In this case the parameter selected is F=13 because it guarantees 85.99% coverage and a maximum distance between satellites of 44.5 km. Although other parameters

## 4.2 – Constellation geometry

F	% Coverage per Latitude																				% Average	Distance min [km]	Rate
	0°	5°	10°	15°	20°	25°	30°	35°	40°	45°	50°	55°	60°	65°	70°	75°	80°	85°	90°				
1	96	68	81.3	85	68.3	100	72	81.7	98.7	69.3	93	100	100	100	100	38.3	0	0	0	84.48	2.56	8.95	
3	96.3	71.7	76.7	91.7	67	92.7	88.7	67.7	98.3	98	78	98	100	100	100	37	0	0	0	85.11	17.99	9.36	
5	94	74.7	71.7	95.3	69	83.3	96.7	73.3	86.7	100	100	95.7	100	100	100	38	0	0	0	86.15	3.25	9.15	
7	91.3	78.7	67.3	96.7	74.7	73.3	93.7	88.3	79.7	97.3	100	100	100	100	100	38	0	0	0	86.19	41.94	9.97	
9	91.3	82	64	96.3	80.3	60.7	89	98.7	91	91.3	96.7	100	100	100	100	36	0	0	0	86.08	25.17	9.61	
11	90.7	81.3	64.3	95.3	79.7	71.3	86.3	95.3	96.3	97	98	100	100	100	100	37	0	0	0	87.03	2.15	9.20	
13	91	78.7	67.3	93.7	75.7	82.3	90	83.3	87.3	97	96.3	99.3	100	100	100	34	0	0	0	85.99	44.50	10.00	
15	92.3	75.7	72.3	89.3	72	89.3	94.7	67.3	95.7	100	100	100	100	100	100	38.3	0	0	0	86.68	17.99	9.53	
17	93.7	71.7	77.7	85.7	71	98	85.3	71.3	100	99.3	93.7	95	100	100	100	36	0	0	0	86.15	3.25	9.15	
19	96	67.7	82.3	79.3	73.3	98.7	71.3	87	99.3	78	86	99	100	100	100	39.3	0	0	0	84.83	2.56	8.99	
21	96.3	63.7	87.3	73	80.7	88.3	64	99.7	78.3	78.7	100	100	100	100	100	36	0	0	0	84.13	32.10	9.55	
23	94	60	92	66.3	88	76	73	95.7	63.7	98.7	90.7	70.3	87.7	100	100	39	0	0	0	80.94	57.65	9.74	
25	91.7	57.9	96	59.4	94.7	63.9	85.7	78.5	78.8	97.1	60.6	95.6	100	100	100	36.4	0	0	0	81.02	64.69	9.89	
27	91.3	57.3	97	54.7	98.7	53	97.7	60.3	97	70.7	87	91	62	87.7	94.3	28.7	0	0	0	76.78	17.99	8.48	
29	90.7	57.3	96	58.7	93.3	60.7	92.3	65.7	93	65.3	99	58.7	100	78	61.3	21.3	0	0	0	74.46	3.25	7.92	
31	91	59	93.3	64.3	86.3	71.3	79.7	83	75.7	90.3	72.3	96.3	72.3	100	79	18.7	0	0	0	77.03	34.24	8.84	
33	92.3	61	89.7	70.3	79.7	82.7	64.7	98.3	61.7	98	73.3	88.7	99.3	100	100	23.7	0	0	0	80.21	8.41	8.64	
35	93.7	64.7	86.3	77.7	73.7	95.3	59.7	97.3	78.7	77.3	100	76.3	95	100	100	29.7	0	0	0	81.59	51.05	9.67	

**Table 4.5:** Coverage per latitude for each F parameter of the  $A_B$  shell.

guarantee slightly higher coverage, that parameter was chosen for anti-collision safety reasons.

For the other shells  $A_{CD}$ ,  $II_E$ ,  $II_G$ ,  $II_H$  and  $II_I$ , on the other hand, it has been shown that the previously estimated parameter provides the best trade-off between coverage and distance.

The only exception is represented by the shell  $A_E$  for which it goes from 92% to 100% coverage with  $F=39$ .

Then Table 4.4 was remade with what are the final values used in this research.

So at the end the values for the F parameter in Table 4.7 have been used:

The choice of these values in a preliminary study may seem inaccurate, and the values used for shells B are a reflection of this. However, for the following analyses that are to be performed, only a small error is found when changing F within a range of values considered acceptable. Hence, all the analysis carried out below, although affected by an error, have an error that can be considered negligible.

In Tables 4.7 and 4.6, shells B have been indicated with an asterisk because for them, due to the excessive calculation time required, the one that guarantees only the maximum distance was assumed to be F (a trade-off that also took coverage into account would have required weeks of calculations).

	0°	5°	10°	15°	20°	25°	30°	35°	40°	45°	50°	55°	60°	65°	70°	75°	80°	85°	90°	average	
	%	%	%	%	%	%	%	%	%	%	%	%	%	%	%	%	%	%	%	%	%
AA	100	100	100	100	100	100	100	100	100	100	100	100	0	0	0	0	0	0	0	0	100.00
AB	91	78.7	67.3	93.7	75.7	82.3	90	83.3	87.3	97	96.3	99.3	100	100	100	34	0	0	0	0	85.99
ACD	65.6	57.5	49.4	40.4	38.4	42.4	48.4	56.7	70.6	90.6	99.6	100	100	100	100	100	100	100	0	0	75.53
AE	100	100	100	100	100	100	100	100	100	100	100	100	0	0	0	0	0	0	0	0	100.00
BA*	73.4	57.6	48.7	74.2	69.7	44.9	46.4	60.6	62.1	19.8	0	0	0	0	0	0	0	0	0	0	55.74
BB*	100	96.8	100	95.7	100	100	100	100	100	100	100	0	0	0	0	0	0	0	0	0	99.32
BC*	100	98.1	83	99.8	100	92.9	100	100	100	100	100	100	0	0	0	0	0	0	0	0	97.82
IIA	100	100	100	100	100	100	100	100	100	100	100	100	0	0	0	0	0	0	0	0	100.00
IIB	100	100	100	100	100	100	100	100	100	100	0	0	0	0	0	0	0	0	0	0	100.00
IIC	100	100	100	100	100	100	100	100	100	0	0	0	0	0	0	0	0	0	0	0	100.00
IID	100	100	100	100	100	100	100	100	100	100	100	100	100	100	100	100	100	100	0	0	100.00
IIE	93.3	100	100	100	100	100	100	100	100	100	100	100	0	0	0	0	0	0	0	0	99.44
IIF	100	100	100	100	100	100	100	100	100	100	0	0	0	0	0	0	0	0	0	0	100.00
IIG	96.9	100	100	100	100	100	100	100	0	0	0	0	0	0	0	0	0	0	0	0	99.61
IIH	66.9	41.5	19	62.5	60.4	67.7	80.6	38.4	0	0	0	0	0	0	0	0	0	0	0	0	54.63
III	71.2	54.2	56.4	40.7	38.4	49.2	53.4	82	65.8	83	79.1	86.3	100	100	0	0	0	0	0	0	68.55

**Table 4.6:** Coverage for each shell with the F parameter that guarantees the best trade-off between coverage and distance.

$A_A$	$A_B$	$A_{CD}$	$A_E$	$B_A^*$	$B_B^*$	$B_C^*$	$II_A$	$II_B$	$II_C$	$II_D$	$II_E$	$II_F$	$II_G$	$II_H$	$II_I$
13	13	0/0	39	1889	1509	201	25	1	35	28	27	11	1	1	1

**Table 4.7:** List of F parameter values used.

## 4.2.4 Satellites ID code

Since we work with a very large number of satellites, it is necessary to give an identification number to each of them to refer to. Specifically, each satellite in each shell is named with an 8-digit code that contains directions for recognizing it.

For instance, we can consider the satellite "s0049.018", in which:

- "s" stands for satellite;
- "0049" identifies the plane in which the satellite orbits;
- "018" uniquely identifies the satellite in its plane.

The only exception is, once again, the shell  $A_{CD}$ . Here the satellites of the  $A_C$  shell are identified with 'c' and the satellites of the  $A_D$  shell with 'd'.

### 4.2.5 Python code

Each calculation previously explained has been implemented in a Python code. The code is available in Appendix B.

Once the various inputs, unique for each shell, have been set, all the minimum distances between satellites that occur for each  $F$  were calculated.

To do this, four nested 'for' loops were constructed. The outermost 'for' loop iterates  $F$  in its own variability interval between 0 and  $P-1$ . Then each value of  $F$  was evaluated for the characteristic orbital period of that shell with a stepsize of  $\Delta t=1$  s.

After that, for each ' $F$ ' and each ' $t$ ' the Walker constellation was constructed and the distance that occurs between each satellite ' $j$ ' and all others arranged in the ' $i$ ' planes was calculated. Finally, for each ' $F$ ' parameter, the minimum possible distance was selected so that the parameter that provides a sufficiently high minimum distance can be selected later.



## Chapter 5

# Starlink performance: evaluation techniques

Once the constellation has been appropriately defined, including the phasing, and the exact position of each satellite over the time range under consideration is known, it is possible to define and quantify some other performance aspects.

The first analyzed feature is the coverage that each shell is able to provide over time. Next, the latency of a given signal sent from one ground station to another was estimated. Further analysis was then performed to see if a stable connection (i.e., without any switches between satellites) is also the fastest connection.

However, due to the scarce available data, it was only possible to evaluate ideal cases in which the possible network congestion is not considered and the internal latency that each satellite requires in order to transmit data is not taken into account.

### 5.1 Earth - satellite communication

When the constellation is completed, it will be possible to put any point on Earth into communication. In other words, each point on Earth at any time will have a certain number of Starlink satellites to establish communication with.

So, the calculation of constellation performance starts right here: knowing how many and which satellites can communicate with a given ground station each instant. Since signal transmission can only take place within a single shell at a time, the following study will analyze each shell individually.

In order to know the number of satellites in view with a ground station, two items must be defined:

- ground station position over time;

- elevation angle;

### 5.1.1 Ground station position over time

By the time the constellation has been completed, any user with an appropriate antenna can be put in direct communication with a satellite. Choosing a random point on the Earth's surface we assume that we know latitude and longitude. However, for the analysis that will be carried out later, it is necessary to know the position of the user or ground station in Cartesian x,y,z coordinates.

For this reason, the following transformation formulas from spherical coordinates to rectangular coordinates are used:

$$\begin{cases} x = R \cdot \cos(lat) \cdot \cos(lon) \\ y = R \cdot \cos(lat) \cdot \sin(lon) \\ z = R \cdot \sin(lat) \end{cases} \quad (5.1)$$

where R is assumed to be the Earth radius.

However, it is necessary to know the position of the ground stations over time, and that is the very reason why the rotation of the Earth must be taken into account. The Earth rotates around its axis, so only the variation in longitude has to be considered while latitude remains constant over time.

Assuming that the Earth completes a full 360° revolution around its axis in 24 h, it is possible to calculate the rotation speed as:

$$\omega = \frac{360}{24 \cdot 3600} \frac{deg}{s} \quad (5.2)$$

As a consequence, before calculating Cartesian coordinates, it is necessary to know latitude and longitude as:

$$\begin{cases} lon = lon_{t=0} + (t - t_0) \cdot \omega \\ lat = lat_{t=0} \end{cases} \quad (5.3)$$

In the following analyses a  $\Delta t=1$  s will be taken and the constellation will be analyzed for 1800 s.

### 5.1.2 Elevation angle

The elevation angle is formed by the line of sight and the horizontal plane for an object above the horizon.

In the early years, users will be equipped with antennas that allow an elevation angle of 40°. Probably in the future the minimum elevation angle will become 25° so as to improve reception in fact Starlink has already submitted a request to the

FCC to lower it. In the analyses conducted in this thesis, a minimum elevation angle  $\alpha$  of  $40^\circ$  was chosen. In addition to being conservative, this choice also allows to reduce the computational time required.

Once the coordinates of the ground stations and the elevation angle are known, the calculation can be set up to allow knowledge of the satellites along line-of-sight. The view of the satellite from the ground station varies for each satellite and for each daily pass. Different views of the satellite from the ground station translate into different durations of visibility between the user and the satellite, so different durations of communication. This is common especially for LEO constellations.

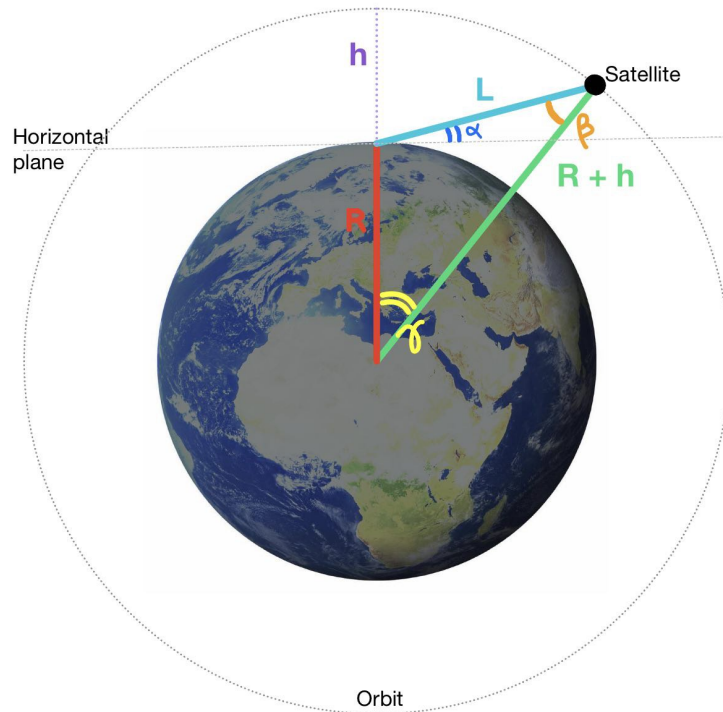


**Figure 5.1:** Necessary values to know in order to determine the satellites in view. Here  $h$  is the altitude of the orbit,  $R$  is the Earth's radius,  $L$  is the slant range and  $\alpha$  is the elevation angle.

Typically, the satellite's passage over the ground station is characterized by three specific events. The first event, known as *Acquisition of the Satellite* (AOS), occurs when the satellite establishes communication with the ground station at an elevation of the satellite equal to the minimum elevation angle. The second event occurs

when the satellite reaches maximum elevation ( $\alpha_{max}$ ). Finally, the third event, known as *Loss of the Satellite* (LOS), occurs when the satellite loses connection with the ground station and occurs at an elevation equal to the minimum elevation angle.

For the satellite passage from the AOS event to the  $\alpha_{max}$  event, the elevation increases, while from the  $\alpha_{max}$  event to the LOS event, the elevation decreases.

The higher the angle at the  $\alpha_{max}$  event, the longer the satellite path. The shorter satellite path (lower  $\alpha_{max}$ ) allows shorter communication with the ground station, and the longer satellite path (higher  $\alpha_{max}$ ) allows longer communication. Thus, the duration of communication between the satellite and the user depends on the maximum elevation  $\alpha_{max}$  from which the user sees the satellite [37].

The imaginary line between the satellite and the ground station is called *slant range* and represents the actual distance between the satellite and the ground station. Its minimum value depends on the maximum elevation  $\alpha_{max}$  of the satellite's path above the ground station. And the slant range is exactly the unknown that needs to be determined to know what the satellites within the cone of view of the user on the ground are.

With reference to Figure 5.1, the goal is to calculate the slant range  $L$ . First the law of sines referring to the triangle is applied, and then the formula is inverted to derive  $\beta$ :

$$\frac{R + h}{\sin(\alpha + 90)} = \frac{R}{\sin \beta} \quad (5.4)$$

$$\sin \beta = \frac{R}{R + h} \sin(\alpha + 90) \quad (5.5)$$

$$\beta = \arcsin \left( \frac{R}{R + h} \sin(\alpha + 90) \right) \quad (5.6)$$

and knowing that:

$$\gamma = 180 - \alpha - \beta - 90 \quad (5.7)$$

and applying Carnot's Theorem the slant range formula is obtained:

$$L = \sqrt{R^2 + (R + h)^2 - 2R(R + h) \cos \gamma} \quad (5.8)$$

The slant range  $L$  represents the maximum distance that can be established between satellite and ground station in order to have communication. As a consequence, in order to know how many and which satellites are in communication with the selected ground station, it is sufficient to calculate the distance between the satellite and the ground station and verify that it is lower than the slant range.

$$distance = \sqrt{(x_s - x_{gs})^2 + (y_s - y_{gs})^2 + (z_s - z_{gs})^2} \quad (5.9)$$

where the subscript 'gs' stands for ground station while the subscript 's' stands for satellite.

So, for each instant of time, the distance between each individual satellite of each individual shell and the ground station has been calculated, and if this distance is lower than the slant range we are sure that communication can take place.

### 5.1.3 Python code

All the calculations seen so far have been implemented in a Python code that can be found in Appendix B.

The code takes as input:

- the coordinates (longitude, latitude, R) of the ground stations;
- the minimum elevation angle;
- the Cartesian coordinates of the satellites in each shell and for each time instant (taken from the first code).

The code returns, as a result, the number of satellites and the identifier of each satellite that can establish a connection with Earth. For large shells this code takes quite a long time to execute. Thus, in order to make the code faster, only satellites that are within a certain range of latitude and longitude dictated by the reference ground station were analyzed.

This code, slightly revised, has also been used for coverage calculations.

## 5.2 Communication link between two cities

A very interesting aspect of evaluating is how data transmission between any two points on the globe occurs. Since the transmission using Starlink is convenient, compared to fiber, only if the distance between ground stations exceeds 3000 km [1], the following cities were selected as reference ground stations:

- **Torino** will be the transmitting ground station from which communications for other cities will start;
- **San Francisco** will be a receiving ground station. It has been chosen because it is at a similar latitude to Torino but at different longitudes;
- **Cape Town** will be a receiving ground station. It has been chosen because it is at a similar longitude to Torino but at different latitude;
- **Buenos Aires** will be a receiving ground station. It has been chosen because it is at a different longitude and latitude from Torino.

So three paths "Torino-San Francisco", "Torino-Cape Town" and "Torino-Buenos Aires" will be established. These are correspondingly "horizontal", "vertical" and "diagonal" paths and will be analyzed to understand how each shell manages to connect these cities. Also for this analysis, each shell was studied individually for a time of 1800 s and a stepsize of  $\Delta t=1$  s.

First, to see if the connection between the selected cities is possible, it was necessary to make sure that both cities have satellites in view at the same instant of time. Only when this has been assured the latency calculation can continue.

### 5.2.1 Constraints in satellites communication

In the scenario under consideration, the range of LISLs is limited only by visibility so each satellite is able to communicate with any other satellite in line-of-sight. However, it must be taken into account that the lowest atmospheric layer without water vapor begins about 80 km above the Earth's surface [51].

The maximum range of LISLs for a LEO satellite operating at a given altitude  $h$  can be easily calculated using:

$$x = 2 \cdot \sqrt{(R + h)^2 - (R + z)^2} \quad (5.10)$$

where  $R$  is the radius of the Earth,  $h$  is the altitude of the satellite and  $z$  is the height of the atmospheric layer above the Earth's surface.  $x$  is the maximum range of the LISL and assuming we are on the shell  $A_E$  with  $h = 550$  km we obtain  $x = 5,016$  km.

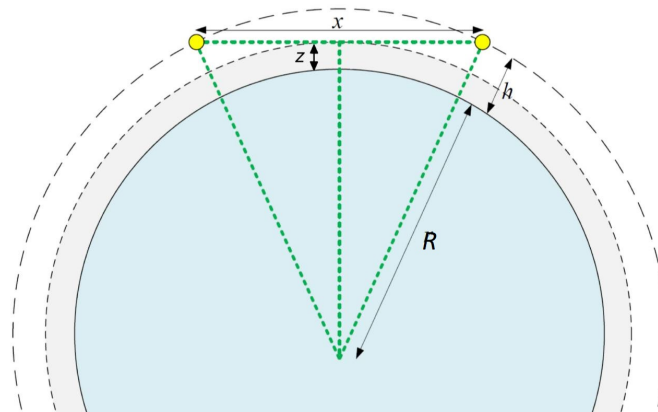


**Figure 5.2:** Geometry for maximum inter-satellite distance calculation. In this figure, the Earth is shown in blue, the atmospheric layer in gray and the satellites in yellow [51].

The higher the shell, the greater the range and the more connections will be available.

### 5.2.2 Dijkstra algorithm

Assuming we want to connect two cities using the network of satellites provided by each shell, it is easy to imagine the large number of possible paths the signal can travel. It is typically a very large number that can involve even so many satellites. However, for satellite communication to be used, it is desirable to select, among all possible paths, the one that provides the lowest latency or, in other words, the shortest path (since time and space are directly proportional at the same speed  $c$ ). It is right here that Dijkstra's algorithm comes to our aid [52].

Dijkstra's algorithm leverages graph theory to find the shortest paths between nodes. Specifically, a graph is defined as a set of elements called nodes that can be connected to each other by lines called edges which are given a certain weight.

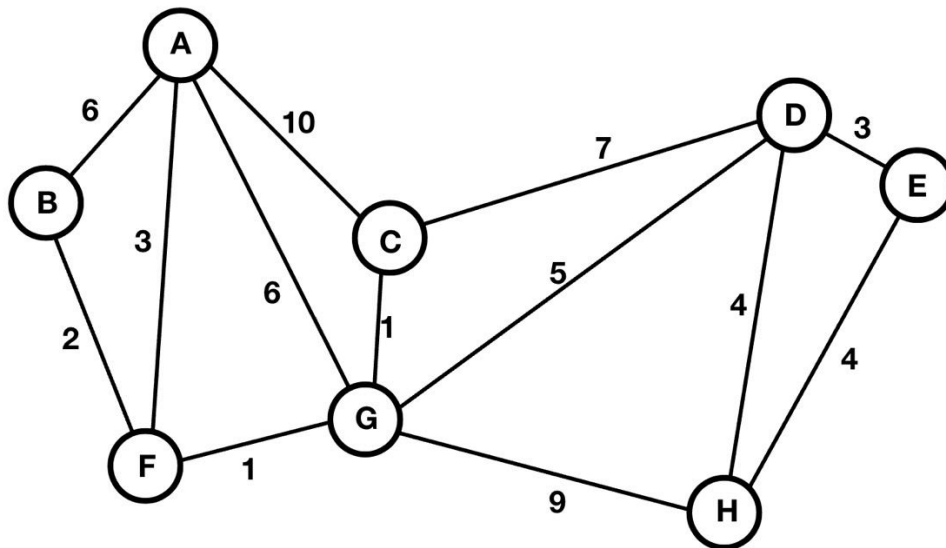


**Figure 5.3:** Example of a graph representation.

Thus, the network of satellites identified by each shell will be represented as a graph in which:

- each satellite is represented as a node;
- each connection between satellites is represented as an edge;
- each edge has an associated value that represents the distance between satellites.

Once the graph is represented, the algorithm can be applied as follows:

1. the starting satellite is chosen;
2. the distances between the starting satellite and all other satellites are set to infinity, except for the distance between the starting satellite and itself, which is set to 0.

After that, the following steps are performed iteratively:

3. node with the smallest value is chosen as the "current node" and all its neighbor nodes are visited. When these are visited, its provisional distance from the starting node is updated;
4. once visited all of the current node's neighbors and update their distances it is possible to mark the current node as "visited". Marking a node as "visited" means that its final cost has been determined;
5. go back to step one. The algorithm loops until it visits all the nodes in the graph.

In our application of the algorithm, the starting node and ending node are chosen according to which satellites are in view with the transmitting and receiving ground stations correspondingly. Under the assumption that each satellite can communicate with every other satellite along the line-of-sight, the weight of each bridge is determined by calculating the distance between them in space. In the end, the algorithm returns, for each time instant,  $m \cdot n$  best paths, where  $m$  is the number of satellites in view with the transmitting ground station and  $n$  is the number of satellites in view with the receiving ground station.

For example, if we analyze the  $A_E$  shell in the path Torino - San Francisco at time  $t=0$ , a given signal can travel 20 possible best paths since there are 4 satellites in line of sight with Torino and 5 satellites in line of sight with San Francisco. Each of them will be characterized by its own length (given by the sum of the segments: initial ground station-satellite(n1) + satellite(n1)-satellite(n2) + ... + satellite(i)-satellite(i+1) + satellite(i+1)-final ground station) and an ideal latency. As can be seen in Figures 5.4 and 5.5 the various paths have different lengths and thus latency times. In order not to idealize our model too much and to be able to simplify it computationally, the average latency will be taken as the reference for subsequent analyses.

### 5.2.3 Python code

In order to determine the average latency that each signal takes to be transmitted from one ground station to another along the best path, Dijkstra's algorithm was implemented in Python. The code can be found in Appendix B.

This code is closely related to the first two as it takes as input all previously

```

The shortest path in time t= 0.0 s between s0048.005 and s0018.022 is 11318.29 km long:
s0048.005 --> s0053.022 --> s0037.009 --> s0018.022
total length: 12759.88 km
total time: 42.56 ms

The shortest path in time t= 0.0 s between s0048.005 and s0021.020 is 10375.39 km long:
s0048.005 --> s0052.001 --> s0036.010 --> s0021.020
total length: 11816.98 km
total time: 39.42 ms

[...]

The shortest path in time t= 0.0 s between s0065.014 and s0042.004 is 9881.28 km long:
s0065.014 --> s0053.022 --> s0037.009 --> s0042.004
total length: 11322.87 km
total time: 37.77 ms

The shortest path in time t= 0.0 s between s0065.014 and s0043.003 is 10433.75 km long:
s0065.014 --> s0056.020 --> s0040.007 --> s0043.003
total length: 11875.34 km
total time: 39.61 ms

Time=0.0s      max:42.56ms   min:37.31ms   average:39.66ms

```

**Figure 5.4:** Output of the code: best possible paths between the two ground stations.

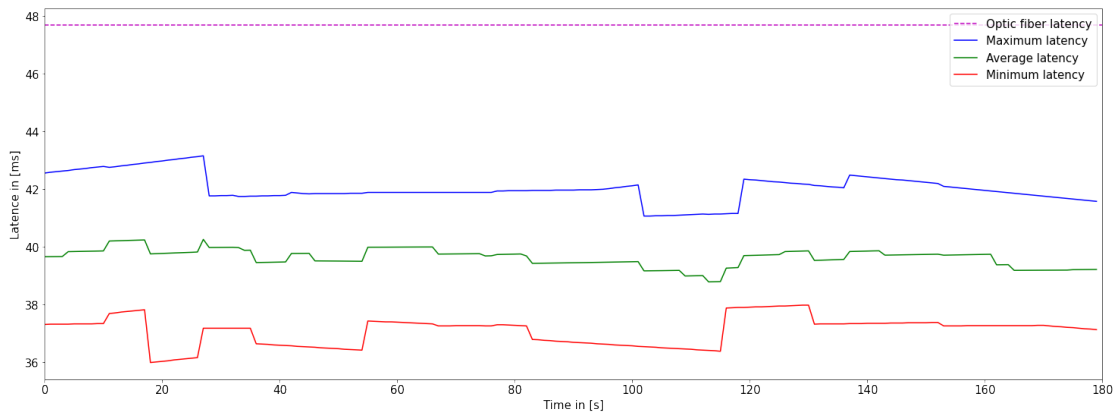


**Figure 5.5:** The figure shows, over a 3 minute range, the communication between Torino and San Francisco through the  $A_E$  shell. Among all the possible paths that may be established over time, those characterized by maximum latency and minimum latency have been shown. Average latency will later be considered as a reference.

calculated information. Once the two ground stations are known and it is known which satellites are in view of them, the code analyzes all the possible best paths there may be and returns as a final value the average latency calculated for each time instant. However, a serious problem related to this code concerns the computational

time required, which is excessive. Therefore, it has been necessary to find a solution that would make feasible the analysis of the most numerous shells. With no effect on the final result, the code has been modified to limit, for each time instant, the area in which possible paths can exist. For example, whereas with the initial code Dijkstra's algorithm analyzed all possible paths, with this modification only the paths considered promising are analyzed. The choice of the area within which to restrict the search for the best path is dictated by the coordinates of the ground stations. Figure 5.6 better captures the idea:



**Figure 5.6:** Analysis of the route between Torino and San Francisco: on the left is the area considered in the original code; on the right is the area considered in the modified code.

This modification greatly reduces computational time and yields identical results. A demonstration is provided by the following graphs, where the simulation was run for a time range of 100 s.

The change made to the algorithm, for the same results, leads to a substantial reduction in code execution time:

- Torino - San Francisco per 100 s through the  $A_A$  shell: the original code takes 1 h 11 min while the modified code takes 9 min (788% improvement);
- Torino - Cape Town per 100 s through the  $B_A$  shell: the original code takes 2 h 1 min while the modified code takes 18 min (672% improvement);
- Torino - San Francisco per 100 s through the  $II_A$  shell: the original code takes 7 h 58 min while the modified code takes 1 h 2 min (770% improvement);

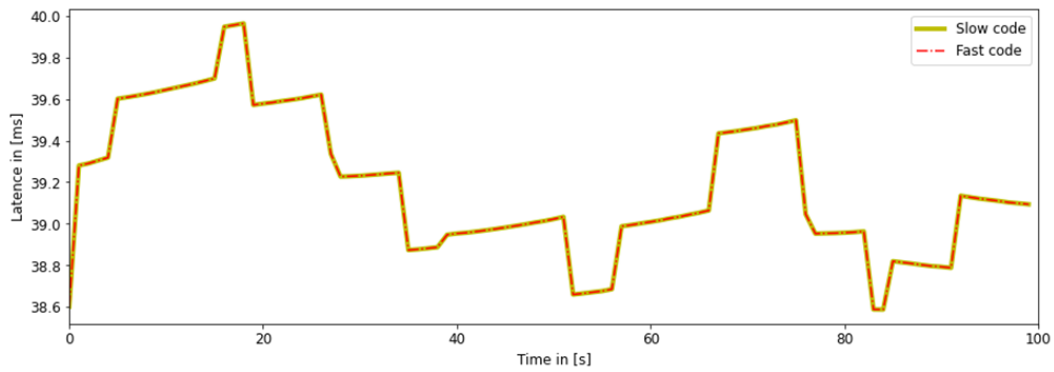


Figure 5.7: Latency for the Torino - San Francisco path, with two codes

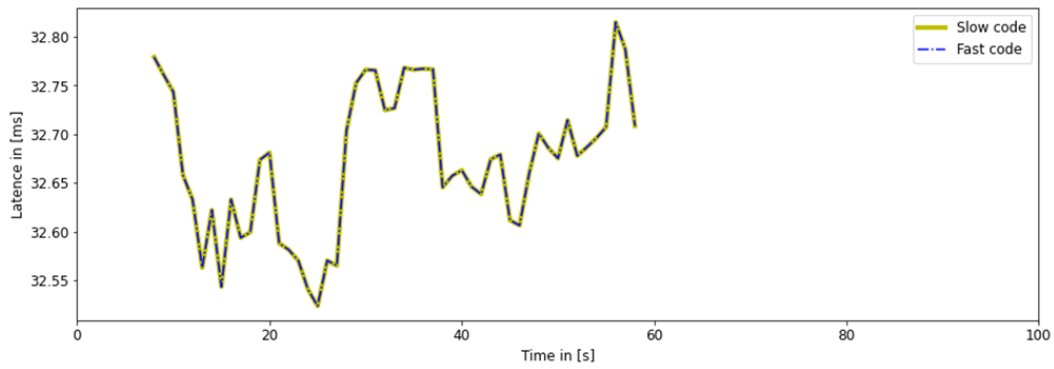


Figure 5.8: Latency for the Torino - Cape Town path, with two codes

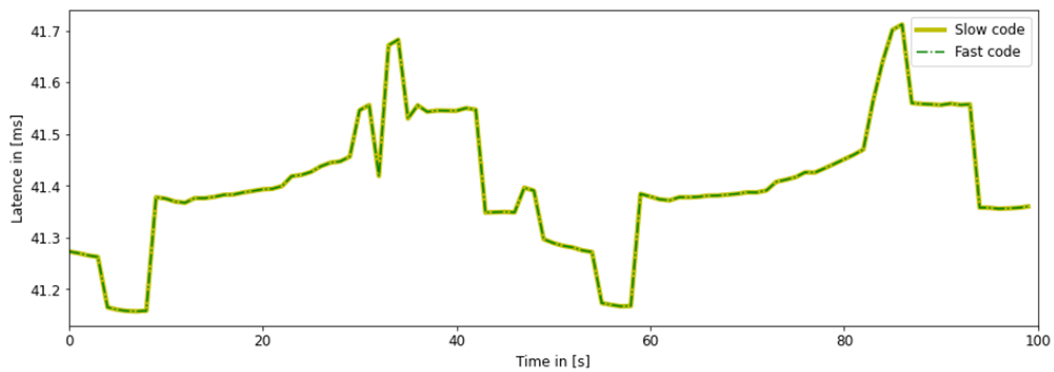


Figure 5.9: Latency for the Torino - Buenos Aires path, with two codes

## 5.3 Connection stability

Another important aspect in determining the best path between satellites and thus the best shell for each couple of cities is the number of satellites involved in the link from the first ground station to the last. Obviously, if the shell under analysis allows it, it is best to use as few satellites as possible to make communication faster. With the data in our hands, it is impossible to make an accurate estimate since all the information concerning the on-board instruments, the used protocols and the operations of the transceivers are unknown. However, it is reasonable to assume that the fewer satellites involved, the less latency will be accumulated on the path. It is also important to study how long the communication established between the two ground stations involves the exact same satellites. Indeed, for long data transmissions it will be more advantageous to use a shell that does not make any switches between satellites. Given the small amount of data of the real constellation, again, it is impossible to make a precise estimate, but it is reasonable to assume that establishing a new connection between the satellites will cause latency to accumulate over the path.

These further evaluations help us to understand better how the constellation works and are to be done in the design phase to choose the best path.

This thesis intends to analyze in-depth how the Starlink constellation works; therefore, the code written, which implements Dijkstra's algorithm calculates for each time instant all possible combinations of paths and evaluates their effectiveness. Each of these paths could involve different satellites and different number of satellites and, therefore, may be faster or slower than others.

A comprehensive assessment that allows us to state which and how many paths are needed to ensure the best link between two cities involves studying all shells individually by analyzing each of all possible paths established over time. Such a work would be too onerous to accomplish and would require too much computational time. For this reason, as shown in the next chapter, only the instant  $t = 300s$  for shell  $A_A$  of the communication between Torino and San Francisco has been analyzed.

This chapter has shown the various tools that have been created to calculate constellation characteristics. Once the F parameter was calculated and the minimum elevation angle was selected, four cities scattered around the world were considered and simulations were carried out by putting them in communication. The data that SpaceX has made public allows us to get interesting results on coverage, latency and connection stability.

## Chapter 6

# Starlink performance: results

After thoroughly describing the procedures that have been used and the tools that have been created to know what the potential of the constellation is, this chapter will show all the results obtained and appropriately commented. So, in the same order as in the previous chapter, the results inherent in coverage, latency and switches will be shown and commented below. All the limitations highlighted in the previous chapters due to the limited computational power and small amount of data are then reflected in the shown final results.

### 6.1 Coverage

One of the primary goals of the Starlink constellation is to connect the entire globe by providing broadband Internet. Once the best F parameter ensuring the best trade-off between coverage and collision avoidance was determined for each shell, it was possible to propagate the orbits and then quantify the features about them. Table 4.6 presented in Chapter 4 describes for all shells, except  $B_A$ ,  $B_B$  and  $B_C$ , the ideal coverage they provide at different latitudes.

While at low latitudes satellites are obliged to orbit even if they do not guarantee global coverage, for high latitudes coverage depends on the inclination of the shells. So only a few shells guarantee good coverage at high latitudes. An example is given in Table 6.1 which describes the coverage of the settlements with higher latitudes and the number of satellites in view every second for 30 minutes.

All the available tables show how Starlink's goal of covering the entire globe has been met. In addition, it is interesting to see how the distribution of satellites by latitude belts is directly proportional to population density. In fact, if Table 4.6 and Figure 6.1 are compared, it can be seen that the areas at latitudes below

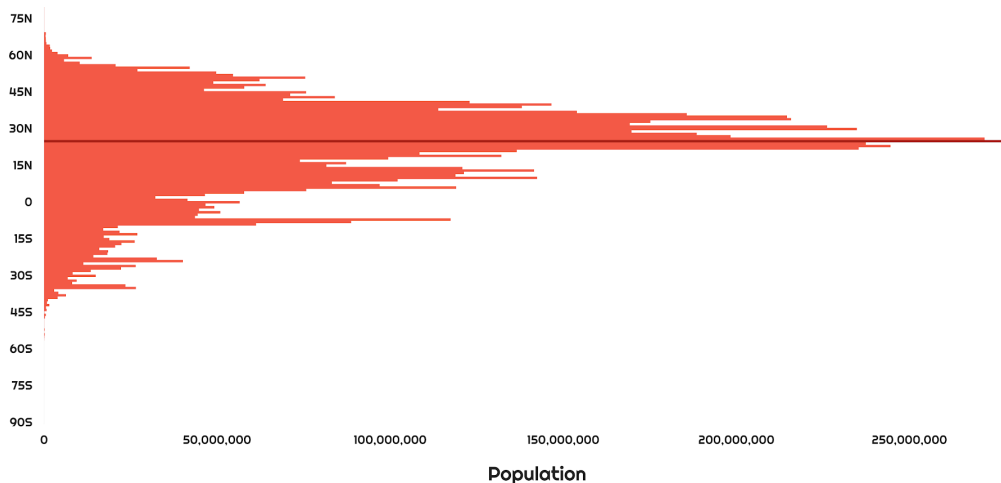


**Figure 6.1:** Population density per latitude [53].

$45^\circ$  are the most populated and those over which all shells guarantee coverage. However, it can be seen that some shells, like  $A_B$ ,  $A_{CD}$ ,  $II_D$  and  $II_I$ , seem to have been specifically designed for high-latitude areas. In fact they provide full coverage with many satellites in view only for high latitudes while for low latitudes they provide partial coverage.

Only the  $A_{CD}$  and  $II_D$  shells, being the ones with the highest inclination (correspondingly  $97.6^\circ$  and  $96.9^\circ$ ), are able to cover the polar areas ensuring full coverage and many satellites in line of sight every second. So, even though these areas are mostly uninhabited, they may still be enabled for Internet reception. As a result, exploration of these lands and research can be encouraged.

While the  $II_D$  shell enables communication with every point on the globe (providing full coverage at every latitude), the  $A_{CD}$  shell is designed specifically to connect areas at high latitudes. However, the shell, when unable to communicate directly, can use ground stations as relay and then other shells to be able to ensure a connection with areas at lower latitudes.

The peak in population density occurs for latitudes of about  $30^\circ$ . It is plausible that the shells with lower inclination were designed for this purpose. In fact, each shell guarantees maximum coverage, with the greatest number of satellites in view, when satellites orbit at the highest latitudes that shell can guarantee.

## 6.2 Latency

One of the most important reasons why Starlink has been developed is to connect people around the world quickly while trying to minimize the effect of latency. By adopting all the techniques and tools presented in the previous chapter, it has been

	Ushuaia (ARGENTINA)		Reykjavik (ICELAND)		McMurdo Station (Antarctica)		Longyearbyen (Norway)		Alert (CANADA)	
	Latitude	Longitude	Latitude	Longitude	Latitude	Longitude	Latitude	Longitude	Latitude	Longitude
	-54.801912	-68.302951	64.145981	-21.9422367	-77.841878	166.686345	79.004959	17.666016	82.508453	-62.410526
	%	n of sats	%	n of sats	%	n of sats	%	n of sats	%	n of sats
AA	100%	3(10s) 4(99s) 5(397s) 6(1037s) 7(220s) 8(39s)	0		0		0		0	
AB	99.34%	1(312s) 2(807s) 3(376s) 4(205s)	100%	2(3s) 3(569s) 4(728s) 5(355s) 6(147s)	0		0		0	
ACD	80.80%	1 (11007s) 2 (4448s)	100%	2(589s) 3(185s) 4(992s) 5(34s)	100%	5(12s) 6(596s) 7(784s) 8(282s) 9(49s) 10(9s) 11(30s) 12(31s) 13(7s)	100%	5(579s) 6(604s) 7(295s) 8(221s) 9(61s) 10(11s) 11(6s) 12(23s)	100%	5(39s) 6(1295s) 7(365s) 8(59s) 9(42s)
AE	100%	3(9s) 4(193s) 5(504s) 6(741s) 7(355s)	0		0		0		0	
BA	0%		0		0		0		0	
BB	0%		0		0		0		0	
BC	100%	3(628s) 4(1112s) 5(62s)	0		0		0		0	
IIA	100%	4(16s) 5(130s) 6(198s) 7(495s) 8(813s) 9(150s)	0		0		0		0	
IIB	0%		0		0		0		0	
IIC	0%		0		0		0		0	
IID	100%	2(4s) 3(744s) 4(871s) 5(183s)	100%	4(134s) 5(985s) 6(611s) 7(72s)	100%	10(67s) 11(226s) 12(448s) 13(410s) 14(352s) 15(219s) 16(80s)	100%	13(26s) 14(298s) 15(362s) 16(463s) 17(445s) 18(172s) 19(36s)	100%	21(609) 22(824) 23(362) 24(6)
IIE	100%	9(6s) 10(298s) 11(730s) 12(690s) 13(75s) 14(3s)	0		0		0		0	
IIF	0%		0		0		0		0	
IIG	0%		0		0		0		0	
IIH	0%		0		0		0		0	
III	84.35%	1(639s) 2(825s) 3(56s)	100%	1(452s) 2(776s) 3(574s)	0		0		0	

**Table 6.1:** Coverage of the higher latitudes settlements on Earth and the number of satellites in view every second for 30 minutes.

possible to evaluate the latency that occurs for the different paths.

Several methods could be used for accurate latency estimation however, due to the lack of information regarding the traffic data, none of them could be considered to be more or less correct than the others. For this reason, the value obtained from the average of the latencies of all the possible  $m \cdot n$  (where  $m$  is the number of satellites in view of the transmitting station and  $n$  is the number of satellites in view of the receiving station) best paths that can be established at a specific time instant was selected as the reference latency for that time instant.

This method was chosen to try to make the problem more realistic: it is like accounting for possible network congestion in which for each instant of time there are  $m \cdot n$  possible paths (with in principle  $m$  and  $n$  varying every second).

It should be emphasized that this is merely an assumption to avoid oversimplifying the problem. In particular, the number of signals to be sent from one specific ground station to another is not known in advance and in a real case the same satellite could not be involved in transceiving (either receiver or transmitter) more than four signals at a time.

Below, communications between Torino and San Francisco, Cape Town and Buenos Aires will be analyzed and the performance of the various shells will be compared.

### 6.2.1 Torino - San Francisco

The cities are at similar latitudes, so the path each signal must take from one station to another is assumed to travel "horizontally" and involve several satellites from different orbital planes, and that is exactly what happens.

However, as shown in Figure 6.2, each shell behaves differently from the others based on its own characteristics.

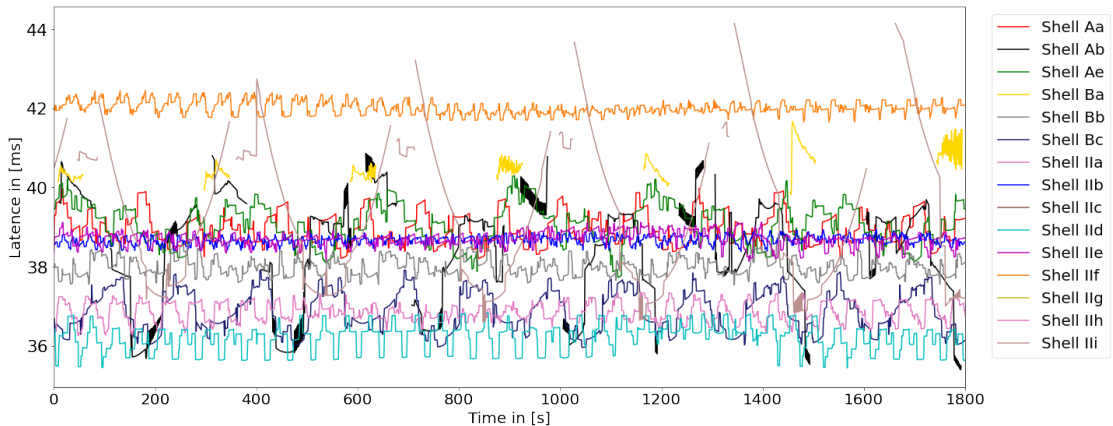


**Figure 6.2:** Average latency of the  $m \cdot n$  best paths for each instant of time over 1800 s between Torino and San Francisco.

It can be seen immediately that the connection between the two cities over the 30 minutes is always guaranteed even though not all shells ensure a continuous connection (look at Table 6.2). It can also be seen in Figure 6.5 that in all cases the satellite connection is more advantageous than the fiber connection, in fact, all the graphs are below the dashed line that symbolizes the ideal latency (since the cable length is assumed to be equal to the spherical distance of the two cities) of the signal assuming that it travels in fiber cables.

Shell	Connection [%]
Shell $A_A$	100
Shell $A_B$	77.89
Shell $A_{CD}$	60.39
Shell $A_E$	100
Shell $B_A$	19.83
Shell $B_B$	100
Shell $B_C$	100
Shell $II_A$	100
Shell $II_B$	100
Shell $II_C$	0
Shell $II_D$	100
Shell $II_E$	100
Shell $II_F$	100
Shell $II_G$	0
Shell $II_H$	0
Shell $II_I$	91.11

**Table 6.2:** Percentage of coverage guaranteed over 1800 s.

Taking a look at Table 6.2 it can be observed that for shells  $II_C$ ,  $II_G$  and  $II_H$  it is impossible to connect the two cities. These are in fact shells that have the inclination too low ( $38^\circ$ ,  $33^\circ$  and  $148^\circ$ ) and as a result there are no satellites in line of sight with the ground stations.

The behavior of the  $B_A$  shell, on the other hand, turns out to be a bit anomalous. In fact, sifting through the data we can see that it guarantees partial coverage of Torino. The fact that creates some suspicion is that shell  $II_F$ , which has an inclination of just one degree higher, guarantees a 100% connection. However, the reason might be that shell  $B_A$  is among those for which the optimal F parameter could not be calculated because of CPU time limitations.

Another aspect that immediately jumps out is that the densest shells provide a latency value with fluctuations in the range of 2 ms while other shells such as  $A_{CD}$  (Figure 6.5) and  $II_I$ , consisting of 520 and 324 satellites correspondingly, have very

unstable latency values that vary even by 30 ms. The reason for this is that, since there are few satellites that can be involved, they may be in inconvenient positions so the path is not so linear.

Special attention is owed to shells  $A_A$  and  $A_E$  which behave in exactly the same way; in fact they present identical orbital characteristics. The average latency value settles on a similar value and sometimes it seems that the trends of the latencies are complementary; in fact the peak of one corresponds to the valley of the other. Similar behavior can be observed for shells  $II_B$  and  $II_E$  despite the fact that they have different orbital characteristics.

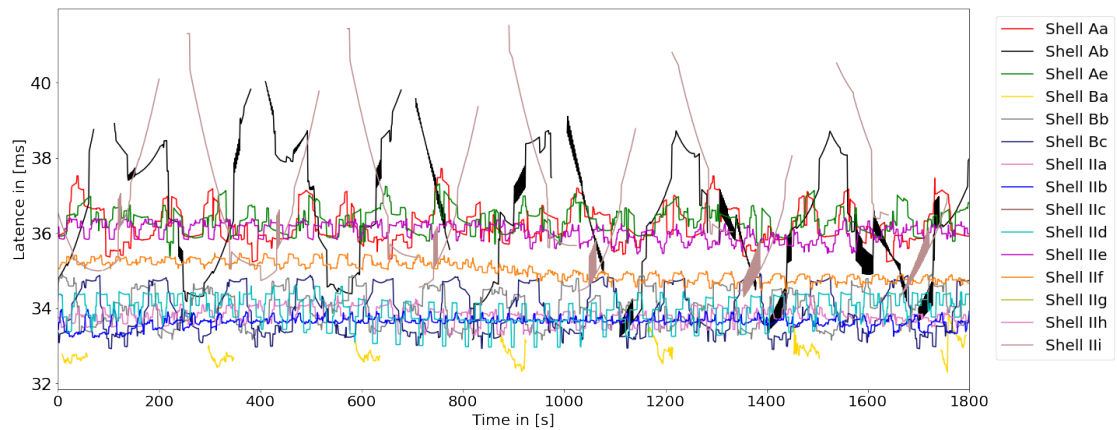
Overall, the shells that perform best in terms of latency are  $II_D$  whose average latency over 1800 s is 36.21 ms and  $II_A$  whose average latency is 36.86 ms. So, although it is useful to have redundancies and more shells to use, in this case it can be seen how the goal of fast connection can be achieved even with shells that have fewer than 5280 satellites.

Figure 6.5 shows in more detail the graphs for each group of shells in the path Torino - San Francisco.

## 6.2.2 Torino - Cape Town

These cities are located at similar longitudes so the path each signal must take from one station to another is assumed to travel "vertically" and involves several satellites that may also belong to the same orbital plane, and this is exactly what happens.

However, as Figure 6.3 shows, each shell behaves differently from the others based on its own characteristics.



**Figure 6.3:** Average latency of the  $m \cdot n$  best paths for each instant of time over 1800 s between Torino and Cape Town.

Also in this case it is immediately noticeable that the connection between the two cities over the 30 minute period is always guaranteed, although not all shells ensure a continuous connection (see Table 6.3). It can also be seen in Figure 6.6 that in all cases, except the shell  $A_{CD}$  that sometimes is not convenient, the satellite connection is more advantageous than the fiber connection; in fact, all the graphs are below the dashed line that symbolizes the ideal latency of the signal under the assumption that it travels by fiber.

Shell	Connection [%]
Shell $A_A$	100
Shell $A_B$	85
Shell $A_{CD}$	82.11
Shell $A_E$	100
Shell $B_A$	19.83
Shell $B_B$	100
Shell $B_C$	100
Shell $II_A$	100
Shell $II_B$	100
Shell $II_C$	0
Shell $II_D$	100
Shell $II_E$	100
Shell $II_F$	100
Shell $II_G$	0
Shell $II_H$	0
Shell $II_I$	77.33

**Table 6.3:** Percentage of coverage guaranteed over 1800 s.

Taking a look at Table 6.3 it can be observed that for shells  $II_C$ ,  $II_G$  and  $II_H$  it is impossible to connect the two cities. These are in fact shells that have a very low inclination and as a result there are no satellites in line of sight with the ground stations.

The behavior of  $B_A$  immediately jumps out, which among all the shells seems to be the one that guarantees the minimum latency of about 33 ms. However, it does not guarantee a full connection because it does not guarantee continuous coverage on Turin, and the reason may be that the F parameter of that shell was unable to be calculated accurately due to CPU time issues.

The shells  $B_B$  and  $B_C$  are among those that provide lower latencies and it is interesting to note that they have a complementary pattern because an increasing oscillation of one corresponds to a decreasing oscillation of the other and vice versa. Also on this path, it is further noticeable how, unlike the more crowded shells that

provide latency oscillations lower than 2 ms, the less dense shells  $A_B$  and  $II_I$  cause latency oscillations of about 6-7 ms. Once again the reason may be related to the low number of satellites that may be involved in communication; in fact they may be in awkward positions and thus the path is not so linear.

Overall, the shells that provide better performance with latencies of about 34 ms are  $B_B$ ,  $B_C$ ,  $II_A$ ,  $II_B$ , and  $II_D$ .

Shell	# of sats.	Latency [ms]
Shell $B_B$	2493	34.02
Shell $B_C$	2547	33.91
Shell $II_A$	5280	33.78
Shell $II_B$	5280	33.63
Shell $II_D$	3600	33.96

**Table 6.4:** Comparison of best performing shells in terms of number of satellites and average latency.

This allows for another reflection on the number of satellites in the shells and the average latency along the path. In fact as can be seen in Table 6.4 there is no great latency advantage in using shells that have more than 2,600 satellites.

Figure 6.6 shows in more detail the graphs for each group of shells for the path Torino - Cape Town.

### 6.2.3 Torino - Buenos Aires

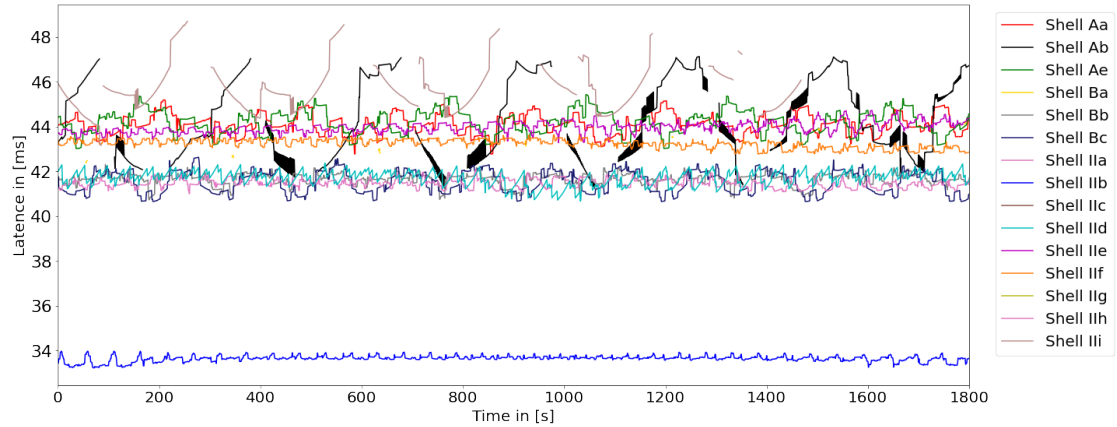


**Figure 6.4:** Average latency of the  $m \cdot n$  best paths for each instant of time over 1800 s between Torino and Buenos Aires.

These two cities are located at different latitudes and longitudes, so it is assumed

that the path each signal must take from one station to another travels "diagonally" and involves several satellites that may even belong to the same orbital plane, and this is exactly what happens.

However, as Figure 6.4 shows, each shell behaves differently from the others based on its own characteristics.

Also in this case it is immediately noticeable that the connection between the two cities over the 30 minute period is always guaranteed, although not all shells ensure a continuous connection (see Table 6.5). It can also be seen in Figure 6.7 that in all cases the satellite connection is more advantageous than the fiber connection; in fact, all the graphs are below the dashed line that symbolizes the ideal latency of the signal under the assumption that it travels by fiber.

Shell	Connection [%]
Shell $A_A$	100
Shell $A_B$	78.83
Shell $A_{CD}$	0
Shell $A_E$	100
Shell $B_A$	1.39
Shell $B_B$	100
Shell $B_C$	100
Shell $II_A$	100
Shell $II_B$	100
Shell $II_C$	0
Shell $II_D$	100
Shell $II_E$	100
Shell $II_F$	100
Shell $II_G$	0
Shell $II_H$	0
Shell $II_I$	62.67

**Table 6.5:** Percentage of coverage guaranteed over 1800 s.

In this case, the shells that do not allow communication between cities are  $A_{CD}$ ,  $II_C$ ,  $II_G$  and  $II_H$  while the  $B_A$  shell guarantees communication for only a few seconds and again the unusual behavior can be attributed to an incorrect estimation of the F parameter, again due to CPU time limitations.

In this path, although there is still a difference on latency stability between dense and less dense shells, it is less marked.

Also in this case, it is possible to recognize groups of shells that, although characterized by different orbital parameters, have the same average latency. In particular, shells  $B_B$ ,  $B_C$ ,  $II_D$  and  $II_A$  are characterized by an average latency of about 41.5

ms, shells  $II_F$  and  $II_E$  are characterized by average latencies of about 43.5 ms, and shells  $A_E$  and  $A_A$  are characterized by average latencies of about 44 ms. Again, therefore, it can be seen that the same result in terms of latency can be obtained with shells characterized by a moderate number of satellites. However, the shell  $II_B$ , composed of 5280 satellites, stands out because it provides significantly lower latency values and certainly the large number of satellites contributes positively to its performance in terms of average latency and stability.

Figure 6.7 shows in more detail the graphs for each group of shells in the path Torino - Buenos Aires.

Only three small examples out of an infinite number of cases that might actually be there have been given, but it is clear from the results just analyzed that each shell has its own characteristics that are different from those of other shells. Very important for a shell to work properly is the path that the signal must follow in terms of both length and orientation. In fact, the results obtained have shown how the orientation of the path affects latency times.

In general, it can be established that denser shells (>1584 satellites) have significantly higher functionalities than less populated ones. But it is important to point out how the benefits in terms of average latency for shells composed of 5280 satellites are sometimes less than for less populated shells, and so it may raise the question of the utility of such dense shells again.

While great efficiency is noted in using dense shells to connect very distant cities, less dense shells will most likely have greater utility in the case of more near-by cities. It is also noticeable that they are also those characterized by greater inclination, consequently providing good coverage only at very high latitudes. Furthermore, in order to link cities at high latitudes with cities at low latitudes, they could use the help of some ground stations.

Shells characterized by very low inclination, on the other hand, will be useful in connecting cities closer to the equator.

## 6.2 – Latency

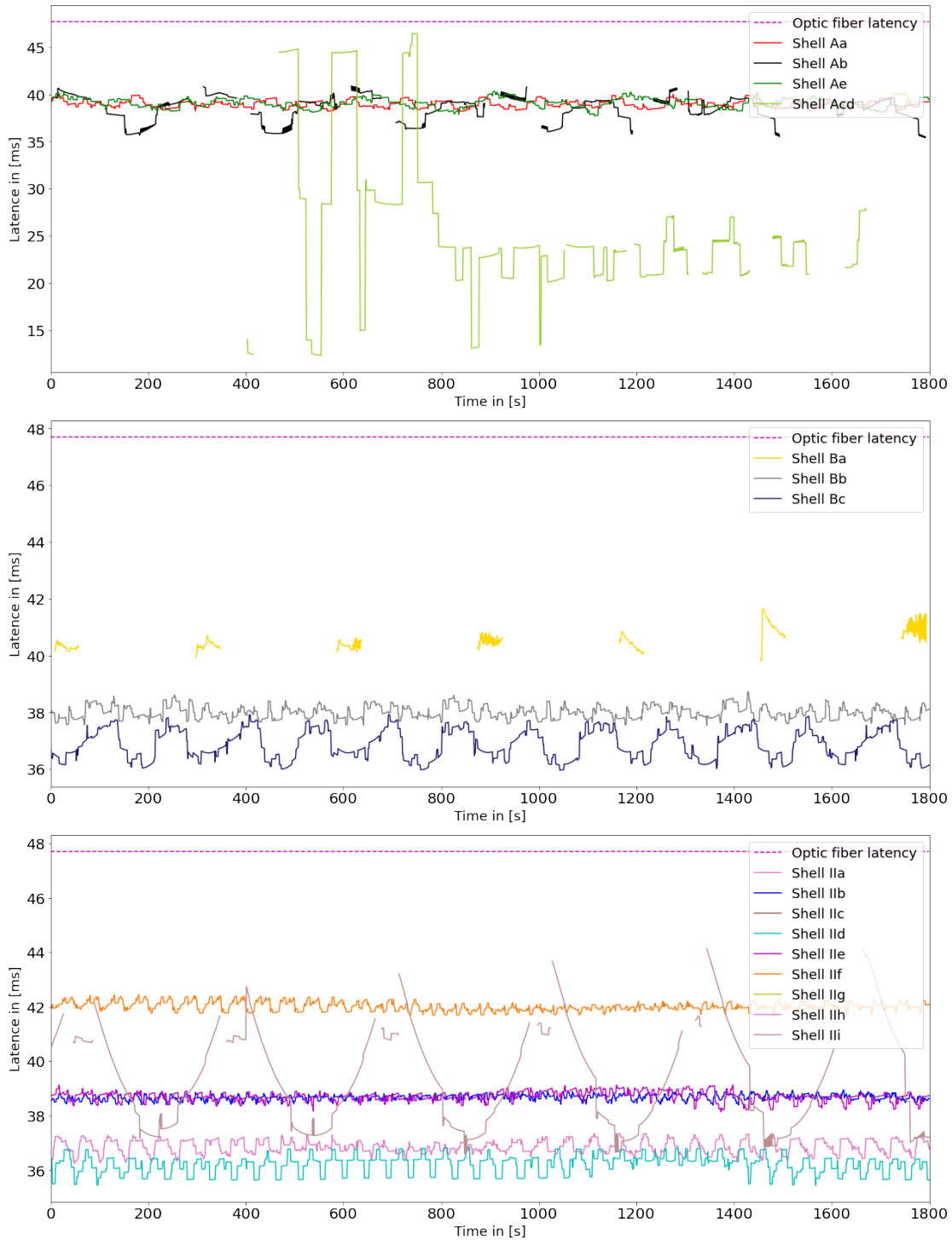


**Figure 6.5:** Average latency of the  $m \cdot n$  best paths between **Torino** and **San Francisco** for each instant of time.

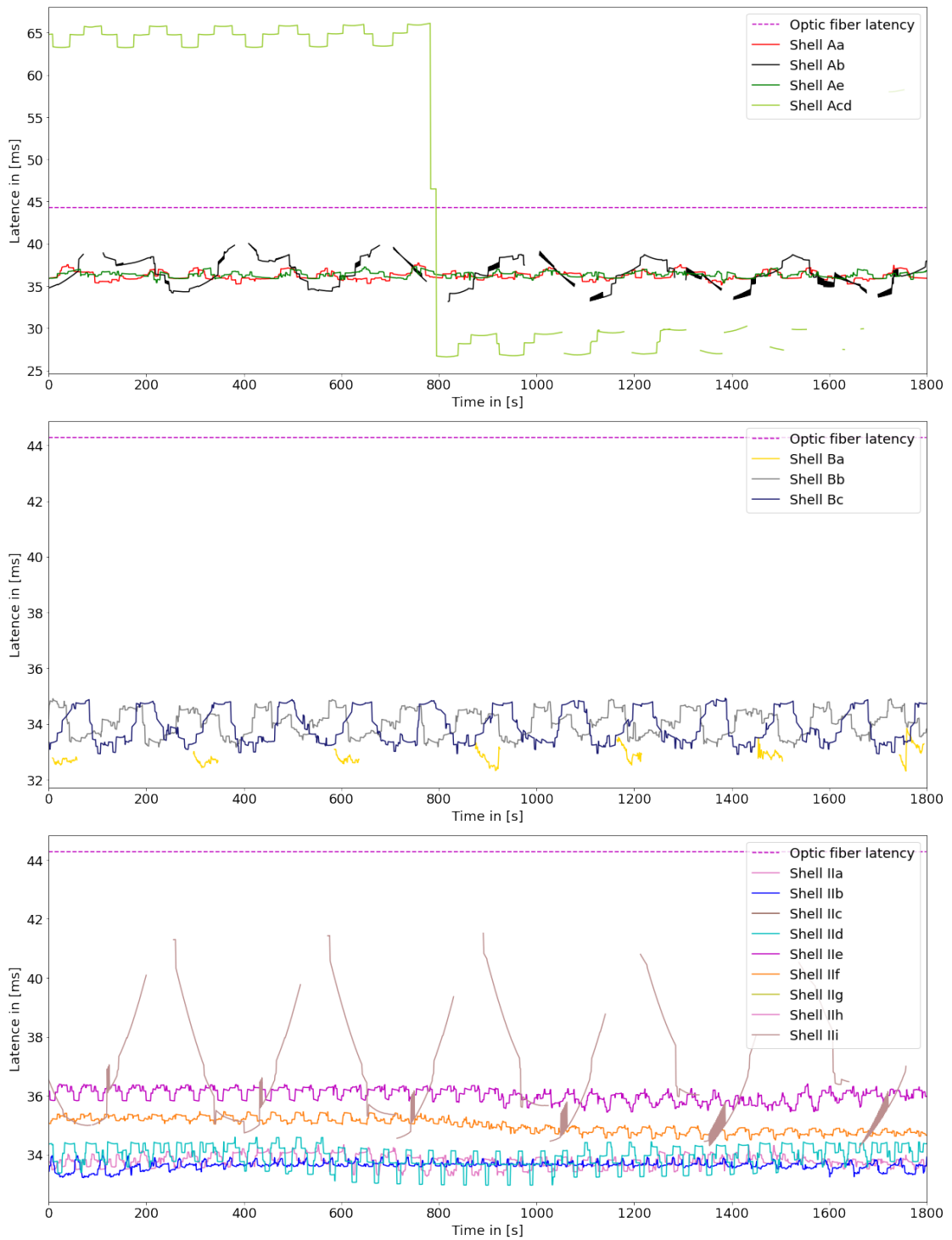


**Figure 6.6:** Average latency of the  $m \cdot n$  best paths between **Torino** and **Cape Town** for each instant of time.

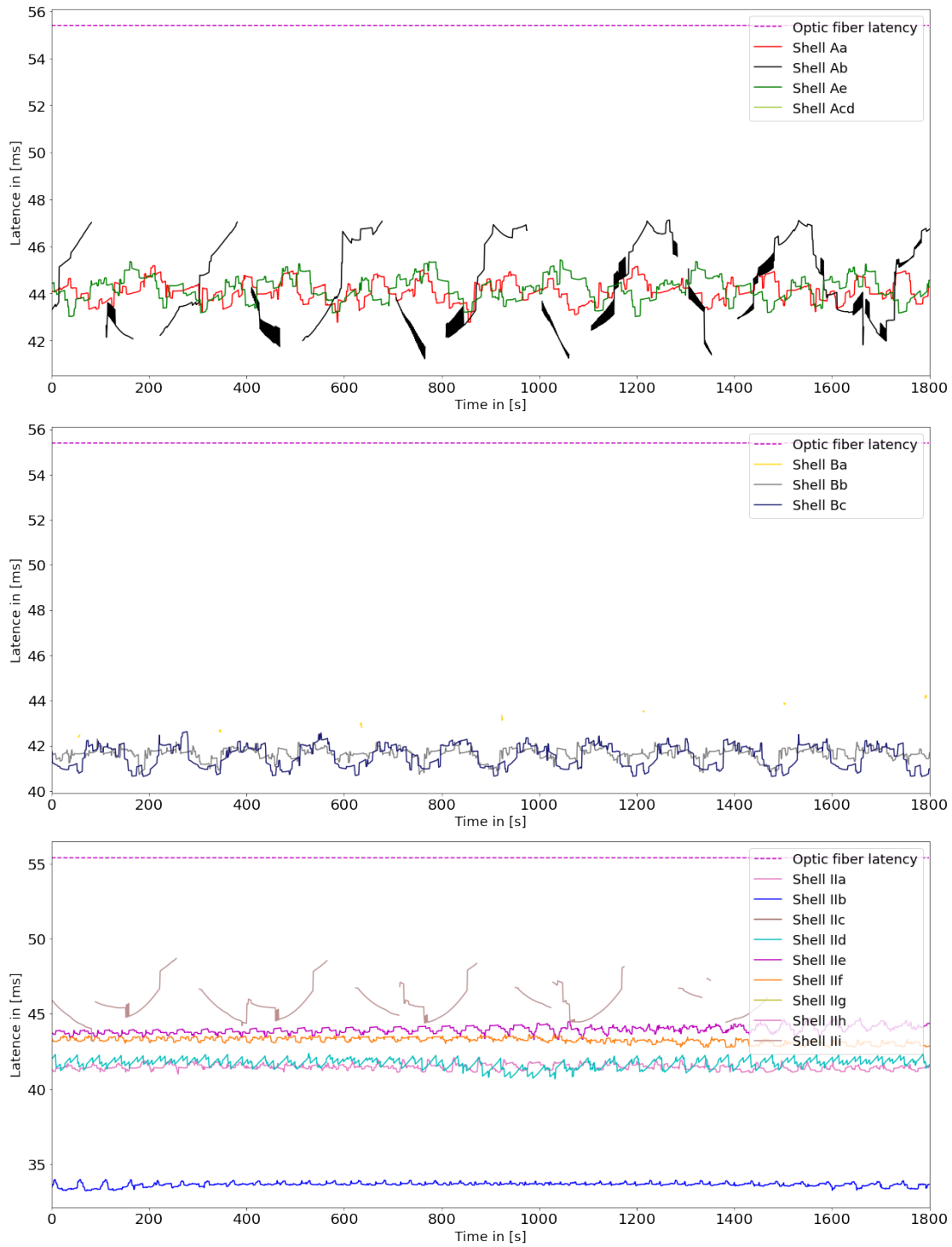


**Figure 6.7:** Average latency of the  $m \cdot n$  best paths between **Torino** and **Buenos Aires** for each instant of time.

### 6.3 Connection stability

As mentioned in Chapter 5, connection stability is another very important aspect. Hence, trying to establish a connection between ground stations that involves the least number of satellite switches can be crucial in lowering latency times.

It is necessary to reiterate that this research does not consider the aspects related to protocols, on-board instruments, and transceiver operations as they are unknown. So, an objective analysis that aims to understand how one can choose the best path in which the phenomena mentioned above have little impact follows.

To best understand how the Starlink constellation works, the code that implements Dijkstra's algorithm calculates for each time instant all possible combinations of paths and evaluates their effectiveness.

Again, for each time instant there are  $m \cdot n$  possible paths (where  $m$  is the number of satellites in view of the first ground station while  $n$  is the number of satellites in view of the last ground station). Each of these paths may involve different satellites or different number of satellites, and thus may be faster or slower than others. A complete assessment that would allow us to determine which and how many paths are needed to ensure the best connection between two cities involves studying all the shells individually and analyzing each of the possible paths established over time. Such work would be too onerous to accomplish and would require too much computational time.

For this reason, as shown in the following example, only the instant  $t = 300s$  for the shell  $A_A$  involved in the communication between Torino and San Francisco was taken into analysis. For the considered shell and at the considered time instant, 24 paths are established, since there are 6 satellites in view of Torino and 4 satellites in view of San Francisco, as shown in Table 6.6.

Torino	San Francisco
<b>s0047.021</b> for 134 s (235s - 368s)	<b>s0021.004</b> for 139 s (225s - 363s)
<b>s0049.020</b> for 166 s (297s - 462s)	<b>s0040.018</b> for 96 s (298s - 393s)
<b>s0050.020</b> for 144 s (208s - 351s)	<b>s0041.018</b> for 159 s (166s - 324s)
<b>s0063.015</b> for 126 s (194s - 319s)	<b>s0043.017</b> for 122 s (263s - 384s)
<b>s0065.014</b> for 168 s (244s - 411s)	
<b>s0066.014</b> for 155 s (154s - 308s)	

**Table 6.6:** Satellites in view of Torino and San Francisco in  $t = 300s$ .

As a result, the possible following 24 paths could be established:

- **s0047.021** → s0049.019 → s0039.020 → **s0021.004** for 128 s (236s - 363s);
- **s0047.021** → s0049.019 → s0039.020 → **s0040.018** for 48 s (298s - 345s)

- **s0047.021** → s0049.019 → s0039.020 → **s0041.018** for 58 s (267s - 324s)
- **s0047.021** → s0050.019 → s0040.020 → **s0043.017** for 60 s (263s - 322s)
- **s0049.020** → s0050.019 → s0040.020 → **s0021.004** for 67 s (297s - 363s)
- **s0049.020** → s0050.019 → s0040.020 → **s0040.018** for 53 s (298s - 350s)
- **s0049.020** → s0050.019 → s0040.020 → **s0041.018** for 28 s (297s - 324s)
- **s0049.020** → s0050.019 → s0040.020 → **s0043.017** for 88 s (297s - 384s)
- **s0050.020** → s0051.019 → s0041.020 → **s0021.004** for 127 s (225s - 351s)
- **s0050.020** → s0051.019 → s0041.020 → **s0040.018** for 34 s (298s - 331s)
- **s0050.020** → s0051.019 → s0041.020 → **s0041.018** for 96 s (208s - 303s)
- **s0050.020** → s0051.019 → s0041.020 → **s0043.017** for 89 s (263s - 351s)
- **s0063.015** → s0051.019 → s0041.020 → **s0021.004** for 72 s (246s - 317s)
- **s0063.015** → s0051.019 → s0041.020 → **s0040.018** for 22 s (298s - 319s)
- **s0063.015** → s0051.019 → s0041.020 → **s0041.018** for 104 s (216s - 319s)
- **s0063.015** → s0051.019 → s0041.020 → **s0043.017** for 50 s (263s - 312s)
- **s0065.014** → s0050.019 → s0040.020 → **s0021.004** for 79 s (285s - 363s)
- **s0065.014** → s0049.019 → s0039.020 → **s0040.018** for 32 s (298s - 329s)
- **s0065.014** → s0049.019 → s0039.020 → **s0041.018** for 72 s (249s - 320s)
- **s0065.014** → s0050.019 → s0040.020 → **s0043.017** for 112 s (263s - 374s)
- **s0066.014** → s0051.019 → s0041.020 → **s0021.004** for 27 s (282s - 308s)
- **s0066.014** → s0051.019 → s0041.020 → **s0040.018** for 11 s (298s - 308s)
- **s0066.014** → s0051.019 → s0041.020 → **s0041.018** for 26 s (283s - 308s)
- **s0066.014** → s0051.019 → s0041.020 → **s0043.017** for 46 s (263s - 308s)

As we can see, the several identified paths use the same satellites as intermediaries and have different durations. However, the LISLs transceivers mounted on the satellites allow communication with 4 satellites at a time and consequently all these paths cannot coexist at the same time. In any case, the code has reported only what are the best paths in terms of latency for each pair of satellites; there are, of course, many other possibilities for putting the two satellites into communication involving either several satellites or a different number of them but with slightly higher latencies.

So the question that needs to be answered now is: how to identify the best

path, which is the one that provides lowest latency but at the same time allows communication that is as stable as possible over time (without many switches)? All paths involve 4 satellites; consequently to critically answer the question we will analyze the paths which guarantee the lowest latency over time.

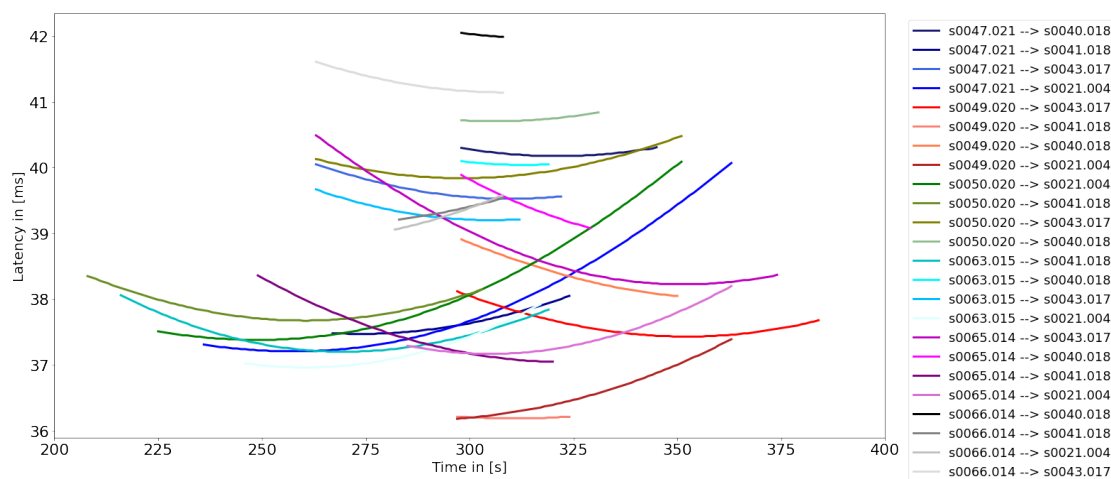


**Figure 6.8:** Latency over time of all the 24 possible paths.

In this case, in the reported time frame (from  $t = 225$  s to  $t = 375$  s), to take full advantage of the shell between Torino and San Francisco, we could follow different routes by making a varying number of switches. In fact, it can be seen (Figure 6.8) that some routes that seem more advantageous from the point of view of duration are actually less efficient from the point of view of latency. Also, because of time-varying latency, it may be more advantageous to switch paths more frequently.

Since each number of switches corresponds to a minimum average latency value, in Figure 6.9, the Pareto front is evaluated over a time interval of 150 s.

The Figure 6.9 confirms what was said before, that is, the higher the number of switches, the lower the ideal latency. Furthermore, the difference in ideal latency between making 1 switch and making 7, in this case, is just 0.4 ms. However, the internal latency times of each satellite remain unknown, so in this study phase, in a real case, it is not known whether it is actually convenient to make more switches or not.

Moreover, as the time interval considered changes, the values in the graph vary, but the curve trend remains constant. As expected, fewer switches correspond to greater path latency.

However, it is difficult to make a wise choice because there are so many possible alternatives, so many parameters to evaluate, and making a trade-off is complicated. In addition, the lack of useful data to estimate the actual latency due to switching

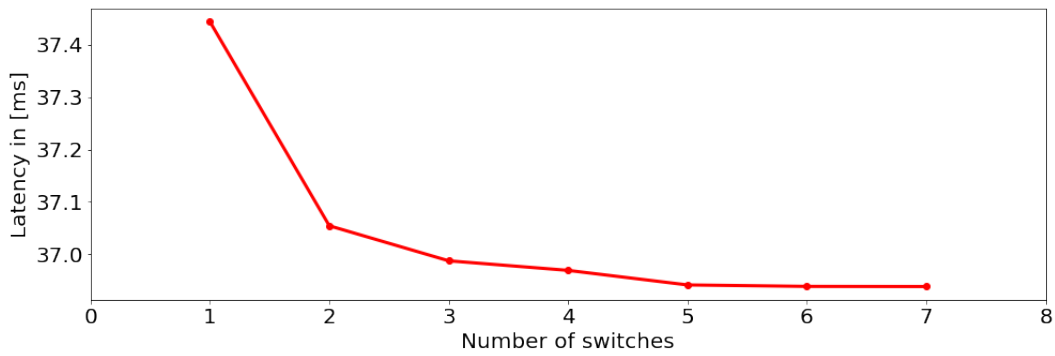


**Figure 6.9:** Pareto front which relates the number of switches and latency.

and the excessive computation time make things complicated.

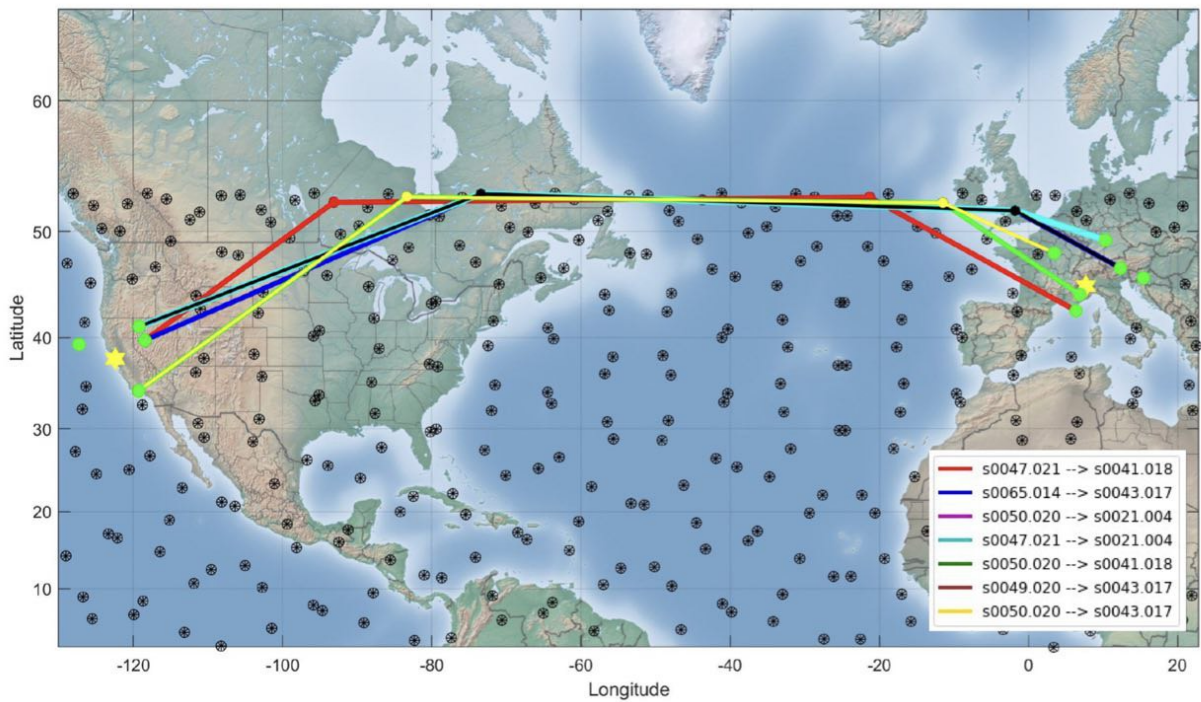


**Figure 6.10:** Link of the most persistent paths at  $t = 300s$ .

Figure 6.10 shows the most persistent paths at  $t = 300 s$  between Torino and San Francisco (both represented with a yellow star on the map). The green dots are the satellites in view of the ground stations, while the black dots are the satellites in the selected shell.

## 6.4 Critical analysis of each shell

The constellation analysis conducted so far has allowed us to understand how it will work when completed.

Despite limited data and computational limitations, interesting aspects of each shell have been analyzed, such that it is now possible to draw conclusions and speculate on the presumed exact purpose of each of them.

### 6.4.1 Shell $A_A$

It is a useful shell for short and long range connections between mid-latitude cities. In fact, full coverage of areas at latitudes below  $60^\circ$  is guaranteed, where there is a greater concentration of the world's population and presumably also greater data traffic. However, some populated areas such as Northern Europe, North Asia and North America as well as the poles remain uncovered.

The shell ensures continuous communication with cities located along both "horizontal", "vertical" and "diagonal" paths with slightly greater effectiveness for "horizontal" and "vertical" connectivities.

In all the paths analyzed, it is found that the average latency trend has fluctuations on the scale of 2 *ms* all better than fiber.

### 6.4.2 Shell $A_B$

With its 720 satellites positioned at an altitude of 570 km and an inclination of  $70^\circ$  it provides continuous coverage only in areas whose latitude is between  $55^\circ$  and  $70^\circ$ . Lower-latitude areas are not continuously covered. Thus, the goal of this shell is to ensure a fast connection to less densely populated areas, where data traffic is not assumed to be very heavy.

The consequence of this is that this shell does not offer good performance when used in connecting cities located in low latitude areas; in fact a discontinuous connection and a very fluctuating latency are observed.

However, it is possible that it is used in the vertical connection with cities located at different latitudes providing lower performance because it uses ground stations as relays.

### 6.4.3 Shell $A_{CD}$

A shell obtained from two shells correspondingly of 348 satellites and 172 satellites, both positioned 560 km and inclined  $97.6^\circ$ . This shell provides excellent coverage in all latitude areas above  $55^\circ$  including the poles while the coverage provided in low latitude areas is quite bad.

Also this shell seems to be designed to ensure connection in the most remote areas of the planet. In fact it is capable of fast communication with only ground stations located in that belt. Although it can also be used at low latitudes, its performance is very poor: in fact very discontinuous connection and very fluctuating average latency values are observed.

Therefore, for "vertical" connection with cities at different latitudes it will use ground stations as relays.

#### 6.4.4 Shell $A_E$

The shell  $A_E$  is currently the only completed shell. It is a shell with the same orbital characteristics as the  $A_A$  shell. Both have 1584 satellites but the shell in question has a  $0.2^\circ$  lower inclination and a 10 km higher altitude. These slight differences balance out and both shells manage to cover continuously all areas with latitude less than  $60^\circ$ .

Moreover, all performance characteristics are also identical and it sometimes happens that they behave in a complementary way.

#### 6.4.5 Shell $B_A$

Considerations about this shell must be taken with a grain of salt because they refer to an F parameter that is not the optimal one. Among the Generation I shells it is the second most numerous nevertheless it does not seem to provide continuous coverage in the areas it is supposed to cover, but this is surely the effect of an incorrect F parameter.

Given the low inclination of  $42^\circ$ , the goal of this shell is to connect the central part of the planet; that is, the part in which most of the data traffic will be concentrated.

#### 6.4.6 Shell $B_B$

The considerations on this shell must also be taken with a pinch of salt because they refer to an F parameter that is not the optimal one. It has similar characteristics to the  $B_A$  shell but has an inclination of  $48^\circ$ . Despite this, probably because of a more accurate estimate of the F parameter, this shell provides almost excellent coverage below the latitude of  $50^\circ$ .

Consequently, it works very well for the purpose for which it was built there, which is to put into communication long-range cities that are in that latitude range.

Performance also seems to be good both in terms of continuity of connection and in terms of guaranteed average latency.

### 6.4.7 Shell $B_C$

Finally, even the considerations about this shell must be taken with a grain of salt because they refer to an F parameter that is not optimal.

It, with its 2547 satellites at an altitude of just 345.6 km, is the most numerous shell of Generation I. The inclination is  $53^\circ$ , and although a suboptimal F parameter was used, this shell provides almost excellent coverage below the latitude of  $55^\circ$  and seems to have been designed as a support to  $A_A$  and  $A_E$  shells.

As a result it works very well for the purpose for which it was built, which is to put in long-range communications cities located in that latitude range. Performance seems to be good both in terms of continuity of connection and in terms of guaranteed average latency.

### 6.4.8 Shell $II_A$

It is part of the most numerous shells. With its 5280 satellites positioned at just 340 km with a  $53^\circ$  inclination, it aims to support shells  $A_A$ ,  $A_E$  and  $B_C$  covering the same area. In addition, the large number of satellites involved and the low altitude are intended to increase performance compared to the Generation I shells. This can be seen from the results obtained; in fact the coverage guaranteed by this shell is continuous everywhere and the latencies are generally lower. High performance is guaranteed for any kind of communication at latitudes below  $60^\circ$ . Although the advantages are evident, this is a slight improvement in performance at the cost of a large increase in satellites in orbit. Thus the reason this shell was designed comes merely from the high data traffic that will be estimated to be very high.

### 6.4.9 Shell $II_B$

This shell is also part of the most numerous shells and with its 5280 satellites positioned at just 345 km with a  $46^\circ$  inclination it aims to support the  $B_A$  shell that covers the same area increasing its performance given the large number of satellites involved and the low altitude.

This can be seen from the results obtained. In fact continuous coverage is guaranteed at latitudes below  $50^\circ$  and latency times are generally lower. In the coverage range of this shell, high performance is guaranteed for any kind of communication. Although the advantages are obvious, again this is a slight improvement in performance at the cost of a large increase in satellites in orbit. Thus the reason this shell was designed comes merely from the high data traffic that will be estimated to be very high.

#### 6.4.10 Shell II<sub>C</sub>

It is the third most numerous of the shells. With its 5280 satellites positioned only 350 km away at an inclination of 38°, it aims to support shells covering a similar area. A large number of satellites focus on the low-latitude part of the Earth because that area will be the busiest. In addition, the large number of satellites involved and the low altitude are intended to increase performance compared with Generation I shells.

As the results show, in fact, the coverage provided by this shell is continuous everywhere and latencies are generally lower. The performance is high for any kind of communication at latitudes below 40°.

Also in this case, although the advantages are evident, it is a slight improvement in performance at the cost of a large increase in the number of satellites in orbit. Therefore, the reason for designing this shell stems solely from the data traffic that is estimated to be very high.

#### 6.4.11 Shell II<sub>D</sub>

With its 3600 satellites positioned at 360 km and an inclination of 96.9°, the goal is to improve communication of the most remote areas of the globe. In fact, it improves the performance of the  $A_{CD}$  shell by ensuring continuous worldwide coverage with more advantageous average latencies. For this very reason, this shell will be able to connect all cities around the globe without using ground stations as relay. The performance guaranteed by this shell is comparable to that of other Generation II shells.

Even in this case, the very large number of satellites that will be at high latitudes is due to the data traffic that is expected to be very heavy in those areas as well.

#### 6.4.12 Shell II<sub>E</sub>

This shell, consisting of 3360 satellites, aims to help the shells  $A_A$ ,  $A_E$ ,  $B_C$  and  $II_A$  since they have a 53° inclination. However, compared to the  $II_A$  shell it has fewer satellites and is located at an altitude of 525 km so, although the coverage is continuous, it provides slightly higher latencies. Nevertheless, it is an example of how shells with lower numbers of satellites can be used without problems.

#### 6.4.13 Shell II<sub>F</sub>

This shell also, consisting of 3360 satellites, concentrates on an area at latitudes lower than 45° but unlike the other shells covering the same area it has a higher altitude at 530 km. Consequently even though it provides continuous coverage like the others it ensures a little higher latency.

The reason this shell seems to have been designed is to overcome a possible situation in which the more performant shells are not available.

#### **6.4.14 Shell II<sub>G</sub>**

This shell, consisting of 3360 satellites, has an inclination of only 33° and focuses on latitudes less than 40° but unlike the other shells covering the same area has an altitude of 535 km. Consequently even though it provides continuous coverage like the others it ensures a little higher latency.

The reason why this shell was designed is to ensure additional support in the area assumed to be the busiest.

#### **6.4.15 Shell II<sub>H</sub>**

With its 144 satellites, it is the least numerous shell, and to make it perform better it was placed at an altitude of 604 km. However, it does not provide continuous coverage and, as a result, may prove useful and competitive only for small-range communications.

Probably the reason it was created is to further support the existing shells and at the same time provide a type of service that uses the ground stations as relays.

#### **6.4.16 Shell II<sub>I</sub>**

With its 324 satellites, it is the second less numerous shell, and to make it perform better it has been placed at an altitude of 614 km. However, it does not provide continuous coverage and, as a result, may prove useful and competitive only for small-range communications.

Probably the reason it was created is to further support the existing shells and at the same time provide a type of service that uses the ground stations as relays.

The results just obtained are unpublished as far as they are not available in literature. Moreover, they are very interesting because they help answer some interrogatives about the constellation. Although the results do not consider data traffic, they are still of great value because they allow us to understand the presumed usefulness of each shell. In addition, it was also shown how sometimes some shells demonstrate better features than denser shells and even the whole construction of Gen2 can be questioned.

## Chapter 7

# Alternative proposals to current constellation

By now, all the features of Starlink have been evaluated and can be considered as known. Using all available data from FCC documents and official websites, the quality and potential of the constellation have been estimated.

As a consequence, from now on, the already analyzed constellation will be compared with some other constellations in which the number of satellites is gradually reduced. The purpose of this analysis is to compare all features to see if it is possible to reduce the number of satellites while maintaining the same performance.

This kind of analysis takes a big amount of computational time, which is why only a few shells have been studied in depth. The choice of shells falls on the following:  $A_A$  and  $II_C$ . The reason these two shells were chosen is that they represent the most crowded shells in their group so the effects of satellites reduction could be more impressive with more interesting considerations to be made.

Other less crowded shells, such as  $A_B$ ,  $A_{CD}$ ,  $II_H$  or  $II_I$ , may be more affected by satellite reduction. For this reason, the best way to greatly reduce the number of satellites for these shells might be to increase the altitude, but this leads to an obvious change in performance due to increased latency.

In the following chapters many different alternatives with the same orbital characteristics but with a reduced number of satellites are proposed for each selected shell. All of them will be compared with the original one in terms of coverage per latitude and latency through the same paths.

In any case, these analyses are not complete and will not be sufficient to state a definitive conclusion, because all traffic data are unknown. Starlink probably does not even know the accurate estimate of future information flow through Starlink's infrastructure. However, this work might reveal that the number of satellites in the Starlink constellation could be reduced.

## 7.1 Shell $A_A$

Seven alternatives are proposed for this shell. All the proposals have the same inclination ( $53.2^\circ$ ) and altitude (540 km) but have a different distribution and number of satellites. The choice was made to keep the number of planes the same but to change the number of satellites per plane in order to reduce the total number of involved satellites.

The seven shells that will be analyzed are:

- Shell  $A_{A1}$ : 1512 sats (-4,5% of sats);
- Shell  $A_{A2}$ : 1440 sats (-9,1% of sats);
- Shell  $A_{A3}$ : 1296 sats (-18,2% of sats);
- Shell  $A_{A4}$ : 1152 sats (-27,3% of sats);
- Shell  $A_{A5}$ : 1008 sats (-36,4% of sats);
- Shell  $A_{A6}$ : 864 sats (-45,4% of sats);
- Shell  $A_{A7}$ : 720 sats (-54,5% of sats);

By reducing the number of satellites, seven new shells have been obtained which have different characteristics than the starting one. For this reason it was necessary to calculate for each of them also the new F parameter that characterizes them. The procedure for determining the parameter follows the one explained in Chapter 4 and all the tables with the trade off to determine the best one are shown in Appendix C.

In the end, seven shells with the following orbital characteristics have been obtained:

Shell	No. of Sats	No. of Planes	Sats per Plane	Interplane Spacing	Phasing parameter
$A_A$	1584	72	22	$16.36^\circ$	13
$A_{A1}$	1512	72	21	$17.14^\circ$	38
$A_{A2}$	1440	72	20	$18^\circ$	43
$A_{A3}$	1296	72	18	$20^\circ$	19
$A_{A4}$	1152	72	16	$22.5^\circ$	19
$A_{A5}$	1008	72	14	$25.7^\circ$	17
$A_{A6}$	864	72	12	$30^\circ$	21
$A_{A7}$	720	72	10	$36^\circ$	23

**Table 7.1:** Original  $A_A$  shell and different alternatives.

As can be easily guessed, a decreasing number of satellites can lead to a reduction in coverage capability. From what can be seen in Appendix C, each shell has its

own best  $F$  parameter that ensures a good trade-off between collision safety and good coverage.

Figure 7.1 describes the coverage as a function of latitude for different shells.

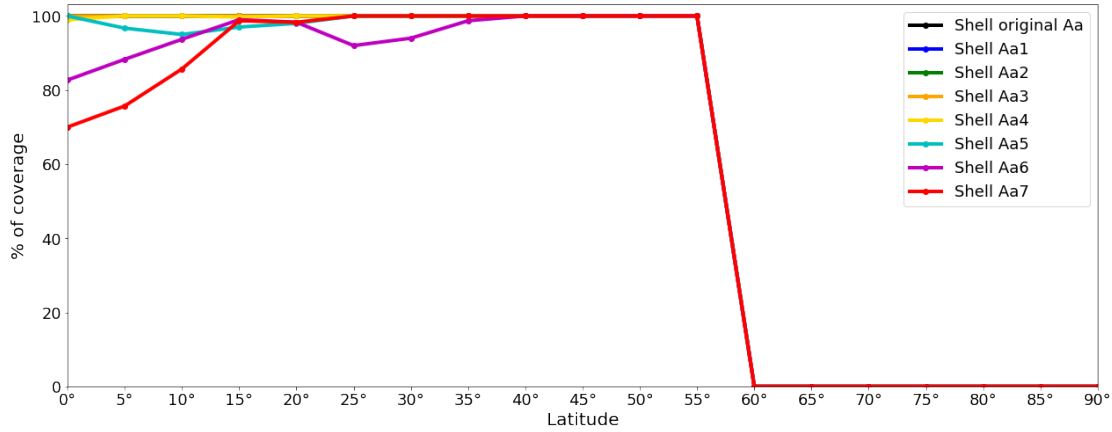


**Figure 7.1:** Coverage as a function of latitude for different  $A_A$  alternative shells.

The plot shows how the less dense shells barely cover the low latitude areas especially in the regions below 15° while for all of the proposed shells the high latitude bands are characterized by continuous coverage. Obviously, since the inclination of the plane is the same for all of them, they have the same upper limit set at about 55° beyond which the satellites cannot provide service.

If, on the other hand, we want to see the graph in another way, by averaging the overall guaranteed coverage according to the number of satellites involved, we can refer to Figure 7.2.

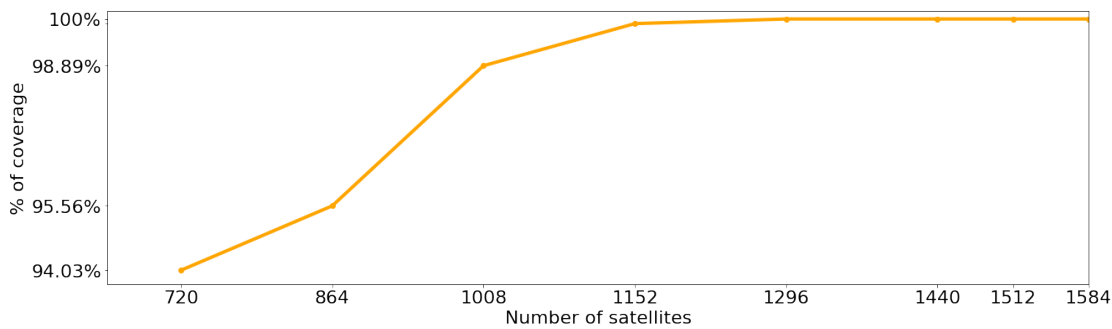


**Figure 7.2:** Coverage as a function of number of satellites for  $A_A$ 's alternatives.

This last graph in particular shows that for a reduction of satellites down to 1152 there is no a significant impact on guaranteed coverage. After that, the link between reduction of satellites and loss of coverage capabilities seems to be exponential.

Although coverage is an essential parameter for judging the efficiency of a shell, latency is as well. Therefore all seven shells are analyzed, as done previously, in the paths Torino - San Francisco, Torino - Cape Town and Torino - Buenos Aires, and very interesting results are obtained.

In Figures 7.3, 7.4 and 7.5 the average latencies of the  $m \cdot n$  paths that instantiate every second for a period of 1800 s have been graphed. Although the total number of paths that can occur each time instant varies as  $m$  and  $n$ , which are the number of satellites in view with the ground stations, vary from shell to shell it can be seen that the average latency value remains similar for all shells.

### 7.1.1 Torino → San Francisco

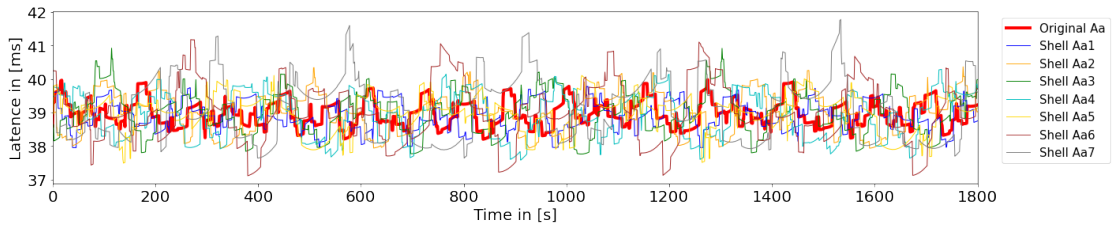


**Figure 7.3:** Average latency of  $A_A$ 's alternatives in Torino - San Francisco.

In this path it can be seen that all the alternatives provide a continuous connection along the 30 minutes and also have identical average latency values, as shown in Table 7.2.

Shell	Coverage [%]	Average Latency [ms]
$A_A$	100	38.96
$A_{A1}$	100	38.89
$A_{A2}$	100	38.98
$A_{A3}$	100	38.98
$A_{A4}$	100	38.92
$A_{A5}$	100	38.98
$A_{A6}$	100	38.98
$A_{A7}$	100	39.06

**Table 7.2:** Coverage and latency of  $A_A$ 's alternatives for Torino - San Francisco.

### 7.1.2 Torino → Cape Town

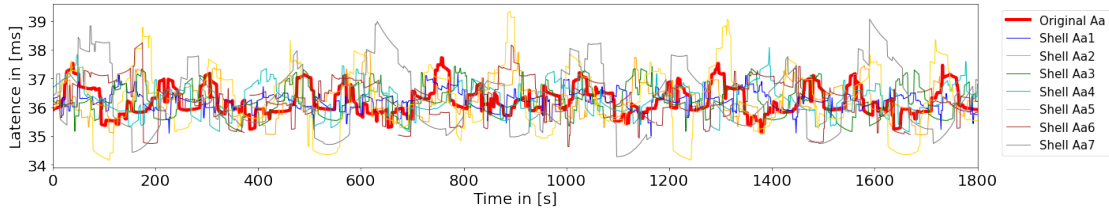


**Figure 7.4:** Average latency of  $A_A$ 's alternatives in Torino - Cape Town.

In this path it can be seen that all of the alternatives guarantee a continuous connection along the 30 minutes except for shell  $A_6$ , which still guarantees a connection that is continuous at 97.6%. Nevertheless, all shells have identical average latency values, as shown in Table 7.3.

Shell	Coverage [%]	Average Latency [ms]
$A_A$	100	36.21
$A_{A1}$	100	36.20
$A_{A2}$	100	36.22
$A_{A3}$	100	36.20
$A_{A4}$	100	36.28
$A_{A5}$	100	36.25
$A_{A6}$	97.6	36.26
$A_{A7}$	100	36.27

**Table 7.3:** Coverage and latency of  $A_A$ 's alternatives for Torino - Cape Town.

### 7.1.3 Torino → Buenos Aires

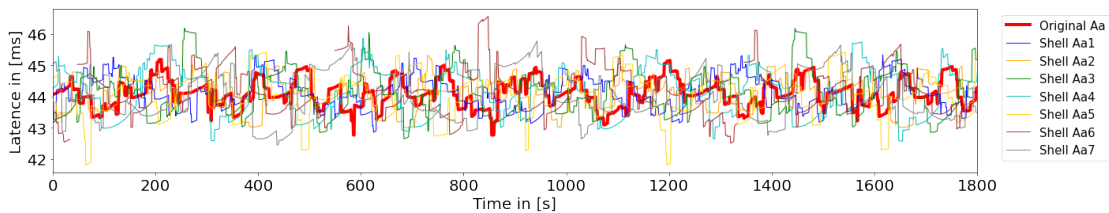


**Figure 7.5:** Average latency of  $A_A$ 's alternatives in Torino - Buenos Aires.

In this path it can be seen that all of the alternatives guarantee a continuous

connection along the 30 minutes except for shell  $A_6$ , which still guarantees a connection that is continuous at 97.7%. Nevertheless, all shells have identical average latency values, as shown in Table 7.4.

Shell	Coverage [%]	Average Latency [ms]
$A_A$	100	44.10
$A_{A1}$	100	44.11
$A_{A2}$	100	44.09
$A_{A3}$	100	44.11
$A_{A4}$	100	44.13
$A_{A5}$	100	44.07
$A_{A6}$	97.7	44.14
$A_{A7}$	100	44.01

**Table 7.4:** Coverage and latency of  $A_A$ 's alternatives for Torino - Buenos Aires.

In the end, it is observed that reducing, even substantially, the number of satellites per shell does not cause performance reductions in terms of average latency.

The reduction of satellites undoubtedly affects the availability of satellites to work; in fact each satellite can process at most four laser transceiver signals per instant. However, since the data traffic is unknown, the effect of satellite reduction cannot be estimated from this point of view.

As mentioned above, the reduction of satellites in a shell causes a reduction in the number of satellites each ground station has in view at any moment in time, and consequently also the number of possible paths the signal can follow. If this does not have a direct impact on latency, it can be seen that the stability of the connection over time may be affected.

Assuming we want to establish a lasting connection between two cities, we see that as we move to a less dense shell the possible solutions for a stable connection decrease.

Once again, the instant  $t = 300$  s of the Torino - San Francisco path is taken into analysis. Figures 7.6 and 7.7 compare all the possible paths that occur at that instant for shells  $A_{A2}$  and  $A_{A7}$  (the other graphs for the other shells are available in Appendix C).

The first thing that jumps out when looking at the graphs is the number of available paths, and as a result it can be seen that in order to ensure a stable connection, the number of possible switches has also dropped dramatically. Thus, the more the number of satellites per shells is reduced, the more the signal is forced to follow a

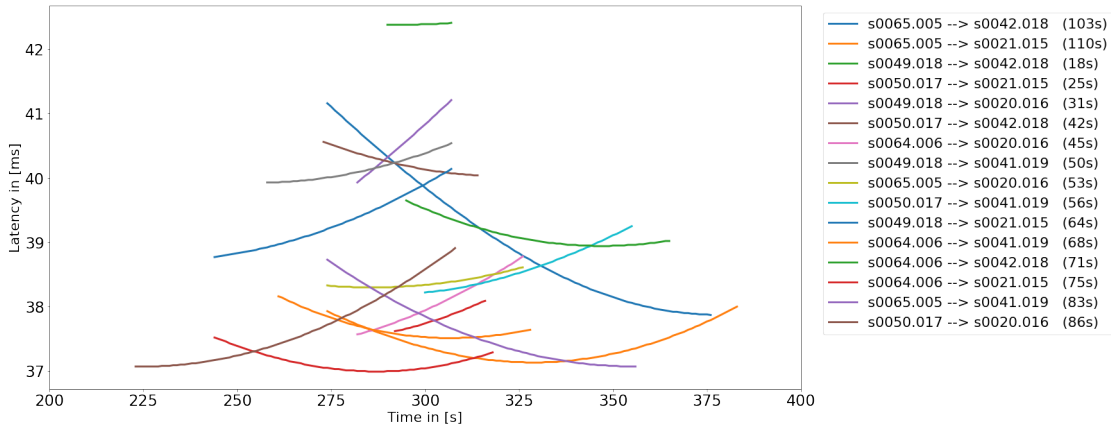


**Figure 7.6:** Latency over time of all the 16 possible paths (shell  $A_{A2}$ ).

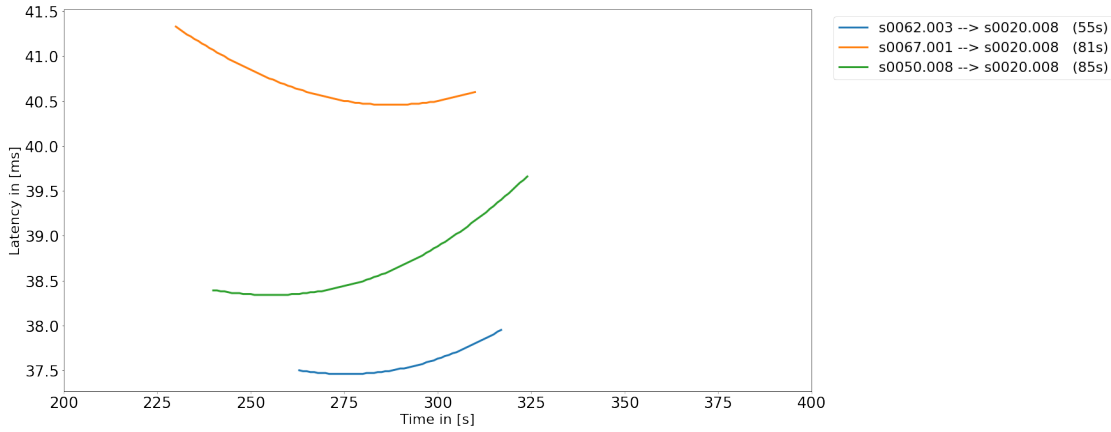


**Figure 7.7:** Latency over time of all the 3 possible paths (shell  $A_{A7}$ ).

given path of satellites without many alternatives. This could cause a significant increase in latency when taking into consideration the protocols and tools used for signal transceiving.

Although from the images shown in Appendix C a direct proportionality between the decrease in the number of satellites in the shells and the decrease in the number of available paths for each time instant is not evident, it can be said that this is correct. To support this, all the possible  $m \cdot n$  paths in the interval of 1800 s were calculated and added together, obtaining Table 7.5.

Obviously a greater number of possible paths guarantees better traffic management even if all the performances analyzed so far remain similar.

Shell	Available paths
A <sub>A1</sub>	34780
A <sub>A2</sub>	31350
A <sub>A3</sub>	25821
A <sub>A4</sub>	20086
A <sub>A5</sub>	15312
A <sub>A6</sub>	11494
A <sub>A7</sub>	8061

**Table 7.5:** Number of available paths of each shell over 1800 s.

## 7.2 Shell $II_C$

As for the  $II_C$  shell, nine alternatives have been proposed. All the proposals have the same inclination ( $38^\circ$ ) and altitude (350 km) but have a different distribution and number of satellites. The choice was made to keep the number of planes the same but to change the number of satellites per plane in order to reduce the total number of involved satellites.

The nine shells that will be analyzed are:

- Shell  $II_{C1}$ : 5040 sats (-5% of sats);
- Shell  $II_{C2}$ : 4752 sats (-10% of sats);
- Shell  $II_{C3}$ : 4224 sats (-20% of sats);
- Shell  $II_{C4}$ : 3696 sats (-30% of sats);
- Shell  $II_{C5}$ : 3169 sats (-40% of sats);
- Shell  $II_{C6}$ : 2640 sats (-50% of sats);
- Shell  $II_{C7}$ : 2112 sats (-60% of sats);
- Shell  $II_{C8}$ : 1584 sats (-70% of sats);
- Shell  $II_{C9}$ : 1056 sats (-80% of sats);

By reducing the number of satellites, nine new shells have been obtained which have different characteristics than the starting one. For this reason it was necessary to calculate for each of them also the new F parameter that characterizes them. The procedure for determining the parameter follows the one explained in Chapter 4 and all the tables with the trade off to determine the best one are shown in Appendix C.

In the end, nine shells with the orbital characteristics shown in Table 7.6 have been obtained.

Shell	No. of Sats	No. of Planes	Sats per Plane	Interplane Spacing	Phasing parameter
$II_C$	5280	48	110	$3.27^\circ$	35
$II_{C1}$	5040	48	105	$3.43^\circ$	10
$II_{C2}$	4752	48	99	$3.64^\circ$	0
$II_{C3}$	4224	48	88	$4.09^\circ$	19
$II_{C4}$	3696	48	77	$4.67^\circ$	16
$II_{C5}$	3168	48	66	$5.45^\circ$	33
$II_{C6}$	2640	48	55	$6.54^\circ$	26
$II_{C7}$	2112	48	44	$8.18^\circ$	43
$II_{C8}$	1584	48	33	$10.9^\circ$	34
$II_{C9}$	1056	48	22	$16.4^\circ$	47

**Table 7.6:** Original  $II_C$  shell and different alternatives.

Also in this case, a decreasing number of satellites leads to a reduction in coverage capability but the reduction is observable only in the last proposed shell. From what can be seen in Appendix C, each shell has its own best F parameter that ensures a good trade-off between collision safety and good coverage and Figure 7.8 describes the coverage as a function of latitude for different shells.

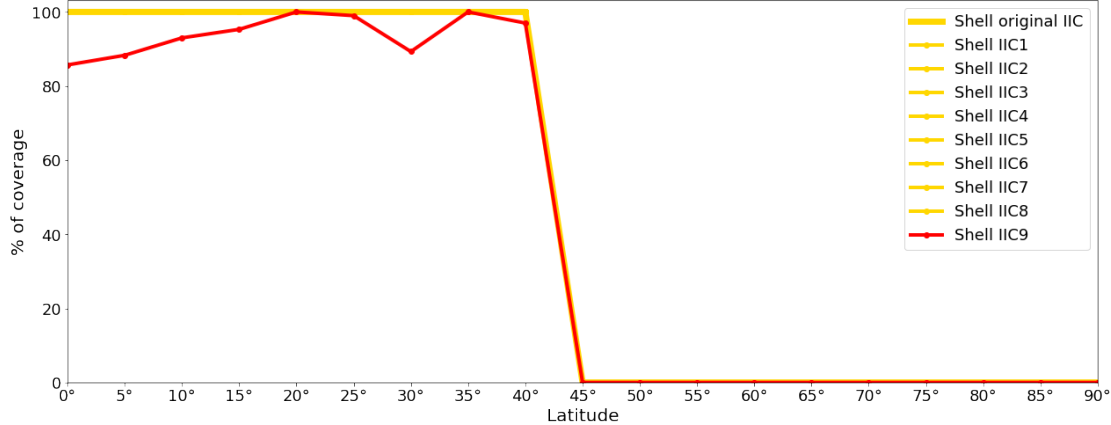


**Figure 7.8:** Coverage as a function of latitude for different  $II_C$  alternative shells.

The plot shows how the least dense shells barely cover the interested areas while all the others are characterized by continuous coverage. Since the inclination of the plane is the same for all of them, they have the same upper limit set at about  $40^\circ$  beyond which the satellites cannot provide service.

If, on the other hand, we want to see the graph in another way, by averaging the

overall guaranteed coverage according to the number of satellites involved, we can refer to Figure 7.9.

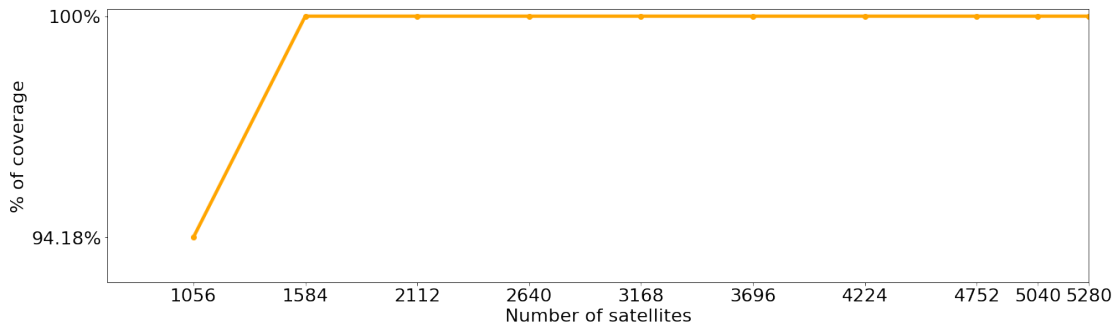


**Figure 7.9:** Coverage as a function of number of satellites for  $II_C$ 's alternatives.

This last graph in particular shows that even reducing the number of satellites by 70% there is no significant impact on guaranteed coverage.

Due to the low inclination of the shell, the cities considered so far are not covered and consequently the classical analysis to know the average latency along Torino - San Francisco, Torino - Cape Town and Torino - Buenos Aires paths could not be performed. Similarly, further analysis on stability and the number of available routes was not performed.

The analyses just conducted give us the opportunity to answer the original questions. Under the assumption of having to transmit only one signal or a few signals at a time, the constellation could very well operate with a very reduced number of satellites because performance is not affected. So even if it is true that there is no information on data traffic, the question remains whether it is really necessary to use all those satellites just to succumb to the high demand.

Out of a total of 16 shells and nearly 42000 satellites, even a slight reduction can make a difference.

## Chapter 8

# Conclusions and recommendations

Nowadays, it is essential to have an Internet connection that allows us to be in continuous communication with the whole world, and various companies are working to ensure a fast and performing service.

It has been seen that among all possible solutions, the most advantageous, especially for long-range connections, turns out to be the satellite connection that uses a constellation of satellites placed in low orbit. SpaceX's Starlink constellation was designed with precisely this goal in mind despite the many controversies surrounding its architecture. Although the constellation promises excellent performance, the huge number of satellites it involves raises quite a few concerns in the scientific community, so further study is essential to fully understand the need to use so many satellites.

The importance of such a study stems from the fact that in the worst-case scenario, such a large number of satellites in close orbits could cause Kessler syndrome and consequently could make space inaccessible for the next decades or centuries.

### 8.1 Conclusions

This thesis has produced a number of important and unpublished results that are not currently available in the literature and that can help the scientific and engineering community answer some of the questions related to the constellation. Despite the limitations related to low data availability and excessive computing power required, the goal of this thesis has been met.

The orbits of all the shells that compose the constellation were propagated, and it was possible to evaluate the performance of the constellation in terms of coverage and average latency. These are two of the most important aspects for which the

constellation was designed, and essential information was derived for each shell. However, the question about the alleged use of some shells remains open.

The most important results that have been obtained concern studies related to alternative shells in which shells with a reduced number of satellites have been analyzed and compared with the original, and surprisingly it has been found that the performance in terms of coverage and latency remains unchanged even when each shell undergoes a drastic reduction in the number of satellites.

In particular, the  $II_C$  shell manages to provide continuous coverage even with 1584 satellites instead of 5280, and the  $A_A$  shell, in front of a reduction of more than 50% of its satellites, provides identical average latency times along the same paths. These are only the two examples analyzed, but further investigations on other shells as well would be able to detect equally satisfactory results.

However, although it is true that the same results can be obtained by reducing the number of satellites per shell does not mean that the solution is feasible. In fact, the study carried out in this thesis does not take data traffic into account because there are no estimates for it.

Therefore, this thesis, with its important results obtained, paves the way for more in-depth research in which other aspects currently unknown are taken into consideration.

## 8.2 Recommendations

The study turns out to be extremely important because it reveals the possibility of achieving outstanding performance even with an extreme reduction in the number of satellites involved. However, it is still necessary to understand whether the high number of satellites serves to succumb to the high and more diverse data traffic. To get more accurate data, one step forward that can help this research is to do a market investigation and estimate, over the next few decades, what the satellite Internet traffic will be and do simulations to see how much each shell can be resized.

Another possible solution that would help to reduce the number of satellites drastically is to implement the LISLs system and make it capable of establishing more than four transceiver connections at a time. Although this would lead Starlink to reinvest many resources in R&D, the benefits are significant because fewer satellites will be employed and the possibility of collision drops.

In the age of space exploration, a small false pass can be lethal and may cause all atmospheric activity to halt for decades, with economic and political consequences that would affect every state in the world. Therefore, it is paramount that all

operations will be carried out with the utmost safety and that only necessary items will be launched into orbit.

There has never been a satellite constellation as large as Starlink, and it will not be the only one to be launched. So it is good to encourage a study to investigate this issue further. Even a small percentage decrease of satellites out of a total of 42,000 can make a significant and attractive difference.



# Appendix A

## Tables

### A.1 F parameter

#### A.1.1 F that guarantees the maximum minimum distance

The table below shows, for different shells, how the minimum guaranteed distance between satellites varies with F. The best F corresponds to the one that guarantees the maximum minimum distance.

Shell	Best F	Max.min.dist	Graph
$A_A$	13	47.94 km	

*(Continued on the next page)*

(Continued on the previous page)

$A_B$	25	64.68 km	
$A_C$	0	60.71 km	
$A_D$	0	67.03 km	

(Continued on the next page)

(Continued on the previous page)

$A_E$	65	71.51 km	
$B_A$	1889	78.66 km	
$B_B$	1509	76.66 km	

(Continued on the next page)

(Continued on the previous page)

$B_C$	201	86.10 km	
$II_A$	25	19.38 km	
$II_B$	1	16.14 km	

(Continued on the next page)

(Continued on the previous page)

$\Pi_C$	35	29.83 km	
$\Pi_D$	28	11.77 km	
$\Pi_E$	27	33.91 km	

(Continued on the next page)

(Continued on the previous page)

$\Pi_F$	11	37.05 km	
$\Pi_G$	1	26.78 km	
$\Pi_H$	1	831.86 km	

(Continued on the next page)

(Continued on the previous page)

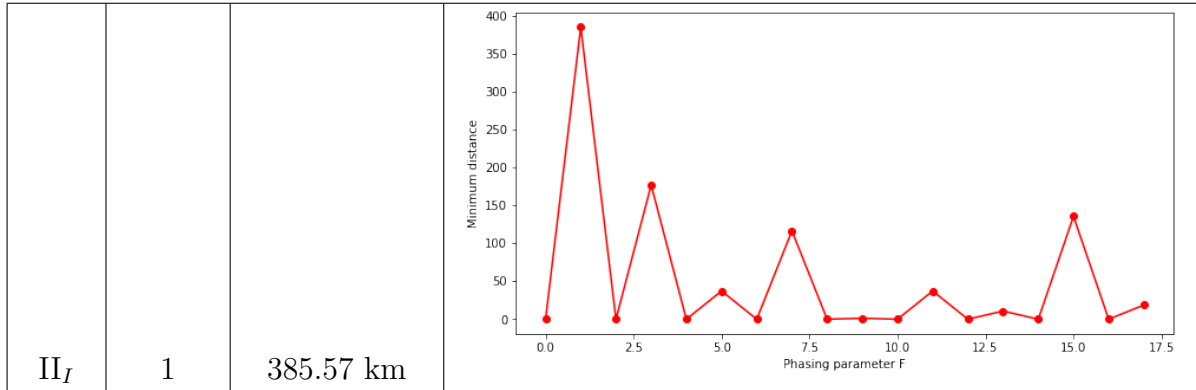


**Table A.1:** Evaluation of the best F parameter based on the minimum guaranteed distance between satellites.

### A.1.2 Best F evaluation

For shells  $A_E$ ,  $II_E$ ,  $II_G$ ,  $II_H$  and  $II_I$  the results that led to the decision of the best F as a trade-off between minimum guaranteed distance and coverage are shown.

F	% Coverage per Latitude																			% Average	Distance min [km]	Rate	
	0°	5°	10°	15°	20°	25°	30°	35°	40°	45°	50°	55°	60°	65°	70°	75°	80°	85°	90°				
1	93.3	100	100	100	100	100	100	100	100	100	100	100	100	100	100	100	100	100	100	100	99.44	4.08	9.00
3	93.3	100	100	100	100	100	100	100	100	100	100	100	100	100	100	100	100	100	100	100	99.44	14.68	9.37
5	93	100	100	100	100	100	100	100	100	100	100	100	100	100	100	100	100	100	100	100	99.42	2.50	8.93
7	92.7	100	100	100	100	100	100	100	100	100	100	100	100	100	100	100	100	100	100	100	99.39	19.39	9.52
9	93	100	100	100	100	100	100	100	100	100	100	100	100	100	100	100	100	100	100	100	99.42	3.68	8.98
11	93	100	100	100	100	100	100	100	100	100	100	100	100	100	100	100	100	100	100	100	99.42	0.13	8.25
13	93	100	100	100	100	100	100	100	100	100	100	100	100	100	100	100	100	100	100	100	99.42	2.52	8.93
15	93.3	100	100	100	100	100	100	100	100	100	100	100	100	100	100	100	100	100	100	100	99.44	0.57	8.75
17	93.3	100	100	100	100	100	100	100	100	100	100	100	100	100	100	100	100	100	100	100	99.44	17.11	9.45
19	93	100	100	100	100	100	100	100	100	100	100	100	100	100	100	100	100	100	100	100	99.42	2.50	8.93
21	92.7	100	100	100	100	100	100	100	100	100	100	100	100	100	100	100	100	100	100	100	99.39	17.11	9.44
23	93	100	100	100	100	100	100	100	100	100	100	100	100	100	100	100	100	100	100	100	99.42	3.68	8.98
25	93	100	100	100	100	100	100	100	100	100	100	100	100	100	100	100	100	100	100	100	99.42	0.13	8.25
27	93	100	100	100	100	100	100	100	100	100	100	100	100	100	100	100	100	100	100	100	99.42	33.91	10.00

**Figure A.1:** Best F evaluation for shell  $II_E$ .

F	% Coverage per Latitude																			% Average	Distance min [km]	Rate								
	0°	5°	10°	15°	20°	25°	30°	35°	40°	45°	50°	55°	60°	65°	70°	75°	80°	85°	90°											
1	100	100	100	86	92	100	100	100	100	100	100	100	100	100	100	100	100	100	100	0	0	0	0	0	0	0	0	98.17	3.38	8.86
3	100	100	100	98.7	87.7	99	100	100	100	100	100	100	100	100	100	100	100	100	100	0	0	0	0	0	0	0	0	98.78	58.24	10.00
5	100	100	100	100	100	96.7	98.3	100	100	100	100	100	100	100	100	100	100	100	100	0	0	0	0	0	0	0	0	99.58	35.51	9.63
7	100	100	100	100	100	100	100	100	100	100	100	100	100	100	100	100	100	100	100	0	0	0	0	0	0	0	0	100.00	12.03	9.21
9	100	100	100	100	100	100	100	100	100	100	100	100	100	100	100	100	100	100	100	0	0	0	0	0	0	0	0	100.00	5.01	9.07
11	100	100	100	100	100	100	100	100	100	100	100	100	100	100	100	100	100	100	100	0	0	0	0	0	0	0	0	100.00	23.64	9.44
13	100	100	100	100	100	100	100	100	100	100	100	100	100	100	100	100	100	100	100	0	0	0	0	0	0	0	0	100.00	30.58	9.57
15	100	100	100	100	100	100	100	100	100	100	100	100	100	100	100	100	100	100	100	0	0	0	0	0	0	0	0	100.00	1.48	8.96
17	100	100	100	100	100	100	100	100	100	100	100	100	100	100	100	100	100	100	100	0	0	0	0	0	0	0	0	100.00	20.18	9.37
19	100	100	100	100	100	100	100	100	100	100	100	100	100	100	100	100	100	100	100	0	0	0	0	0	0	0	0	100.00	10.04	9.17
21	100	100	100	100	100	100	100	100	100	100	100	100	100	100	100	100	100	100	100	0	0	0	0	0	0	0	0	100.00	13.33	9.24
23	100	100	100	100	100	100	100	100	100	100	100	100	100	100	100	100	100	100	100	0	0	0	0	0	0	0	0	100.00	1.99	8.98
25	100	100	100	100	100	100	100	100	100	100	100	100	100	100	100	100	100	100	100	0	0	0	0	0	0	0	0	100.00	30.58	9.57
27	100	100	100	100	100	100	100	100	100	100	100	100	100	100	100	100	100	100	100	0	0	0	0	0	0	0	0	100.00	5.01	9.07
29	100	100	100	100	100	100	100	100	100	100	100	100	100	100	100	100	100	100	100	0	0	0	0	0	0	0	0	100.00	18.00	9.33
31	100	100	100	100	100	100	100	100	100	100	100	100	100	100	100	100	100	100	100	0	0	0	0	0	0	0	0	100.00	21.03	9.39
33	100	100	100	100	100	100	100	100	100	100	100	100	100	100	100	100	100	100	100	0	0	0	0	0	0	0	0	100.00	31.74	9.60
35	100	100	100	100	100	100	100	100	100	100	100	100	100	100	100	100	100	100	100	0	0	0	0	0	0	0	0	100.00	23.64	9.44
37	100	100	100	100	100	100	100	100	100	100	100	100	100	100	100	100	100	100	100	0	0	0	0	0	0	0	0	100.00	22.40	9.42
39	100	100	100	100	100	100	100	100	100	100	100	100	100	100	100	100	100	100	100	0	0	0	0	0	0	0	0	100.00	49.81	9.95
41	100	100	100	100	100	100	100	100	100	100	100	100	100	100	100	100	100	100	100	0	0	0	0	0	0	0	0	100.00	35.51	9.67
43	100	100	99.7	89.3	89	96.7	98.3	100	100	100	100	100	100	100	100	100	100	100	100	0	0	0	0	0	0	0	0	97.75	21.01	9.19
45	100	100	89.7	86	99.7	100	100	100	100	100	100	100	100	100	100	100	100	100	100	0	0	0	0	0	0	0	0	97.95	1.95	8.80
47	100	98.3	77.3	94	100	100	100	100	100	100	100	100	100	100	100	100	100	100	100	0	0	0	0	0	0	0	0	97.47	40.49	9.54
49	100	91.7	77.7	100	100	95	79	82	86.7	100	100	100	100	100	100	100	100	100	100	0	0	0	0	0	0	0	0	92.68	0.56	8.19
51	100	85	82.7	100	93.7	68	94	100	100	100	100	100	100	100	100	100	100	100	100	0	0	0	0	0	0	0	0	93.62	1.48	8.39
53	100	79.3	88.7	100	71.3	89	100	94	81.3	83.3	100	100	100	100	100	100	100	100	100	0	0	0	0	0	0	0	0	90.58	20.18	8.53
55	100	74.3	94.7	91	70.7	100	85	77.7	100	100	100	96.7	100	100	100	100	100	100	100	0	0	0	0	0	0	0	0	90.84	21.03	8.57
57	100	69.7	100	75.7	88.3	93.7	73.7	100	84.3	66.3	82.3	71.3	100	100	100	100	100	100	100	0	0	0	0	0	0	0	0	83.78	20.82	7.93
59	100	65	100	62.7	100	72.3	100	80.3	83.3	100	77.3	61	100	100	100	100	100	100	100	0	0	0	0	0	0	0	0	83.49	1.99	7.50
61	100	67.3	100	70.3	99.3	78.7	96.7	79	98.7	79.3	100	63.3	100	100	100	100	100	100	100	0	0	0	0	0	0	0	0	86.05	30.58	8.32
63	100	72.3	97.7	85	84	100	68.3	100	78	100	100	84.3	100	100	100	100	100	100	100	0	0	0	0	0	0	0	0	89.13	5.01	8.09
65	100	77.3	91	100	69	100	91.7	82.3	100	100	100	100	100	100	100	100	100	100	100	0	0	0	0	0	0	0	0	92.61	71.52	9.70
67	100	83.7	85.3	100	85.3	86.3	100	99.3	80	100	100	100	100	100	100	100	100	100	100	0	0	0	0	0	0	0	0	93.33	21.01	8.79
69	100	90.7	79.7	100	100	80.7	94.7	100	100	100	100	100	100	100	100	100	100	100	100	0	0	0	0	0	0	0	0	95.48	31.74	9.19
71	100	98.7	74.7	99	100	100	94	90.7	100	100	100	100	100	100	100	100	100	100	100	0	0	0	0	0	0	0	0	96.43	8.04	8.81

Figure A.2: Best F evaluation for shell  $A_E$ .

F	% Coverage per Latitude																			% Average	Distance min [km]	Rate							
	0°	5°	10°	15°	20°	25°	30°	35°	40°	45°	50°	55°	60°	65°	70°	75°	80°	85°	90°										
1	67.3	41.3	18.7	62.7	60	67.7	80	38.3	0	0	0	0	0	0	0	0	0	0	0	0	0	0	0	0	0	0	54.50	831.86	10.00
3	67.3	41.3	21.7	51.7	58.3	60.3	91	39	0	0	0	0	0	0	0	0	0	0	0	0	0	0	0	0	0	0	53.83	214.75	8.51
5	67.3	41.3	21	42.7	37.3	48.3	83.3	37	0	0	0	0	0	0	0	0	0	0	0	0	0	0	0	0	0	0	47.28	163.07	7.42
7	67.3	41.3	17.3	62	57.3	59	88.7	38	0	0	0	0	0	0	0	0	0	0	0	0	0	0	0	0	0	0	53.86	214.75	8.52
9	67.3	41.3	14.7	53.7	60.7	62.7	55.3	31.7	0	0	0	0	0	0	0	0	0	0	0	0	0	0	0	0	0	0	48.43	254.49	7.80
11	67.3	41.3	16.7	44	37.3	35.7	48	31.7	0	0	0	0	0	0	0	0	0	0	0	0	0	0	0	0	0	0	40.25	163.07	6.37

Figure A.3: Best F evaluation for shell  $II_H$ .

A.1 – F parameter

F	% Coverage per Latitude																		% Average	Distance min [km]	Rate	
	0°	5°	10°	15°	20°	25°	30°	35°	40°	45°	50°	55°	60°	65°	70°	75°	80°	85°				90°
<b>1</b>	71.3	53.7	56	40	38.7	49.3	53	82.3	65.3	82.7	79	86	100	100	0	0	0	0	0	68.38	385.57	<b>10.00</b>
<b>3</b>	71.3	53.7	56	38.7	42	49.7	64.3	60	79	66.7	70.3	98.7	100	100	0	0	0	0	0	67.89	177.07	<b>9.10</b>
<b>5</b>	71.3	53.7	56	38.7	42	46.7	74	54.3	71	56.3	93	71.3	100	83	0	0	0	0	0	65.09	37.28	<b>8.20</b>
<b>7</b>	71.3	53.7	56	38.7	38.7	47.7	64.7	76.7	56	81	58	89.3	83	57	0	0	0	0	0	62.27	116.61	<b>8.17</b>
<b>9</b>	71.3	53.7	56	40.3	34.3	48.7	56.3	89.7	54.7	65	91.3	66.3	64.7	71.3	0	0	0	0	0	61.69	1.33	<b>7.58</b>
<b>11</b>	71.3	53.7	56	42.3	29.7	48	59.3	73.3	71	50.7	65	97.7	100	100	0	0	0	0	0	65.57	37.28	<b>8.25</b>
<b>13</b>	71.3	53.7	56	44	24.3	49	68.7	52	76.3	77.3	80.3	72.7	100	100	0	0	0	0	0	66.11	10.81	<b>8.21</b>
<b>15</b>	71.3	53.7	56	43.7	30	48.7	67	68	63.7	63	82	100	100	100	0	0	0	0	0	67.65	135.76	<b>8.91</b>
<b>17</b>	71.3	53.7	56	42.3	34.7	48	55	86.7	58	52.3	76.7	93.7	99	100	0	0	0	0	0	66.24	18.72	<b>8.26</b>

Figure A.4: Best F evaluation for shell  $II_I$ .



# Appendix B

## Python codes

The following are the codes that constituted the results previously shown. Obviously, these are some more important code snippets.

### B.1 Walker constellation

This code was used both for finding the best  $F$  parameter and for orbit propagation using Walker's pattern.

```
1 #Import necessary packages
2 from cProfile import label
3 import numpy as np
4 import math
5 import pandas as pd
6 import itertools as it
7 import csv
8 import matplotlib.pyplot as plt
9
10 #-----SET PARAMETERS-----#
11
12 shell_name= 'Shell_A_a'
13 h=540           #altitude in km
14 P=72           #num. of planes
15 N=22           #num sat. per plane
16 inc=math.radians(53.2) #inclination
17 dt =1         #timestep in seconds
18 R=6378        #Earth radius in km
19 mu= 3.986e5   #Earth gravitational parameter (km3 per s2)
20 a=R+h        #semi-major axis in km
21 e=0          #eccentricity
22 N_tot=P*N    #total num. of satellites
```

```

23 | omega=0                                #argument of periapsis in degrees
24 | S=N_tot/P
25 | tau=0                                  #constant
26 | n = ((math.sqrt(mu/(a**3)))) #mean angular motion (rad per second)
27 | T = (2*math.pi/math.sqrt(mu))*a**(3/2) #orbital period in seconds
28 | time = 1*T #Choose how many orbital periods to run simulation
29 | number_Timesteps = int(time/dt)+1 #number of timesteps
30 | print("\nThe simulation will run for " + str(number_Timesteps) + "
    |         timesteps.\n")
31 | Timestamps = np.arange(0,time,dt)
32 |
33 | #-----CREATE DATA-----#
34 |
35 | x=np.zeros((N,P))
36 | y=np.zeros((N,P))
37 | z=np.zeros((N,P))
38 | cos_omega=math.cos(omega)
39 | sin_omega=math.sin(omega)
40 | cos_inc=math.cos(inc)
41 | sin_inc=math.sin(inc)
42 | min_distances_each_F=np.zeros(P)
43 |
44 | for F in range(0,P):
45 |     min_distances_each_t=np.zeros(number_Timesteps)
46 |     tt=0
47 |     for t in (Timestamps):
48 |         min_distance_t=1000000000
49 |         for i in range(1,P+1):
50 |             raan=((2*math.pi)/P)*(i-1) #DELTA Walker
51 |             #raan=((math.pi)/P)*(i-1) #STAR Walker
52 |             cos_raan=math.cos(raan)
53 |             sin_raan=math.sin(raan)
54 |             l1= cos_omega*cos_raan - sin_omega*sin_raan*cos_inc
55 |             m1= cos_omega*sin_raan + sin_omega*cos_raan*cos_inc
56 |             n1= sin_omega*sin_inc
57 |             l2= -sin_omega*cos_raan - cos_omega*sin_raan*cos_inc
58 |             m2= -sin_omega*sin_raan + cos_omega*cos_raan*cos_inc
59 |             n2= cos_omega*sin_inc
60 |             for j in range(1,N+1):
61 |                 M_o=((2*math.pi)/S)*(j-1)+((2*math.pi)/N_tot)*F*(i-1)
62 |                 E=M_o+n*t
63 |                 teta=E
64 |                 cos_teta=math.cos(teta)
65 |                 sin_teta=math.sin(teta)
66 |                 r=(a*(1-e**2)) / (1+e*cos_teta)
67 |                 x[j-1,i-1]= r*(l1*cos_teta + l2*sin_teta)
68 |                 y[j-1,i-1]= r*(m1*cos_teta + m2*sin_teta)
69 |                 z[j-1,i-1]= r*(n1*cos_teta + n2*sin_teta)
70 |                 if j!=1 or (i!=1 and j==1):

```

```

71         distance=math.sqrt((x[0,0]-x[j-1,i-1])**2+(y
[0,0]-y[j-1,i-1])**2+(z[0,0]-z[j-1,i-1])**2)
72         if distance<min_distance_t:
73             min_distance_t=distance
74             min_distances_each_t[tt]=min_distance_t
75             tt=tt+1
76     min_distance_f=min(min_distances_each_t)
77     print('The minimum distance with F= ' + str(F) + ' is ' + str(
min_distance_f) + ' km')
78     min_distances_each_F[F]=min_distance_f
79     max_min_distance=max(min_distances_each_F)
80     f=np.argmax(min_distances_each_F)
81     print('\nThe maximum distance between satellites is ' + str(
max_min_distance) + ' with F=' + str(f) +'\n')

```

## B.2 Communication link between two cities

This code was used to determine what satellites are in view with both the transmitting and receiving ground stations.

```

1  [...] #Import necessary packages
2  [...] #import data from the previous code
3  el= 40 #Elevation angle in deg
4  name_of_the_city_i="Torino" #First Ground Station
5  latitude_i= 45.0781
6  longitude_i=7.6761
7  altitude_i= R
8  name_of_the_city_f="San Francisco" #Last Ground Station
9  latitude_f= 37.774929
10 longitude_f=-122.419416
11 altitude_f= R
12
13 #-----CREATE DATA-----#
14
15 # Converting lat/long to cartesian
16 def get_cartesian(lat=None,lon=None):
17     lat, lon = np.deg2rad(lat), np.deg2rad(lon)
18     x = R * np.cos(lat) * np.cos(lon)
19     y = R * np.cos(lat) * np.sin(lon)
20     z = R *np.sin(lat)
21     return x,y,z

```

```

22 (x_gsii , y_gsii , z_gsii)=get_cartesian(latitude_i , longitude_i) #xyz GSi
23 (x_gsff , y_gsff , z_gsff)=get_cartesian(latitude_f , longitude_f) #xyz GSf
24
25 # Calculate distance between the two city
26 from numpy import sin , cos , arccos , pi , round , zeros
27 def rad2deg(radians):
28     degrees = radians * 180 / pi
29     return degrees
30 def deg2rad(degrees):
31     radians = degrees * pi / 180
32     return radians
33 def getDistanceBetweenPoints(latitude1 , longitude1 , latitude2 ,
34     longitude2):
35     theta = longitude1 - longitude2
36     distance = 60 * 1.1515 * rad2deg(arccos((sin(deg2rad(latitude1))
37     * sin(deg2rad(latitude2))) + (cos(deg2rad(latitude1)) * cos(
38     deg2rad(latitude2)) * cos(deg2rad(theta))))))
39     return round(distance * 1.609344 , 2)
40
41 distance=getDistanceBetweenPoints(latitude_i , longitude_i , latitude_f
42     , longitude_f)
43 if distance > 3000:
44     print("\nThe distance between " + name_of_the_city_i + " and " +
45     name_of_the_city_f + " is " + str(distance)+ " km so using
46     Starlink can be convenient")
47 else:
48     warnings.warn("The distance between " + name_of_the_city_i + " and
49     " + name_of_the_city_f + " is " + str(distance) + " so using
50     Starlink couldn't be convenient")
51
52 with open(str(shell_name)+'_distance_between_gs' , 'w' , newline="") as
53     file:
54     writer = csv.writer(file)
55     file.write(str(distance))
56
57 #Earth rotation
58 x_gsi=np.zeros(len(Timestamps))
59 y_gsi=np.zeros(len(Timestamps))
60 z_gsi=np.zeros(len(Timestamps))
61 x_gsf=np.zeros(len(Timestamps))
62 y_gsf=np.zeros(len(Timestamps))
63 z_gsf=np.zeros(len(Timestamps))
64 x_gsi[0]=x_gsii
65 y_gsi[0]=y_gsii
66 z_gsi[0]=z_gsii
67 x_gsf[0]=x_gsff
68 y_gsf[0]=y_gsff
69 z_gsf[0]=z_gsff
70 w=(360/(24*3600))*dt #angular velocity of the earth in deg/s

```

```

62 for i in range (1, len(Timestamps)):
63     longitude_i=longitude_i+w
64     latitude_i=latitude_i
65     longitude_f=longitude_f+w
66     latitude_f=latitude_f
67     (x_gsi[i],y_gsi[i],z_gsi[i])=get_cartesian(latitude_i,longitude_i
68     ) # x,y,z first ground station
69     (x_gsf[i],y_gsf[i],z_gsf[i])=get_cartesian(latitude_f,longitude_f
70     ) # x,y,z final ground station
71
72 # Calculate the maximum range between Ground Station and satellites
73 # (look at the picture made on the ipad)
74 beta=rad2deg(math.asin((R/(R+h))*math.sin(deg2rad(el+90))))
75 gamma=180-el-beta-90
76 max_distance=math.sqrt(R**2+(R+h)**2-2*R*(R+h)*math.cos(deg2rad(
77     gamma)))
78
79 [...]# Import coordinates of satellites
80 [...]# Import the name of the satellites
81
82 #Find satellites than can communicate with first ground station
83 with open(str(shell_name)+'_sats_to_first_gs.csv', 'w', newline="")
84 as file:
85     writer = csv.writer(file)
86     writer.writerow(['time','plane','satellite','x','y','z'])
87     for j in range (0,len(Timestamps)):
88         for i in range (0,len(sats)):
89             if float(sats[i][0])==j:
90                 lat= math.asin(float(sats[i][5])/a)*(180/math.pi)
91                 lon= math.atan2(float(sats[i][4]),float(sats[i][3]))
92                 *(180/math.pi)
93                 if ((lon>0 and lon<30) or (lon<0 and lon>-15)) and (lat
94                 >30 and lat<60):
95                     if float(sats[i][0]) ==Timestamps[j]:
96                         distance=math.sqrt( (float(sats[i][3])-x_gsi[j])**2
97                         + (float(sats[i][4])-y_gsi[j])**2 + (float(sats[i][5])-z_gsi[j])
98                         **2 )
99
100                     if distance < max_distance:
101                         writer.writerow(sats[i])
102
103 #to find satellites than can communicate with last ground station
104 with open(str(shell_name)+'_sats_to_last_gs.csv', 'w', newline="") as
105     file:
106         writer = csv.writer(file)
107         writer.writerow(['time','plane','satellite','x','y','z'])
108         for j in range (0,len(Timestamps)):
109             for i in range (0,len(sats)):
110                 if float(sats[i][0])==j:
111                     lat= math.asin(float(sats[i][5])/a)*(180/math.pi)

```

```

102         lon= math.atan2(float(sats[i][4]), float(sats[i][3]))
    *(180/math.pi)
103         if (lon<-95 and lon>-145) and (lat>20 and lat<60):
104             if float(sats[i][0]) ==Timestamps[j]:
105                 distance=math.sqrt( (float(sats[i][3])-x_gsf[j])
    **2 + (float(sats[i][4])-y_gsf[j])**2 + (float(sats[i][5])-z_gsf[j]
    )**2 )
106                 if distance < max_distance:
107                     writer.writerow(sats[i])

```

### B.3 Latency calculation along the best path

This code was used to estimate the ideal latency time it takes for a signal to be transmitted between two ground stations. It takes the best possible path into analysis because Dijkstra's algorithm was implemented.

```

1  [...] #Import necessary packages
2  [...] #Import data from the previous code
3  k=80 #km height of the atmospheric layer above the surface of Earth
4  [...] #Import satellites coordinates from the previous code
5  [...] #Import GS coordinates from the previous code
6  [...] #import satellites that can communicate with the first GS
7  [...] #Import satellites that can communicate with the last GS
8  [...] #Import the name of the satellites
9  [...] #Import the distance between ground station
10
11 class Graph(object):
12     def __init__(self, nodes, init_graph):
13         self.nodes = nodes
14         self.graph = self.construct_graph(nodes, init_graph)
15
16     def construct_graph(self, nodes, init_graph):
17         graph = {}
18         for node in nodes:
19             graph[node] = {}
20         graph.update(init_graph)
21         for node, edges in graph.items():
22             for adjacent_node, value in edges.items():
23                 if graph[adjacent_node].get(node, False) == False:
24                     graph[adjacent_node][node] = value
25     return graph

```

```

26
27 def get_nodes(self):
28     return self.nodes
29
30 def get_outgoing_edges(self, node):
31     connections = []
32     for out_node in self.nodes:
33         if self.graph[node].get(out_node, False) != False:
34             connections.append(out_node)
35     return connections
36
37 def value(self, node1, node2):
38     return self.graph[node1][node2]
39
40 def dijkstra_algorithm(graph, start_node):
41     unvisited_nodes = list(graph.get_nodes())
42     shortest_path = {}
43     previous_nodes = {}
44     max_value = sys.maxsize
45     for node in unvisited_nodes:
46         shortest_path[node] = max_value
47     shortest_path[start_node] = 0
48     while unvisited_nodes:
49         current_min_node = None
50         for node in unvisited_nodes:
51             if current_min_node == None:
52                 current_min_node = node
53             elif shortest_path[node] < shortest_path[current_min_node]:
54                 current_min_node = node
55         neighbors = graph.get_outgoing_edges(current_min_node)
56         for neighbor in neighbors:
57             tentative_value = shortest_path[current_min_node] + graph
58             .value(current_min_node, neighbor)
59             if tentative_value < shortest_path[neighbor]:
60                 shortest_path[neighbor] = tentative_value
61                 previous_nodes[neighbor] = current_min_node
62         unvisited_nodes.remove(current_min_node)
63     return previous_nodes, shortest_path
64
65 def print_result(previous_nodes, shortest_path, start_node,
66 target_node):
67     path = []
68     node = target_node
69     while node != start_node:
70         path.append(node)
71         node = previous_nodes[node]
72     path.append(start_node)

```

```

71     print ("The shortest path in time t= " +str(t) + " s is " + str(
72     round(shortest_path[target_node],2)) + " km long:")
73     print ("The shortest path in time t= " +str(t) + " s between " +
74     start_node + " and " + target_node + " is " + str(round(
75     shortest_path[target_node],2)) + " km long:")
76     print("We found the following best path with a value of {}".format(
77     shortest_path[target_node]))
78     print(" -> ".join(reversed(path)))
79     writer2.writerow([t,(round(shortest_path[target_node],2)),rtt,"",
80     .join(reversed(path))])
81
82 #-----CREATE DATA-----#
83
84 max_range=(math.sqrt((R+h)**2-(R+k)**2))*2
85 print('The maximum LILS range is ' + str(round(max_range,2)) + ' km')
86 rtt_avarage=[]
87 rtt_min=[]
88 rtt_max=[]
89 with open(str(shell_name)+'_time_path.csv', 'w', newline="") as
90     filetime:
91     writer = csv.writer(filetime)
92     writer.writerow(["time", "max", "average", "min"])
93     with open(str(shell_name)+'_switch.csv', 'w', newline="") as
94         file_switch:
95         writer2 = csv.writer(file_switch)
96         writer2.writerow(["time", "length", "rtt", "path"])
97         k=0
98         v=-1
99         w=-1
100        for t in (Timestamps):
101            init_graph = {}
102            new_sats=[]
103            nodes=[]
104            for i in range(0,len(sats)):
105                if float(sats[i][0])==t:
106                    lat= math.asin(float(sats[i][5])/a)*(180/math.pi)
107                    lon= math.atan2(float(sats[i][4]),float(sats[i][3]))
108                    *(180/math.pi)
109                    if ((lon>0 and lon<40) or (lon<0 and lon>-140)) and (lat
110                    >20 and lat<70):
111                        nodes.append(nodi[int(i-num_of_sat*t)])
112                        new_sats.append(sats[i][:])
113            num_of_sats=len(nodes)
114            for node in nodes:
115                init_graph[node] = {}
116            min_lens=[]
117            rttt=[]
118            for n in range(0,len(nodes)):
119                x_ref=float(new_sats[n][3])

```

```

111     y_ref=float(new_sats[n][4])
112     z_ref=float(new_sats[n][5])
113     for i in range(0,len(nodes)):
114         if i!=n:
115             x_neighbor=float(new_sats[i][3])
116             y_neighbor=float(new_sats[i][4])
117             z_neighbor=float(new_sats[i][5])
118             distance=math.sqrt( (x_ref-x_neighbor)**2 + (y_ref-
y_neighbor)**2 + (z_ref-z_neighbor)**2 )
119             if distance<max_range:
120                 init_graph[n][nodes[i]] = distance
121     graph = Graph(nodes, init_graph)
122     for i in range(0,len(sats_gsi)):
123         if float(sats_gsi[i][0])==t:
124             name_first_sat = 's' + str(sats_gsi[i][1]).zfill(4)+'.'+
str(sats_gsi[i][2]).zfill(3)
125             name_first_sat=str(name_first_sat)
126             v=v+1
127             k=w
128             for j in range(0,len(sats_gsf)):
129                 if float(sats_gsf[j][0])==t:
130                     name_last_sat = 's' + str(sats_gsf[j][1]).zfill(4)+'.'+
+str(sats_gsf[j][2]).zfill(3)
131                     name_last_sat=str(name_last_sat)
132                     k=k+1
133                     previous_nodes, shortest_path = dijkstra_algorithm(
graph=graph, start_node=name_first_sat)
134                     #calculate the RTT (one direction)
135                     distance1=math.sqrt( (float(x_gsi[int(t)])-float(
sats_gsi[int(v)][3]))**2+(float(y_gsi[int(t)])-float(sats_gsi[int(
v)][4]))**2+(float(z_gsi[int(t)])-float(sats_gsi[int(v)][5]))**2)
136                     distance2=math.sqrt( (float(x_gsf[int(t)])-float(
sats_gsf[int(k)][3]))**2+(float(y_gsf[int(t)])-float(sats_gsf[int(
k)][4]))**2+(float(z_gsf[int(t)])-float(sats_gsf[int(k)][5]))**2)
137                     length_path=round(distance1+distance2+shortest_path[
name_last_sat],2)
138                     c=299792.458 #km/s
139                     rtt=round( (length_path/c)*1000, 2) #ms
140                     rttt.append(rtt)
141                     print_result(previous_nodes, shortest_path,
start_node=name_first_sat, target_node=name_last_sat)
142                     min_lens.append(shortest_path[name_last_sat])
143     w=k
144     if rttt==[]:
145         print('Time='+str(t)+'s      no connection available')
146         rtt_avarage.append(math.nan)
147         rtt_min.append(math.nan)
148         rtt_max.append(math.nan)
149         writer.writerow([t, math.nan,math.nan, math.nan])

```

```
150     else :
151         rtt_avarage.append(sum(rttt)/len(rttt))
152         rtt_min.append(min(rttt))
153         rtt_max.append(max(rttt))
154         writer.writerow([t, max(rttt),sum(rttt)/len(rttt), min(
rttt)])
155         print('Time='+str(t)+'s          max: '+str(max(rttt))+'ms
min: '+str(min(rttt))+'ms  average: '+str(round(sum(rttt)/len(
rttt),2))+'ms')
```

# Appendix C

## Alternative proposals

This appendix will include all the material used that adds detail to the alternatives to the original shells.

### C.1 F parameter evaluation of $A_A$ alternatives

There are seven alternative shells to the original and for each of them some details are reported. Similar to the original shell case, also in the derivatives, the study for every odd (or even, as the case may be) F led to the collision.

Hence only half of all possible parameters appear in the next tables.

### C.2 Switches available for $A_A$ alternatives

For each of the seven alternatives proposed to the  $A_A$  shell, all the paths and their relative durations that are established at the instant  $t = 300$  s of the connection between Torino and San Francisco are given below.

### C.3 F parameter evaluation of $II_C$ alternatives

There are nine alternative shells to the original and for each of them some details are reported. Similar to the original shell case, also in the derivatives, the study for every odd (or even, as the case may be) F led to the collision.

Hence only half of all possible parameters appear in the next tables.

Alternative proposals

F	% Coverage per Latitude																			% Average	Distance min [km]	Rate
	0°	5°	10°	15°	20°	25°	30°	35°	40°	45°	50°	55°	60°	65°	70°	75°	80°	85°	90°			
0	100	94.3	73.3	99.7	100	98.7	84	97.7	100	100	100	100	0	0	0	0	0	0	0	95.64	16.98	8.84
2	100	99.7	78.7	94	100	100	100	100	100	100	100	100	0	0	0	0	0	0	0	97.70	10.74	8.90
4	100	100	93.3	86.3	100	100	100	100	100	100	100	100	0	0	0	0	0	0	0	98.30	3.99	8.82
6	100	100	100	96	92	98	100	100	100	100	100	100	0	0	0	0	0	0	0	98.83	59.57	9.90
8	100	100	100	100	100	100	100	100	100	100	100	100	0	0	0	0	0	0	0	100.00	28.53	9.44
10	100	100	100	100	100	100	100	100	100	100	100	100	0	0	0	0	0	0	0	100.00	39.29	9.63
12	100	100	100	100	100	100	100	100	100	100	100	100	0	0	0	0	0	0	0	100.00	21.87	9.32
14	100	100	100	100	100	100	100	100	100	100	100	100	0	0	0	0	0	0	0	100.00	12.87	9.15
16	100	100	100	100	100	100	100	100	100	100	100	100	0	0	0	0	0	0	0	100.00	12.94	9.15
18	100	100	100	99.3	100	100	100	100	100	100	100	100	0	0	0	0	0	0	0	99.94	4.39	8.98
20	100	100	100	100	100	100	100	100	100	100	100	100	0	0	0	0	0	0	0	100.00	28.53	9.44
22	100	100	100	100	100	100	100	100	100	100	100	100	0	0	0	0	0	0	0	100.00	3.99	8.97
24	100	100	100	100	100	100	100	100	100	100	100	100	0	0	0	0	0	0	0	100.00	34.41	9.55
26	100	100	100	100	100	100	100	100	100	100	100	100	0	0	0	0	0	0	0	100.00	13.87	9.17
28	100	100	100	100	100	100	100	100	100	100	100	100	0	0	0	0	0	0	0	100.00	17.18	9.23
30	100	100	100	100	100	100	100	100	100	100	100	100	0	0	0	0	0	0	0	100.00	24.48	9.36
32	100	100	100	100	100	100	100	100	100	100	100	100	0	0	0	0	0	0	0	100.00	18.91	9.26
34	100	100	100	100	100	100	100	100	100	100	100	100	0	0	0	0	0	0	0	100.00	59.15	10.00
36	100	100	100	100	100	100	100	100	100	100	100	100	0	0	0	0	0	0	0	100.00	53.66	9.90
38	100	100	100	100	100	100	100	100	100	100	100	100	0	0	0	0	0	0	0	100.00	59.36	10.00
40	100	100	100	100	100	100	100	100	100	100	100	100	0	0	0	0	0	0	0	100.00	3.99	8.97
42	100	100	100	100	100	100	100	100	100	100	100	100	0	0	0	0	0	0	0	100.00	37.84	9.61
44	100	100	98.3	88.7	82.7	86.7	90.7	100	100	100	100	100	0	0	0	0	0	0	0	95.59	6.64	8.64
46	100	99.7	86.7	78	92.7	100	100	100	100	100	100	100	0	0	0	0	0	0	0	96.43	15.24	8.87
48	100	96.3	74.7	86.7	100	100	100	100	100	100	100	100	0	0	0	0	0	0	0	96.48	21.87	9.00
50	100	88.7	70	95.3	100	96.7	83.7	76.7	82.7	100	100	100	0	0	0	0	0	0	0	91.15	12.87	8.36
52	100	81.7	75.3	100	94.7	69.3	83.7	100	100	100	100	100	0	0	0	0	0	0	0	92.06	61.32	9.33
54	100	75.7	81.7	100	73.3	78.7	100	96.3	83.3	82.7	100	100	0	0	0	0	0	0	0	89.31	15.13	8.24
56	100	70	88.3	91.3	62.3	99.3	87.3	65.7	89.7	100	100	91.7	0	0	0	0	0	0	0	87.13	28.53	8.29
58	100	65.3	95	76.7	78.3	95	62.7	97	87	61	71.7	65.3	0	0	0	0	0	0	0	79.58	3.99	7.16
60	100	62	100	62.7	97	74	89	83.7	70	100	78.3	58	0	0	0	0	0	0	0	81.23	16.79	7.55
62	100	63	100	61	100	69	100	65.3	100	70	100	63	0	0	0	0	0	0	0	82.61	9.55	7.54
64	100	67.7	97	76.7	86.3	92.3	71.3	100	68	100	100	88	0	0	0	0	0	0	0	87.28	14.07	8.04
66	100	74	89.7	93.3	72	100	79.7	88	100	96	100	100	0	0	0	0	0	0	0	91.06	24.48	8.57
68	100	80	83.7	100	79	89.3	100	88	86.3	100	100	100	0	0	0	0	0	0	0	92.19	18.91	8.56
70	100	87.7	79.3	100	98.7	70.7	100	100	100	100	100	100	0	0	0	0	0	0	0	94.70	33.82	9.06

Figure C.1: Best F evaluation for shell  $A_{41}$ .

C.3 – F parameter evaluation of  $II_C$  alternatives

F	% Coverage per Latitude																			% Average	Distance min [km]	Rate
	0°	5°	10°	15°	20°	25°	30°	35°	40°	45°	50°	55°	60°	65°	70°	75°	80°	85°	90°			
1	100	92	74.3	100	100	91	83.7	100	100	100	100	100	0	0	0	0	0	0	0	95.08	3.05	8.47
3	100	99	74.3	96.3	100	100	100	100	100	100	100	100	0	0	0	0	0	0	0	97.47	5.53	8.73
5	100	100	88.3	89	100	100	100	100	100	100	100	100	0	0	0	0	0	0	0	98.11	3.05	8.74
7	100	100	99	91.3	93.3	99.7	100	100	100	100	100	100	0	0	0	0	0	0	0	98.61	52.53	9.49
9	100	100	100	100	100	100	100	100	100	100	100	100	0	0	0	0	0	0	0	100.00	2.24	8.88
11	100	100	100	100	100	100	100	100	100	100	100	100	0	0	0	0	0	0	0	100.00	38.04	9.42
13	100	100	100	100	100	100	100	100	100	100	100	100	0	0	0	0	0	0	0	100.00	3.05	8.90
15	100	100	100	100	100	100	100	100	100	100	100	100	0	0	0	0	0	0	0	100.00	69.75	9.86
17	100	100	100	100	100	100	100	100	100	100	100	100	0	0	0	0	0	0	0	100.00	3.05	8.90
19	100	100	100	100	100	100	100	100	100	100	100	100	0	0	0	0	0	0	0	100.00	21.78	9.19
21	100	100	100	100	100	100	100	100	100	100	100	100	0	0	0	0	0	0	0	100.00	3.05	8.90
23	100	100	100	100	100	100	100	100	100	100	100	100	0	0	0	0	0	0	0	100.00	23.24	9.21
25	100	100	100	100	100	100	100	100	100	100	100	100	0	0	0	0	0	0	0	100.00	3.05	8.90
27	100	100	98	100	100	100	100	100	100	100	100	100	0	0	0	0	0	0	0	99.83	18.65	9.13
29	100	100	100	100	100	100	100	100	100	100	100	100	0	0	0	0	0	0	0	100.00	3.05	8.90
31	100	100	100	100	100	100	100	100	100	100	100	100	0	0	0	0	0	0	0	100.00	32.51	9.34
33	100	100	100	100	100	100	100	100	100	100	100	100	0	0	0	0	0	0	0	100.00	2.24	8.88
35	100	100	100	100	100	100	100	100	100	100	100	100	0	0	0	0	0	0	0	100.00	46.55	9.53
37	100	100	100	100	100	100	100	100	100	100	100	100	0	0	0	0	0	0	0	100.00	3.05	8.90
39	100	100	100	100	100	100	100	100	100	100	100	100	0	0	0	0	0	0	0	100.00	19.54	9.16
41	100	100	100	100	100	100	100	100	100	100	100	100	0	0	0	0	0	0	0	100.00	3.05	8.90
43	100	100	100	100	100	100	100	100	100	100	100	100	0	0	0	0	0	0	0	100.00	80.12	10.00
45	100	100	98	90.3	84	83.7	90	100	100	100	100	100	0	0	0	0	0	0	0	95.50	3.05	8.50
47	100	99.3	86.7	74.3	84	95.3	99.3	100	94	100	100	100	0	0	0	0	0	0	0	94.41	33.31	8.85
49	100	94.3	74.7	79.3	97.7	100	100	100	100	100	100	100	0	0	0	0	0	0	0	95.50	3.05	8.50
51	100	86.3	63.7	88	100	99.3	86.7	81	86.3	100	100	100	0	0	0	0	0	0	0	90.94	80.12	9.19
53	100	79.3	68.7	97.7	97	72.7	71.7	90.3	100	100	100	100	0	0	0	0	0	0	0	89.78	3.05	8.00
55	100	72.7	74.7	100	75.7	69	97.3	100	87	86	100	100	0	0	0	0	0	0	0	88.53	22.61	8.18
57	100	67	82	93	56.3	91	91	62	78	96	100	83.3	0	0	0	0	0	0	0	83.30	2.24	7.40
59	100	62.3	89.3	79.3	72	99	61	86.3	94.3	66.7	64	61.3	0	0	0	0	0	0	0	77.96	80.12	8.04
61	100	58.7	98.7	66.3	89.3	76	79.3	91	62.3	99.7	80.3	54	0	0	0	0	0	0	0	79.63	3.05	7.10
63	100	58.3	100	57.7	100	59.3	100	57.7	100	62.7	100	68.3	0	0	0	0	0	0	0	80.33	18.65	7.40
65	100	62.7	98	72.3	89	84	79.7	97	70	100	100	91	0	0	0	0	0	0	0	86.98	3.05	7.75
67	100	70	92	89	74	100	72	94	100	89.7	100	100	0	0	0	0	0	0	0	90.06	71.11	8.99
69	100	77.3	86	100	71	95	100	79.7	94.7	100	100	100	0	0	0	0	0	0	0	91.98	3.05	8.19
71	100	84	79.7	100	91.7	75	100	100	100	100	100	100	0	0	0	0	0	0	0	94.20	17.44	8.61

Figure C.2: Best F evaluation for shell  $A_{A2}$ .

Alternative proposals

F	% Coverage per Latitude																			% Average	Distance min [km]	Rate
	0°	5°	10°	15°	20°	25°	30°	35°	40°	45°	50°	55°	60°	65°	70°	75°	80°	85°	90°			
1	100	79	83	100	79.3	85.7	100	100	96.3	100	100	100	0	0	0	0	0	0	0	93.61	10.29	8.51
3	100	86	77.7	100	99.7	75.7	96.3	100	100	100	100	100	0	0	0	0	0	0	0	94.62	51.52	9.30
5	100	94.3	73.7	99	100	100	94	92.3	100	100	100	100	0	0	0	0	0	0	0	96.11	18.39	8.88
7	100	99.7	79.7	93	100	100	100	100	100	100	100	100	0	0	0	0	0	0	0	97.70	17.95	9.01
9	100	100	93.3	86.7	98.7	100	100	100	100	100	100	100	0	0	0	0	0	0	0	98.23	2.63	8.77
11	100	100	98.3	96	96.7	99.7	100	100	100	100	100	100	0	0	0	0	0	0	0	99.23	11.42	9.03
13	100	100	100	100	100	100	100	100	100	100	100	100	0	0	0	0	0	0	0	100.00	10.29	9.08
15	100	100	100	100	100	100	100	100	100	100	100	100	0	0	0	0	0	0	0	100.00	3.99	8.96
17	100	100	100	100	100	100	100	100	100	100	100	100	0	0	0	0	0	0	0	100.00	21.62	9.28
19	100	100	100	100	100	100	100	100	100	100	100	100	0	0	0	0	0	0	0	100.00	64.43	10.00
21	100	100	100	100	100	97.3	100	100	100	100	100	100	0	0	0	0	0	0	0	99.78	16.19	9.16
23	99.3	100	100	97	100	100	99.3	100	100	100	100	100	0	0	0	0	0	0	0	99.63	43.93	9.62
25	98	100	100	100	100	98.7	100	100	99.7	100	100	99	0	0	0	0	0	0	0	99.62	10.29	9.05
27	98.3	96.7	100	100	100	100	100	98.3	100	100	100	100	0	0	0	0	0	0	0	99.44	66.27	9.98
29	100	96.7	95.3	100	99.7	100	100	100	100	100	100	100	0	0	0	0	0	0	0	99.31	42.53	9.57
31	100	98.3	95.3	100	100	100	100	100	100	100	100	100	0	0	0	0	0	0	0	99.47	45.81	9.64
33	100	100	99.3	100	100	100	100	100	100	100	100	100	0	0	0	0	0	0	0	99.94	3.99	8.96
35	100	100	100	100	100	100	100	100	100	100	100	100	0	0	0	0	0	0	0	100.00	11.42	9.10
37	100	100	100	99	100	100	100	100	100	100	100	100	0	0	0	0	0	0	0	99.92	10.29	9.07
39	100	100	100	99.7	99	99.7	100	100	100	100	100	100	0	0	0	0	0	0	0	99.87	51.52	9.77
41	100	100	100	100	100	99.3	98.7	100	100	100	100	100	0	0	0	0	0	0	0	99.83	9.41	9.05
43	100	100	100	100	100	100	100	100	100	100	100	100	0	0	0	0	0	0	0	100.00	17.95	9.21
45	100	100	100	100	100	100	100	100	100	100	100	100	0	0	0	0	0	0	0	100.00	42.53	9.63
47	100	100	97.7	92.3	87.7	90	98	100	100	100	100	100	0	0	0	0	0	0	0	97.14	48.40	9.48
49	100	98.7	86	75.3	70	77.7	81.7	81	99.7	100	100	100	0	0	0	0	0	0	0	89.18	10.29	8.12
51	100	91.7	74	66.7	81.7	94.3	100	100	100	93.3	100	100	0	0	0	0	0	0	0	91.81	3.99	8.23
53	100	84	63.3	75	94.3	100	94.3	89	95.3	100	100	100	0	0	0	0	0	0	0	91.27	42.53	8.85
55	100	78.3	59.7	85	100	77.7	60	65.3	76	78.7	100	100	0	0	0	0	0	0	0	81.73	3.35	7.32
57	100	72	65.7	94	78.7	51	73.3	98.3	96.3	93.3	100	93.7	0	0	0	0	0	0	0	84.69	61.01	8.58
59	99.3	67.7	72.3	95	57	68.7	99.7	74	58.7	75.7	83.3	71	0	0	0	0	0	0	0	76.87	11.42	7.04
61	98	63	80.3	80	52	92.7	72.3	67	96.7	73.7	51	45.3	0	0	0	0	0	0	0	72.67	0.39	6.32
63	98.3	60	88	66	71.7	85.3	62.7	100	57.3	79	88.7	57.7	0	0	0	0	0	0	0	76.23	59.89	7.80
65	100	57.3	97.3	54	92.3	66	91	65.7	87.7	76.7	100	71	0	0	0	0	0	0	0	79.92	21.62	7.49
67	100	58.3	98.7	57	95	69.7	89.3	76.3	84.7	100	100	98.3	0	0	0	0	0	0	0	85.61	4.41	7.69
69	100	65.7	93	74.3	82.3	94	63.7	100	91.3	80.3	100	100	0	0	0	0	0	0	0	87.05	3.99	7.81
71	100	72	87	92	69.7	100	88	78.7	100	100	100	100	0	0	0	0	0	0	0	90.62	7.67	8.20

Figure C.3: Best F evaluation for shell  $A_{43}$ .

C.3 – F parameter evaluation of  $II_C$  alternatives

F	% Coverage per Latitude																			% Average	distance min [km]	Rate
	0°	5°	10°	15°	20°	25°	30°	35°	40°	45°	50°	55°	60°	65°	70°	75°	80°	85°	90°			
1	100	64	91.3	81.3	74.3	100	72.3	91.3	100	100	100	100	0	0	0	0	0	0	0	89.54	29.97	8.50
3	100	72.7	86.7	99.3	66.7	97.7	100	88.7	89.7	100	100	100	0	0	0	0	0	0	0	91.79	3.03	8.22
5	100	80.7	82.3	100	88.7	81.3	100	100	100	100	100	100	0	0	0	0	0	0	0	94.42	9.48	8.58
7	100	88.3	78.3	100	100	90.3	88	100	100	100	100	100	0	0	0	0	0	0	0	95.41	12.53	8.72
9	100	97.3	73.7	98.7	100	100	100	100	100	100	100	100	0	0	0	0	0	0	0	97.48	32.58	9.25
11	100	100	85	91.3	100	100	100	100	100	100	100	100	0	0	0	0	0	0	0	98.03	4.38	8.81
13	100	100	94.7	93	95.7	99	100	100	100	100	100	100	0	0	0	0	0	0	0	98.53	19.18	9.12
15	100	99.3	99.3	99	99.3	99.3	100	100	100	100	100	100	0	0	0	0	0	0	0	99.68	57.30	9.87
17	100	100	100	100	97.7	100	100	100	100	100	100	100	0	0	0	0	0	0	0	99.81	45.10	9.67
19	99	100	100	99.7	100	100	100	100	100	100	100	100	0	0	0	0	0	0	0	99.89	64.16	10.00
21	94.7	100	96	100	99	100	100	100	100	100	100	100	0	0	0	0	0	0	0	99.14	8.65	8.99
23	90.7	100	95	100	99.3	100	99.3	100	100	100	100	100	0	0	0	0	0	0	0	98.69	1.22	8.76
25	88	100	99.3	86.7	100	99	100	100	100	100	100	100	0	0	0	0	0	0	0	97.75	21.09	9.08
27	87	99.3	100	99	90.3	100	100	89	100	100	100	84	0	0	0	0	0	0	0	95.72	3.03	8.57
29	88.7	95.7	100	100	99.3	92.3	97.3	100	100	100	100	100	0	0	0	0	0	0	0	97.78	4.38	8.78
31	92.7	93.7	97	100	100	100	100	100	100	100	100	100	0	0	0	0	0	0	0	98.62	14.35	9.04
33	97.7	94.7	87	97.3	98.3	96.3	100	100	100	100	100	100	0	0	0	0	0	0	0	97.61	22.84	9.10
35	100	97	92	100	100	100	100	100	100	100	100	100	0	0	0	0	0	0	0	99.08	17.88	9.14
37	100	98	94.3	99.3	100	100	100	100	100	100	100	100	0	0	0	0	0	0	0	99.30	2.95	8.89
39	100	99	98	93.3	99.7	100	100	100	100	100	100	100	0	0	0	0	0	0	0	99.17	19.80	9.18
41	100	100	100	99	91	100	100	100	100	100	100	100	0	0	0	0	0	0	0	99.17	54.10	9.77
43	100	100	100	100	96.7	89	100	100	100	100	100	100	0	0	0	0	0	0	0	98.81	58.17	9.80
45	100	100	100	100	100	98.7	92	100	100	100	100	100	0	0	0	0	0	0	0	99.23	32.58	9.41
47	100	100	100	100	100	100	100	97	100	100	100	100	0	0	0	0	0	0	0	99.75	4.38	8.96
49	100	100	97.7	94.3	94	96.7	100	100	100	100	100	100	0	0	0	0	0	0	0	98.56	59.73	9.81
51	100	97	86.7	79.3	73.7	72	75	85.3	100	100	100	100	0	0	0	0	0	0	0	89.08	3.03	7.98
53	100	89.3	76	62.7	67.3	77.7	86	88.7	84.7	99	100	100	0	0	0	0	0	0	0	85.95	34.43	8.25
55	99	82.3	64	62.3	80	94.3	100	99	100	100	100	100	0	0	0	0	0	0	0	90.08	64.16	9.12
57	99	82.3	64	62.3	80	94.3	100	99	100	100	100	100	0	0	0	0	0	0	0	90.08	8.65	8.18
59	90.7	68.3	53.7	80.3	84	58	53.3	75	92.3	100	100	78.3	0	0	0	0	0	0	0	77.83	1.22	6.91
61	88	62.7	60.7	88	64.7	51	81.3	81.3	59.7	53.3	63.7	56.3	0	0	0	0	0	0	0	67.56	9.98	6.19
63	87	58	67.3	83.3	46.7	74.3	78.3	46.7	74	85.7	60	40.7	0	0	0	0	0	0	0	66.83	34.50	6.55
65	88.7	54	76.7	72	57.7	90.3	52.3	80.7	73	62.3	97.3	57	0	0	0	0	0	0	0	71.83	4.38	6.47
67	92.7	52	86	60.7	78	70.7	70.7	80.7	70	86.7	100	79.7	0	0	0	0	0	0	0	77.33	24.74	7.32
69	97.7	50.3	98	51	99	52.3	100	59.7	96.3	95.7	100	100	0	0	0	0	0	0	0	83.33	34.43	8.02
71	100	55.7	95.3	65	87.3	78	77.7	100	74	97	100	100	0	0	0	0	0	0	0	85.83	66.14	8.78

Figure C.4: Best F evaluation for shell  $A_{44}$ .

Alternative proposals

F	% Coverage per Latitude																			% Average	Distance min [km]	Rate
	0°	5°	10°	15°	20°	25°	30°	35°	40°	45°	50°	55°	60°	65°	70°	75°	80°	85°	90°			
1	97.7	55.7	97.7	49.3	96	67	88.7	84	77.7	100	100	100	0	0	0	0	0	0	0	84.48	90.49	8.5
3	100	62.7	92.7	68.7	83.7	92.3	62.7	100	100	100	100	100	0	0	0	0	0	0	0	88.57	46.02	8.58
5	100	71	88.3	87.7	72.7	100	90.7	80.7	100	100	100	100	0	0	0	0	0	0	0	90.93	91.36	9.11
7	100	78	84.7	100	78.7	88.3	100	100	100	100	100	100	0	0	0	0	0	0	0	94.14	10.92	8.86
9	100	85	80	100	98	77.3	99.3	100	100	100	100	100	0	0	0	0	0	0	0	94.97	46.02	9.18
11	100	93	75.3	100	100	100	95	99.7	100	100	100	100	0	0	0	0	0	0	0	96.92	42.82	9.34
13	100	99.7	76	97	100	100	100	100	100	100	100	100	0	0	0	0	0	0	0	97.73	8.97	9.18
15	100	99	89.7	91.3	98	100	100	100	100	100	100	100	0	0	0	0	0	0	0	98.17	43.94	9.46
17	100	96.7	95	97	98	100	100	100	100	100	100	100	0	0	0	0	0	0	0	98.89	112.42	10
19	95.3	96.3	99.7	99.7	93	96	100	100	100	100	100	100	0	0	0	0	0	0	0	98.33	83.17	9.75
21	89	100	100	85.7	98	100	99.7	100	100	100	100	100	0	0	0	0	0	0	0	97.7	46.02	9.43
23	83.7	100	89.3	98.7	100	86	100	100	100	100	100	100	0	0	0	0	0	0	0	96.48	102.15	9.7
25	79.7	100	78.3	100	80	100	86	100	100	100	100	100	0	0	0	0	0	0	0	93.67	171.07	9.91
27	77	100	88	94.7	100	81	100	79	100	97	86	82.7	0	0	0	0	0	0	0	90.45	27.75	8.63
29	76.7	97.7	99	76.7	99.7	100	78.3	100	100	89.3	100	82.7	0	0	0	0	0	0	0	91.68	34.6	8.79
31	79	92.7	100	99.3	82	92.7	100	100	99	93	100	100	0	0	0	0	0	0	0	94.81	10.92	8.92
33	83.7	89.3	97	100	100	100	99.3	97.3	99	100	100	100	0	0	0	0	0	0	0	97.13	46.02	9.38
35	90.3	88.3	88.7	94.3	99.7	99.7	100	99.3	100	100	100	100	0	0	0	0	0	0	0	96.69	57.84	9.42
37	97.7	94	82	99	97.7	99.7	100	100	100	100	100	100	0	0	0	0	0	0	0	97.51	0.66	8.97
39	100	96.7	90.3	94.7	100	99.3	100	100	100	100	100	100	0	0	0	0	0	0	0	98.42	46.02	9.5
41	100	98.3	91.3	89.3	99.7	100	99.3	100	100	100	100	100	0	0	0	0	0	0	0	98.16	76.77	9.69
43	100	99.7	94.3	84	87.7	100	100	100	100	100	100	100	0	0	0	0	0	0	0	97.14	37.46	9.32
45	100	100	97.7	93.7	85	87.7	100	100	100	100	100	100	0	0	0	0	0	0	0	97.01	46.02	9.37
47	100	100	100	100	96	86.7	83	100	100	100	100	100	0	0	0	0	0	0	0	97.14	42.76	9.36
49	100	100	100	100	100	99.3	93.7	81.3	100	100	100	100	0	0	0	0	0	0	0	97.86	27.09	9.32
51	100	99.3	98.7	95.7	96.7	100	100	100	90.3	100	100	100	0	0	0	0	0	0	0	98.39	46.02	9.5
53	100	93	85.3	78	75	74	79.7	92.3	100	100	100	100	0	0	0	0	0	0	0	89.78	46.24	8.7
55	95.3	85.3	72.3	62	52.7	57.3	62.7	64	66.3	100	100	100	0	0	0	0	0	0	0	76.49	10.92	7.21
57	89	77.7	61	46.3	61.3	75.3	86	92.7	95.3	89.7	100	100	0	0	0	0	0	0	0	81.19	46.02	7.89
59	83.7	70	50.3	56	75.7	85.7	78.3	67.3	62.3	70.7	100	92.3	0	0	0	0	0	0	0	74.36	102.15	7.64
61	79.7	65	41.7	66.7	79.7	66.3	44	52.3	68.7	80	82.3	63.7	0	0	0	0	0	0	0	65.84	10.84	6.22
63	77	60.7	50	78.3	70	41	59.3	78	70.3	51.3	45	43.7	0	0	0	0	0	0	0	60.38	1.16	5.6
65	76.7	57.3	59	77.7	51	54.7	78.3	59	56.7	81.7	66.3	39	0	0	0	0	0	0	0	63.12	34.6	6.13
67	79	55	68.7	73	40.3	80	64.7	63.7	84.3	43.7	100	64.7	0	0	0	0	0	0	0	68.09	13.95	6.45
69	83.7	53.7	79.3	61.7	61	82	58	91.7	48.7	100	100	86.3	0	0	0	0	0	0	0	75.51	46.01	7.36
71	90.3	53.3	89.7	51	83.3	64.3	89	59	100	84.7	100	100	0	0	0	0	0	0	0	80.38	2.63	7.49

Figure C.5: Best F evaluation for shell  $A_{45}$ .

C.3 – F parameter evaluation of  $II_C$  alternatives

F	% Coverage per Latitude																			% Average	Distance min [km]	Rate
	0	5	10	15	20	25	30	35	40	45	50	55	60	65	70	75	80	85	90			
1	84	51	80.7	59	71	72	73	76.3	88.7	74	100	100	0	0	0	0	0	0	0	77.48	3.99	7.48
3	92.3	51.3	93.3	50.3	95.3	56	99.3	69	91	100	100	100	0	0	0	0	0	0	0	83.15	9.48	8.09
5	97.3	55.3	95.7	59.3	89.7	76.7	79.3	100	96.3	100	100	100	0	0	0	0	0	0	0	87.47	8.54	8.49
7	100	61.3	91	76.7	76	100	74	91.7	100	100	100	100	0	0	0	0	0	0	0	89.23	3.07	8.60
9	100	70.3	86.7	94.7	68.3	98	100	94.3	100	100	100	100	0	0	0	0	0	0	0	92.69	57.3	9.42
11	100	78.7	81	100	83.7	84.3	98.7	100	100	100	100	100	0	0	0	0	0	0	0	93.87	46.89	9.45
13	100	86	78	97.3	99	87.7	96	97.7	100	100	100	100	0	0	0	0	0	0	0	95.14	39.76	9.51
15	100	90.7	74	95	98.7	96.7	100	95	100	100	100	100	0	0	0	0	0	0	0	95.84	29.97	9.49
17	97.7	92.3	75.3	84	97	100	98	98	100	100	100	94.7	0	0	0	0	0	0	0	94.75	8.11	9.19
19	91	89	84	94.7	95.7	96.7	98	95.7	100	100	100	100	0	0	0	0	0	0	0	95.40	3.99	9.21
21	82.7	88.3	93.7	99	98.3	92	94	98.7	100	100	100	100	0	0	0	0	0	0	0	95.56	65.52	9.77
23	75.7	91.7	100	80.7	79.7	96.7	99.7	100	100	100	100	100	0	0	0	0	0	0	0	93.68	34.64	9.32
25	70.7	97.3	89	74.3	100	92.3	74.3	96.7	100	100	100	100	0	0	0	0	0	0	0	91.22	39.29	9.13
27	67.7	100	68.3	97.3	83.7	84	99.7	70.7	91	100	100	98.7	0	0	0	0	0	0	0	88.43	56.86	9.01
29	67	99.7	68	97.3	77	95.7	78.7	98.7	76	100	82.7	61.7	0	0	0	0	0	0	0	83.54	20.07	8.22
31	69	96.3	86.3	76.3	100	75.3	92.3	99	71	100	100	89	0	0	0	0	0	0	0	87.88	15.19	8.59
33	71.7	93.3	100	78.7	80.7	100	98.3	80.3	93.3	100	100	100	0	0	0	0	0	0	0	91.36	64.16	9.35
35	77.3	88	96.7	97	91	83	89.3	100	100	100	100	100	0	0	0	0	0	0	0	93.53	53.48	9.47
37	84	83.3	89	94.3	100	99.7	100	100	100	100	100	100	0	0	0	0	0	0	0	95.86	3.99	9.25
39	92.3	87.3	76.7	93.3	91	94	100	96.7	100	100	100	100	0	0	0	0	0	0	0	94.28	107.14	10.00
41	97.3	94	77	90	96.3	97.7	96.3	92	100	100	100	94.7	0	0	0	0	0	0	0	94.61	32.22	9.39
43	100	96	83.3	86.3	98	99.3	92	99	99.3	100	100	100	0	0	0	0	0	0	0	96.10	3.07	9.26
45	100	97.7	85.7	74.7	89	99.7	96.7	100	100	100	100	100	0	0	0	0	0	0	0	95.29	47.56	9.59
47	100	98.7	90.3	75	72.3	93.3	100	97	100	100	100	100	0	0	0	0	0	0	0	93.88	44.89	9.43
49	100	99.3	94.7	84.3	78.7	68	90.7	100	93.7	100	100	100	0	0	0	0	0	0	0	92.45	59.28	9.42
51	100	99.3	97.3	94.7	92.3	81.3	68.7	87	100	100	100	100	0	0	0	0	0	0	0	93.38	62.29	9.53
53	97.7	98.7	98	97.3	100	98.7	92.7	80.7	78.3	100	100	100	0	0	0	0	0	0	0	95.18	27.44	9.41
55	91	91	85.7	83	82	83.7	88.7	100	100	78.7	100	100	0	0	0	0	0	0	0	90.32	3.99	8.72
57	82.7	83.7	75	68.7	63	59.7	59	65	78.3	100	100	100	0	0	0	0	0	0	0	77.93	141.4	8.72
59	75.7	77.3	65.7	52.7	50.3	61.7	69	74.3	76	71.3	100	100	0	0	0	0	0	0	0	72.83	34.64	7.31
61	70.7	71.7	53.7	46	64.3	76.7	74.3	72.7	68	74	100	80.3	0	0	0	0	0	0	0	71.03	39.29	7.18
63	67.7	66	42.3	57	71	65.7	49.7	31.7	41	52.7	56.7	44.3	0	0	0	0	0	0	0	53.82	20.02	5.36
65	67	61	40.3	68.7	65.7	45	36	61.7	69.3	63.3	45.7	34.3	0	0	0	0	0	0	0	54.83	9.61	5.36
67	69	56.7	50.3	70	56	35.7	66.7	71	40.7	71	75.3	40.7	0	0	0	0	0	0	0	58.59	59.28	6.15
69	71.7	53.7	60.3	72.7	39.7	63.3	75	45.7	85	57.7	100	72.7	0	0	0	0	0	0	0	66.46	64.16	6.95
71	77.3	52.3	70.3	67.3	47	83	50.7	85	60	100	100	98	0	0	0	0	0	0	0	74.24	6.21	7.20

Figure C.6: Best F evaluation for shell  $A_{46}$ .

Alternative proposals

F	% Coverage per Latitude																			% Average	Distance min [km]	Rate
	0°	5°	10°	15°	20°	25°	30°	35°	40°	45°	50°	55°	60°	65°	70°	75°	80°	85°	90°			
0	100	94.3	73.3	99.7	100	98.7	84	97.7	100	100	100	100	0	0	0	0	0	0	0	95.64	16.98	8.84
2	100	99.7	78.7	94	100	100	100	100	100	100	100	100	0	0	0	0	0	0	0	97.70	10.74	8.90
4	100	100	93.3	86.3	100	100	100	100	100	100	100	100	0	0	0	0	0	0	0	98.30	3.99	8.82
6	100	100	100	96	92	98	100	100	100	100	100	100	0	0	0	0	0	0	0	98.83	59.57	9.90
8	100	100	100	100	100	100	100	100	100	100	100	100	0	0	0	0	0	0	0	100.00	28.53	9.44
10	100	100	100	100	100	100	100	100	100	100	100	100	0	0	0	0	0	0	0	100.00	39.29	9.63
12	100	100	100	100	100	100	100	100	100	100	100	100	0	0	0	0	0	0	0	100.00	21.87	9.32
14	100	100	100	100	100	100	100	100	100	100	100	100	0	0	0	0	0	0	0	100.00	12.87	9.15
16	100	100	100	100	100	100	100	100	100	100	100	100	0	0	0	0	0	0	0	100.00	12.94	9.15
18	100	100	100	99.3	100	100	100	100	100	100	100	100	0	0	0	0	0	0	0	99.94	4.39	8.98
20	100	100	100	100	100	100	100	100	100	100	100	100	0	0	0	0	0	0	0	100.00	28.53	9.44
22	100	100	100	100	100	100	100	100	100	100	100	100	0	0	0	0	0	0	0	100.00	3.99	8.97
24	100	100	100	100	100	100	100	100	100	100	100	100	0	0	0	0	0	0	0	100.00	34.41	9.55
26	100	100	100	100	100	100	100	100	100	100	100	100	0	0	0	0	0	0	0	100.00	13.87	9.17
28	100	100	100	100	100	100	100	100	100	100	100	100	0	0	0	0	0	0	0	100.00	17.18	9.23
30	100	100	100	100	100	100	100	100	100	100	100	100	0	0	0	0	0	0	0	100.00	24.48	9.36
32	100	100	100	100	100	100	100	100	100	100	100	100	0	0	0	0	0	0	0	100.00	18.91	9.26
34	100	100	100	100	100	100	100	100	100	100	100	100	0	0	0	0	0	0	0	100.00	59.15	10.00
36	100	100	100	100	100	100	100	100	100	100	100	100	0	0	0	0	0	0	0	100.00	53.66	9.90
38	100	100	100	100	100	100	100	100	100	100	100	100	0	0	0	0	0	0	0	100.00	59.36	10.00
40	100	100	100	100	100	100	100	100	100	100	100	100	0	0	0	0	0	0	0	100.00	3.99	8.97
42	100	100	100	100	100	100	100	100	100	100	100	100	0	0	0	0	0	0	0	100.00	37.84	9.61
44	100	100	98.3	88.7	82.7	86.7	90.7	100	100	100	100	100	0	0	0	0	0	0	0	95.59	6.64	8.64
46	100	99.7	86.7	78	92.7	100	100	100	100	100	100	100	0	0	0	0	0	0	0	96.43	15.24	8.87
48	100	96.3	74.7	86.7	100	100	100	100	100	100	100	100	0	0	0	0	0	0	0	96.48	21.87	9.00
50	100	88.7	70	95.3	100	96.7	83.7	76.7	82.7	100	100	100	0	0	0	0	0	0	0	91.15	12.87	8.36
52	100	81.7	75.3	100	94.7	69.3	83.7	100	100	100	100	100	0	0	0	0	0	0	0	92.06	61.32	9.33
54	100	75.7	81.7	100	73.3	78.7	100	96.3	83.3	82.7	100	100	0	0	0	0	0	0	0	89.31	15.13	8.24
56	100	70	88.3	91.3	62.3	99.3	87.3	65.7	89.7	100	100	91.7	0	0	0	0	0	0	0	87.13	28.53	8.29
58	100	65.3	95	76.7	78.3	95	62.7	97	87	61	71.7	65.3	0	0	0	0	0	0	0	79.58	3.99	7.16
60	100	62	100	62.7	97	74	89	83.7	70	100	78.3	58	0	0	0	0	0	0	0	81.23	16.79	7.55
62	100	63	100	61	100	69	100	65.3	100	70	100	63	0	0	0	0	0	0	0	82.61	9.55	7.54
64	100	67.7	97	76.7	86.3	92.3	71.3	100	68	100	100	88	0	0	0	0	0	0	0	87.28	14.07	8.04
66	100	74	89.7	93.3	72	100	79.7	88	100	96	100	100	0	0	0	0	0	0	0	91.06	24.48	8.57
68	100	80	83.7	100	79	89.3	100	88	86.3	100	100	100	0	0	0	0	0	0	0	92.19	18.91	8.56
70	100	87.7	79.3	100	98.7	70.7	100	100	100	100	100	100	0	0	0	0	0	0	0	94.70	33.82	9.06

Figure C.7: Best F evaluation for shell  $A_{A1}$ .

C.3 – F parameter evaluation of  $II_C$  alternatives

F	% Coverage per Latitude																			% Average	Distance min [km]	Rate
	0	5	10	15	20	25	30	35	40	45	50	55	60	65	70	75	80	85	90			
1	72.3	51.3	62.7	72.7	36.3	77.3	63	68.7	78	90.3	100	100	0	0	0	0	0	0	0	72.72	24.22	7.56
3	79.7	51.3	75.7	65	58	83.3	59.3	92	73.3	89	100	100	0	0	0	0	0	0	0	77.22	13.56	7.97
5	87.3	51.3	88	55.7	82	68	93	60.7	100	100	100	100	0	0	0	0	0	0	0	82.17	2.83	8.41
7	94	56.3	97	50.7	97	65	90.7	95	81.3	99	100	100	0	0	0	0	0	0	0	85.50	45.04	8.96
9	95	61.7	93.3	64	86	89.3	69	99.3	100	100	100	100	0	0	0	0	0	0	0	88.13	8.53	9.07
11	96.3	67	89	84.3	74	98.7	90.3	88.7	96	100	100	100	0	0	0	0	0	0	0	90.36	59.74	9.52
13	97.3	73.3	82	93	73.7	86.3	97.7	96.3	99	100	100	100	0	0	0	0	0	0	0	91.55	114.93	9.87
15	95.7	74	78.3	85.3	91	82	88	100	100	100	100	100	0	0	0	0	0	0	0	91.19	156.67	10.00
17	93.7	76.3	73	91	84.3	95.7	77	100	93	99	100	100	0	0	0	0	0	0	0	90.25	84.24	9.61
19	88	80.7	58	88	92.7	84.3	90	100	94.3	100	100	87.7	0	0	0	0	0	0	0	88.64	12.01	9.14
21	78.7	78.7	71.3	75.7	79.3	82	89.7	100	100	100	100	100	0	0	0	0	0	0	0	87.95	43.95	9.20
23	70	75.7	85.7	98.7	98.3	100	100	100	100	100	100	100	0	0	0	0	0	0	0	94.03	74.83	9.96
25	62.7	78.7	95.3	87.7	72.7	66.3	80	90.7	91.7	98	100	100	0	0	0	0	0	0	0	85.32	45.04	8.94
27	57.3	84.7	90.7	60	78.3	100	83.7	66.3	67	72.7	100	100	0	0	0	0	0	0	0	80.06	13.57	8.27
29	55	91	70	70.7	93	57	84.3	91.3	64	69.3	81.7	70	0	0	0	0	0	0	0	74.78	59.74	7.92
31	55.3	93.7	54.7	94.7	58	92.7	64.7	85.7	78	78.3	96.7	58	0	0	0	0	0	0	0	75.88	82.54	8.12
33	59.3	93	65.7	83.7	83.7	67	99.7	64.3	96.7	100	100	99.7	0	0	0	0	0	0	0	84.40	15.51	8.72
35	65	88.3	89.3	63.7	94.3	93.3	71.7	92	100	100	100	100	0	0	0	0	0	0	0	88.13	12.78	9.09
37	72.3	80.7	91	87.7	70.7	90	98.7	100	100	100	100	100	0	0	0	0	0	0	0	90.93	24.23	9.43
39	79.7	71.3	85	87.3	94.7	87	85.7	99.7	100	100	100	100	0	0	0	0	0	0	0	90.87	66.27	9.60
41	87.3	72.3	78.3	85	82.3	96.7	79.7	100	91	99	100	100	0	0	0	0	0	0	0	89.30	79.56	9.49
43	94	80.7	57	90.3	96.3	81.7	88.7	100	96	98	100	87.3	0	0	0	0	0	0	0	89.17	45.04	9.33
45	95	86.3	66	73.3	85.3	88.3	93.7	100	100	100	100	100	0	0	0	0	0	0	0	90.66	8.53	9.33
47	96.3	89	68	69.3	90	98.3	89.3	97.3	99	100	100	100	0	0	0	0	0	0	0	91.38	59.74	9.62
49	97.3	92	73	60.7	69.7	97.3	97.7	87.7	100	100	100	100	0	0	0	0	0	0	0	89.62	30.06	9.32
51	95.7	93	80	72	58.7	70.3	95.3	98.3	95	100	100	100	0	0	0	0	0	0	0	88.19	1.60	9.00
53	93.7	93.7	85.7	82.3	72	63	60.7	95.3	100	100	100	100	0	0	0	0	0	0	0	87.20	99.88	9.36
55	88	88.7	88.7	90.3	87	83	75.3	60.7	89.3	100	100	100	0	0	0	0	0	0	0	87.58	91.37	9.36
57	78.7	79.7	80	81.7	81.7	86.3	95.3	91.7	76.7	88.3	100	100	0	0	0	0	0	0	0	86.68	69.57	9.18
59	70	70.7	70.7	65	61.7	60	61	68	83.7	99.7	100	100	0	0	0	0	0	0	0	75.88	96.67	8.18
61	62.7	64	59	49.3	40.7	37	45	49	49.7	51.7	100	90	0	0	0	0	0	0	0	58.18	2.64	5.96
63	57.3	57.7	48.3	33	41.3	54.7	60.7	62.7	65	72	82.3	61.3	0	0	0	0	0	0	0	58.03	8.98	5.99
65	55	55	37.3	37.3	55	55.7	56	46.7	32.7	34.7	40.7	35	0	0	0	0	0	0	0	45.09	14.95	4.69
67	55.3	54	28.3	51	56.7	56.3	33.3	44	57.3	58.7	49	29	0	0	0	0	0	0	0	47.74	41.05	5.07
69	59.3	52	35.3	60	60	36	52	64.3	51.3	54	89	50.3	0	0	0	0	0	0	0	55.29	114.93	6.14
71	65	51.7	49.7	66.7	49.3	48	71.3	50.7	68.7	75.7	100	80	0	0	0	0	0	0	0	64.73	78.95	6.97

Figure C.8: Best F evaluation for shell  $A_{A7}$ .

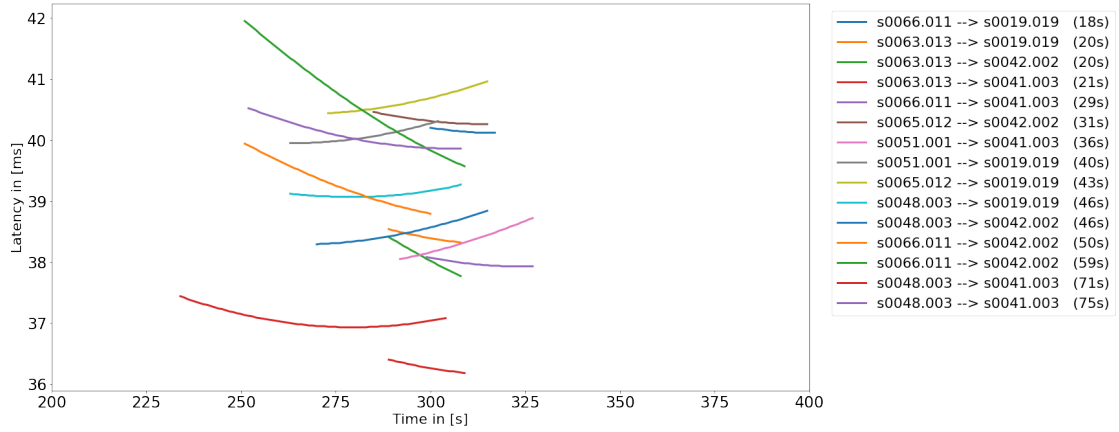


Figure C.9: Latency over time of all the 15 possible paths (shell  $A_{A1}$ ).

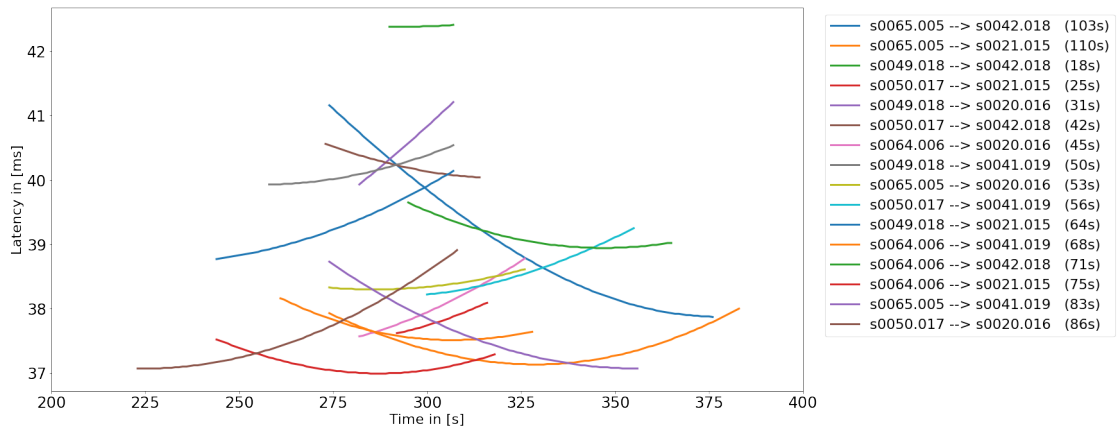


Figure C.10: Latency over time of all the 16 possible paths (shell  $A_{A2}$ ).

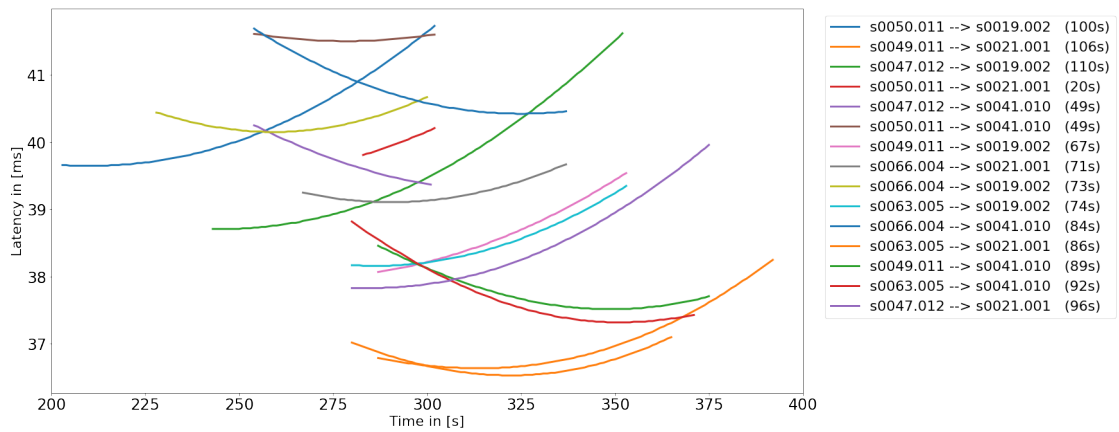
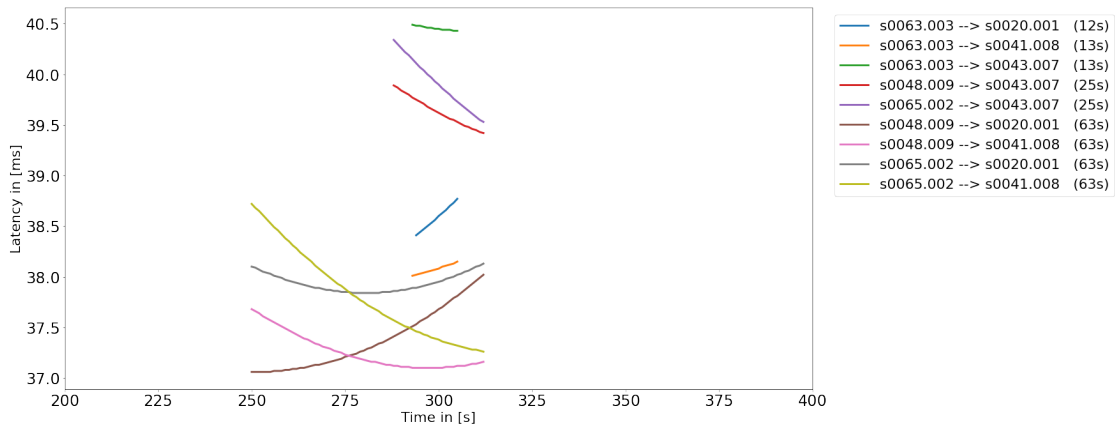
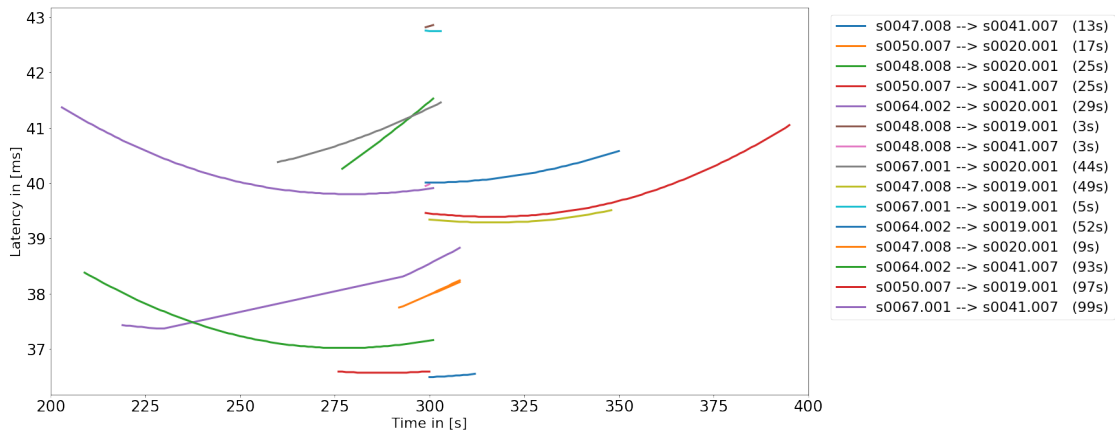


Figure C.11: Latency over time of all the 15 possible paths (shell  $A_{A3}$ ).



**Figure C.12:** Latency over time of all the 9 possible paths (shell  $A_{44}$ ).



**Figure C.13:** Latency over time of all the 15 possible paths (shell  $A_{45}$ ).

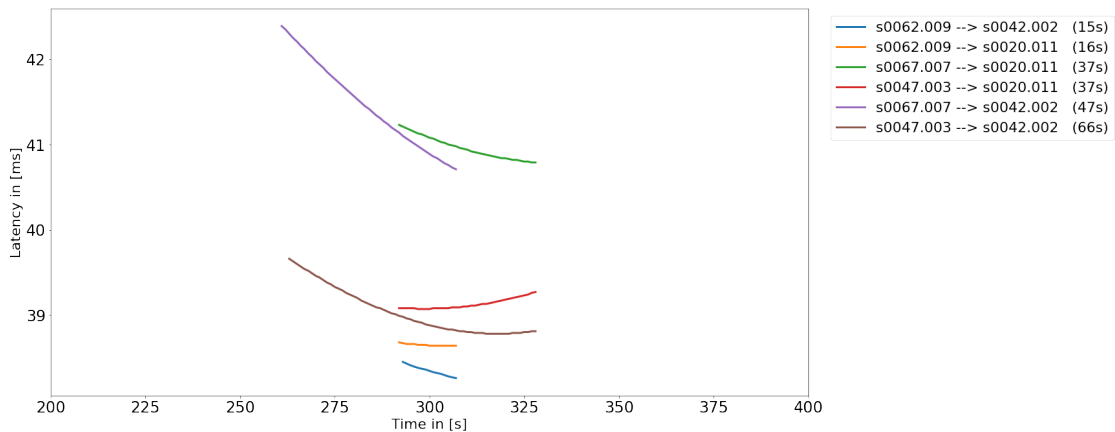


**Figure C.14:** Latency over time of all the 6 possible paths (shell  $A_{46}$ ).

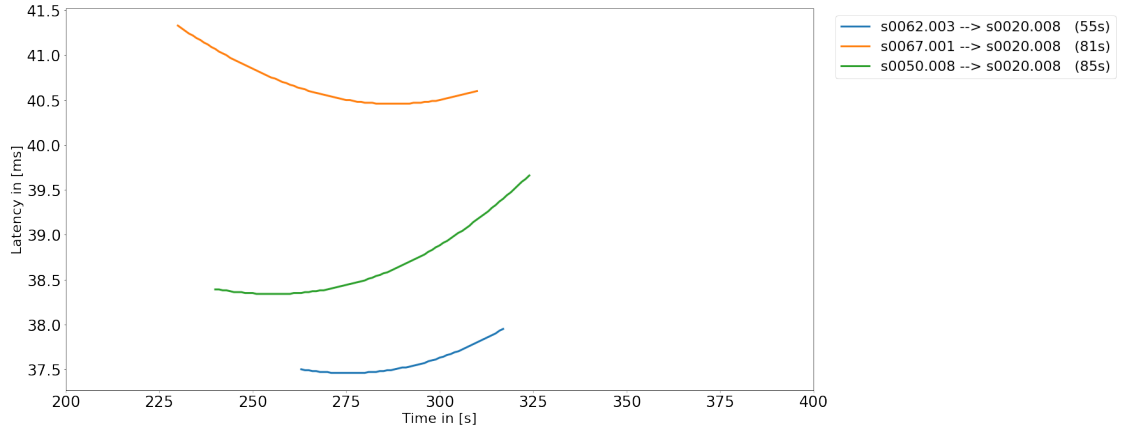


Figure C.15: Latency over time of all the 3 possible paths (shell  $A_{A7}$ ).

F	% Coverage per Latitude																			% Average	Distance min [km]	Rate
	0°	5°	10°	15°	20°	25°	30°	35°	40°	45°	50°	55°	60°	65°	70°	75°	80°	85°	90°			
0	100	100	100	100	100	100	100	100	100	0	0	0	0	0	0	0	0	0	0	100.00	3.37	9.02
2	100	100	100	100	100	100	100	100	100	0	0	0	0	0	0	0	0	0	0	100.00	3.21	9.01
4	100	100	100	100	100	100	100	100	100	0	0	0	0	0	0	0	0	0	0	100.00	3.68	9.04
6	100	100	100	100	100	100	100	100	100	0	0	0	0	0	0	0	0	0	0	100.00	14.81	9.57
8	100	100	100	100	100	100	100	100	100	0	0	0	0	0	0	0	0	0	0	100.00	10.05	9.35
10	100	100	100	100	100	100	100	100	100	0	0	0	0	0	0	0	0	0	0	100.00	24.10	10.00
12	100	100	100	100	100	100	100	100	100	0	0	0	0	0	0	0	0	0	0	100.00	5.61	9.14
14	100	100	100	100	100	100	100	100	100	0	0	0	0	0	0	0	0	0	0	100.00	6.59	9.18
16	100	100	100	100	100	100	100	100	100	0	0	0	0	0	0	0	0	0	0	100.00	3.37	9.02
18	100	100	100	100	100	100	100	100	100	0	0	0	0	0	0	0	0	0	0	100.00	5.10	9.11
20	100	100	100	100	100	100	100	100	100	0	0	0	0	0	0	0	0	0	0	100.00	4.78	9.09
22	100	100	100	100	100	100	100	100	100	0	0	0	0	0	0	0	0	0	0	100.00	10.84	9.38
24	100	100	100	100	100	100	100	100	100	0	0	0	0	0	0	0	0	0	0	100.00	10.49	9.37
26	100	100	100	100	100	100	100	100	100	0	0	0	0	0	0	0	0	0	0	100.00	6.53	9.18
28	100	100	100	100	100	100	100	100	100	0	0	0	0	0	0	0	0	0	0	100.00	3.68	9.04
30	100	100	100	100	100	100	100	100	100	0	0	0	0	0	0	0	0	0	0	100.00	14.80	9.57
32	100	100	100	100	100	100	100	100	100	0	0	0	0	0	0	0	0	0	0	100.00	3.37	9.02
34	100	100	100	100	100	100	100	100	100	0	0	0	0	0	0	0	0	0	0	100.00	2.66	8.98
36	100	100	100	100	100	100	100	100	100	0	0	0	0	0	0	0	0	0	0	100.00	4.78	9.09
38	100	100	100	100	100	100	100	100	100	0	0	0	0	0	0	0	0	0	0	100.00	11.65	9.42
40	100	100	100	100	100	100	100	100	100	0	0	0	0	0	0	0	0	0	0	100.00	7.61	9.23
42	100	100	100	100	100	100	100	100	100	0	0	0	0	0	0	0	0	0	0	100.00	14.80	9.57
44	100	100	100	100	100	100	100	100	100	0	0	0	0	0	0	0	0	0	0	100.00	11.65	9.42
46	100	100	100	100	100	100	100	100	100	0	0	0	0	0	0	0	0	0	0	100.00	16.12	9.63

Figure C.16: Best F evaluation for shell  $II_{C1}$ .

C.3 – F parameter evaluation of  $II_C$  alternatives

F	% Coverage per Latitude																			% Average	Distance min [km]	Rate
	0°	5°	10°	15°	20°	25°	30°	35°	40°	45°	50°	55°	60°	65°	70°	75°	80°	85°	90°			
0	100	100	100	100	100	100	100	100	100	0	0	0	0	0	0	0	0	0	0	100.00	12.29	10.00
2	100	100	100	100	100	100	100	100	100	0	0	0	0	0	0	0	0	0	0	100.00	0.22	8.54
4	100	100	100	100	100	100	100	100	100	0	0	0	0	0	0	0	0	0	0	100.00	9.04	9.70
6	100	100	100	100	100	100	100	100	100	0	0	0	0	0	0	0	0	0	0	100.00	1.40	8.96
8	100	100	100	100	100	100	100	100	100	0	0	0	0	0	0	0	0	0	0	100.00	12.29	10.00
10	100	100	100	100	100	100	100	100	100	0	0	0	0	0	0	0	0	0	0	100.00	0.22	8.54
12	100	100	100	100	100	100	100	100	100	0	0	0	0	0	0	0	0	0	0	100.00	12.29	10.00
14	100	100	100	100	100	100	100	100	100	0	0	0	0	0	0	0	0	0	0	100.00	3.26	9.16
16	100	100	100	100	100	100	100	100	100	0	0	0	0	0	0	0	0	0	0	100.00	5.39	9.37
18	100	100	100	100	100	100	100	100	100	0	0	0	0	0	0	0	0	0	0	100.00	0.22	8.54
20	100	100	100	100	100	100	100	100	100	0	0	0	0	0	0	0	0	0	0	100.00	0.90	8.88
22	100	100	100	100	100	100	100	100	100	0	0	0	0	0	0	0	0	0	0	100.00	9.89	9.78
24	100	100	100	100	100	100	100	100	100	0	0	0	0	0	0	0	0	0	0	100.00	12.29	10.00
26	100	100	100	100	100	100	100	100	100	0	0	0	0	0	0	0	0	0	0	100.00	0.22	8.54
28	100	100	100	100	100	100	100	100	100	0	0	0	0	0	0	0	0	0	0	100.00	11.41	9.92
30	100	100	100	100	100	100	100	100	100	0	0	0	0	0	0	0	0	0	0	100.00	11.67	9.94
32	100	100	100	100	100	100	100	100	100	0	0	0	0	0	0	0	0	0	0	100.00	12.29	10.00
34	100	100	100	100	100	100	100	100	100	0	0	0	0	0	0	0	0	0	0	100.00	0.22	8.54
36	100	100	100	100	100	100	100	100	100	0	0	0	0	0	0	0	0	0	0	100.00	5.61	9.39
38	100	100	100	100	100	100	100	100	100	0	0	0	0	0	0	0	0	0	0	100.00	3.26	9.16
40	100	100	100	100	100	100	100	100	100	0	0	0	0	0	0	0	0	0	0	100.00	12.29	10.00
42	100	100	100	100	100	100	100	100	100	0	0	0	0	0	0	0	0	0	0	100.00	0.22	8.54
44	100	100	100	100	100	100	100	100	100	0	0	0	0	0	0	0	0	0	0	100.00	0.90	8.88
46	100	100	100	100	100	100	100	100	100	0	0	0	0	0	0	0	0	0	0	100.00	11.85	9.96

Figure C.17: Best F evaluation for shell  $II_{C2}$ .

F	% Coverage per Latitude																			% Average	Distance min [km]	Rate
	0°	5°	10°	15°	20°	25°	30°	35°	40°	45°	50°	55°	60°	65°	70°	75°	80°	85°	90°			
1	100	100	100	100	100	100	100	100	100	0	0	0	0	0	0	0	0	0	0	100.00	3.08	8.99
3	100	100	100	100	100	100	100	100	100	0	0	0	0	0	0	0	0	0	0	100.00	9.88	9.30
5	100	100	100	100	100	100	100	100	100	0	0	0	0	0	0	0	0	0	0	100.00	18.47	9.67
7	100	100	100	100	100	100	100	100	100	0	0	0	0	0	0	0	0	0	0	100.00	11.69	9.38
9	100	100	100	100	100	100	100	100	100	0	0	0	0	0	0	0	0	0	0	100.00	1.41	8.89
11	100	100	100	100	100	100	100	100	100	0	0	0	0	0	0	0	0	0	0	100.00	6.44	9.15
13	100	100	100	100	100	100	100	100	100	0	0	0	0	0	0	0	0	0	0	100.00	5.94	9.13
15	100	100	100	100	100	100	100	100	100	0	0	0	0	0	0	0	0	0	0	100.00	5.51	9.11
17	100	100	100	100	100	100	100	100	100	0	0	0	0	0	0	0	0	0	0	100.00	17.46	9.62
19	100	100	100	100	100	100	100	100	100	0	0	0	0	0	0	0	0	0	0	100.00	26.36	10.00
21	100	100	100	100	100	100	100	100	100	0	0	0	0	0	0	0	0	0	0	100.00	4.94	9.08
23	100	100	100	100	100	100	100	100	100	0	0	0	0	0	0	0	0	0	0	100.00	11.44	9.37
25	100	100	100	100	100	100	100	100	100	0	0	0	0	0	0	0	0	0	0	100.00	5.55	9.11
27	100	100	100	100	100	100	100	100	100	0	0	0	0	0	0	0	0	0	0	100.00	3.82	9.03
29	100	100	100	100	100	100	100	100	100	0	0	0	0	0	0	0	0	0	0	100.00	5.94	9.13
31	100	100	100	100	100	100	100	100	100	0	0	0	0	0	0	0	0	0	0	100.00	5.51	9.11
33	100	100	100	100	100	100	100	100	100	0	0	0	0	0	0	0	0	0	0	100.00	1.41	8.89
35	100	100	100	100	100	100	100	100	100	0	0	0	0	0	0	0	0	0	0	100.00	7.13	9.18
37	100	100	100	100	100	100	100	100	100	0	0	0	0	0	0	0	0	0	0	100.00	24.06	9.90
39	100	100	100	100	100	100	100	100	100	0	0	0	0	0	0	0	0	0	0	100.00	17.13	9.61
41	100	100	100	100	100	100	100	100	100	0	0	0	0	0	0	0	0	0	0	100.00	5.55	9.11
43	100	100	100	100	100	100	100	100	100	0	0	0	0	0	0	0	0	0	0	100.00	20.37	9.75
45	100	100	100	100	100	100	100	100	100	0	0	0	0	0	0	0	0	0	0	100.00	4.21	9.05
47	100	100	100	100	100	100	100	100	100	0	0	0	0	0	0	0	0	0	0	100.00	5.51	9.11

Figure C.18: Best F evaluation for shell  $II_{C3}$ .

Alternative proposals

F	% Coverage per Latitude																			% Average	Distance min [km]	Rate
	0°	5°	10°	15°	20°	25°	30°	35°	40°	45°	50°	55°	60°	65°	70°	75°	80°	85°	90°			
0	100	100	100	100	100	100	100	100	100	0	0	0	0	0	0	0	0	0	0	100.00	1.62	8.88
2	100	100	100	100	100	100	100	100	100	0	0	0	0	0	0	0	0	0	0	100.00	9.18	9.14
4	100	100	100	100	100	100	100	100	100	0	0	0	0	0	0	0	0	0	0	100.00	12.13	9.23
6	100	100	100	100	100	100	100	100	100	0	0	0	0	0	0	0	0	0	0	100.00	1.62	8.88
8	100	100	100	100	100	100	100	100	100	0	0	0	0	0	0	0	0	0	0	100.00	3.04	8.95
10	100	100	100	100	100	100	100	100	100	0	0	0	0	0	0	0	0	0	0	100.00	9.18	9.14
12	100	100	100	100	100	100	100	100	100	0	0	0	0	0	0	0	0	0	0	100.00	1.62	8.88
14	100	100	100	100	100	100	100	100	100	0	0	0	0	0	0	0	0	0	0	100.00	15.04	9.31
16	100	100	100	100	100	100	100	100	100	0	0	0	0	0	0	0	0	0	0	100.00	39.24	10.00
18	100	100	100	100	100	100	100	100	100	0	0	0	0	0	0	0	0	0	0	100.00	1.62	8.88
20	100	100	100	100	100	100	100	100	100	0	0	0	0	0	0	0	0	0	0	100.00	0.59	8.76
22	100	100	100	100	100	100	100	100	100	0	0	0	0	0	0	0	0	0	0	100.00	2.85	8.94
24	100	100	100	100	100	100	100	100	100	0	0	0	0	0	0	0	0	0	0	100.00	1.62	8.88
26	100	100	100	100	100	100	100	100	100	0	0	0	0	0	0	0	0	0	0	100.00	1.40	8.87
28	100	100	100	100	100	100	100	100	100	0	0	0	0	0	0	0	0	0	0	100.00	5.88	9.04
30	100	100	100	100	100	100	100	100	100	0	0	0	0	0	0	0	0	0	0	100.00	1.62	8.88
32	100	100	100	100	100	100	100	100	100	0	0	0	0	0	0	0	0	0	0	100.00	3.04	8.95
34	100	100	100	100	100	100	100	100	100	0	0	0	0	0	0	0	0	0	0	100.00	4.94	9.01
36	100	100	100	100	100	100	100	100	100	0	0	0	0	0	0	0	0	0	0	100.00	1.62	8.88
38	100	100	100	100	100	100	100	100	100	0	0	0	0	0	0	0	0	0	0	100.00	2.85	8.94
40	100	100	100	100	100	100	100	100	100	0	0	0	0	0	0	0	0	0	0	100.00	6.07	9.05
42	100	100	100	100	100	100	100	100	100	0	0	0	0	0	0	0	0	0	0	100.00	1.62	8.88
44	100	100	100	100	100	100	100	100	100	0	0	0	0	0	0	0	0	0	0	100.00	5.61	9.03
46	100	100	100	100	100	100	100	100	100	0	0	0	0	0	0	0	0	0	0	100.00	4.25	8.99

Figure C.19: Best F evaluation for shell  $II_{C4}$ .

F	% Coverage per Latitude																			% Average	Distance min [km]	Rate
	0°	5°	10°	15°	20°	25°	30°	35°	40°	45°	50°	55°	60°	65°	70°	75°	80°	85°	90°			
1	100	100	100	100	100	100	100	100	100	0	0	0	0	0	0	0	0	0	0	100.00	9.86	9.22
3	100	100	100	100	100	100	100	100	100	0	0	0	0	0	0	0	0	0	0	100.00	2.21	8.93
5	100	100	100	100	100	100	100	100	100	0	0	0	0	0	0	0	0	0	0	100.00	3.71	9.00
7	100	100	100	100	100	100	100	100	100	0	0	0	0	0	0	0	0	0	0	100.00	15.91	9.44
9	100	100	100	100	100	100	100	100	100	0	0	0	0	0	0	0	0	0	0	100.00	9.08	9.20
11	100	100	100	100	100	100	100	100	100	0	0	0	0	0	0	0	0	0	0	100.00	2.21	8.93
13	100	100	100	100	100	100	100	100	100	0	0	0	0	0	0	0	0	0	0	100.00	26.78	9.82
15	100	100	100	100	100	100	100	100	100	0	0	0	0	0	0	0	0	0	0	100.00	3.50	8.99
17	100	100	100	100	100	100	100	100	100	0	0	0	0	0	0	0	0	0	0	100.00	10.12	9.23
19	100	100	100	100	100	100	100	100	100	0	0	0	0	0	0	0	0	0	0	100.00	2.21	8.93
21	100	100	100	100	100	100	100	100	100	0	0	0	0	0	0	0	0	0	0	100.00	3.71	9.00
23	100	100	100	100	100	100	100	100	100	0	0	0	0	0	0	0	0	0	0	100.00	14.88	9.40
25	100	100	100	100	100	100	100	100	100	0	0	0	0	0	0	0	0	0	0	100.00	9.86	9.22
27	100	100	100	100	100	100	100	100	100	0	0	0	0	0	0	0	0	0	0	100.00	2.21	8.93
29	100	100	100	100	100	100	100	100	100	0	0	0	0	0	0	0	0	0	0	100.00	9.80	9.22
31	100	100	100	100	100	100	100	100	100	0	0	0	0	0	0	0	0	0	0	100.00	3.50	8.99
33	100	100	100	100	100	100	100	100	100	0	0	0	0	0	0	0	0	0	0	100.00	32.09	10.00
35	100	100	100	100	100	100	100	100	100	0	0	0	0	0	0	0	0	0	0	100.00	2.21	8.93
37	100	100	100	100	100	100	100	100	100	0	0	0	0	0	0	0	0	0	0	100.00	3.71	9.00
39	100	100	100	100	100	100	100	100	100	0	0	0	0	0	0	0	0	0	0	100.00	28.25	9.87
41	100	100	100	100	100	100	100	100	100	0	0	0	0	0	0	0	0	0	0	100.00	19.67	9.57
43	100	100	100	100	100	100	100	100	100	0	0	0	0	0	0	0	0	0	0	100.00	2.21	8.93
45	100	100	100	100	100	100	100	100	100	0	0	0	0	0	0	0	0	0	0	100.00	9.61	9.22
47	100	100	100	100	100	100	100	100	100	0	0	0	0	0	0	0	0	0	0	100.00	3.50	8.99

Figure C.20: Best F evaluation for shell  $II_{C5}$ .

C.3 – F parameter evaluation of  $II_C$  alternatives

F	% Coverage per Latitude																		% Average	Distance min [km]	Rate	
	0°	5°	10°	15°	20°	25°	30°	35°	40°	45°	50°	55°	60°	65°	70°	75°	80°	85°				90°
0	100	100	100	100	100	100	100	100	100	0	0	0	0	0	0	0	0	0	0	100.00	11.53	9.17
2	100	100	100	100	100	100	100	100	95.3	0	0	0	0	0	0	0	0	0	0	99.48	3.55	8.91
4	100	100	100	100	100	100	100	100	87.7	0	0	0	0	0	0	0	0	0	0	98.63	5.61	8.89
6	100	100	100	100	100	100	100	100	85.7	0	0	0	0	0	0	0	0	0	0	98.41	21.82	9.29
8	100	100	100	100	100	100	100	100	88.3	0	0	0	0	0	0	0	0	0	0	98.70	11.13	9.05
10	100	100	100	100	100	100	100	100	97	0	0	0	0	0	0	0	0	0	0	99.67	39.06	9.84
12	100	100	100	100	100	100	100	100	100	0	0	0	0	0	0	0	0	0	0	100.00	15.05	9.26
14	100	100	100	100	100	100	100	100	100	0	0	0	0	0	0	0	0	0	0	100.00	11.67	9.17
16	100	100	100	100	100	100	100	100	100	0	0	0	0	0	0	0	0	0	0	100.00	17.50	9.32
18	100	100	100	100	100	100	100	100	100	0	0	0	0	0	0	0	0	0	0	100.00	28.48	9.60
20	100	100	100	100	100	100	100	100	100	0	0	0	0	0	0	0	0	0	0	100.00	17.59	9.33
22	100	100	100	100	100	100	100	100	100	0	0	0	0	0	0	0	0	0	0	100.00	41.23	9.92
24	100	100	100	100	100	100	100	100	100	0	0	0	0	0	0	0	0	0	0	100.00	8.37	9.09
26	100	100	100	100	100	100	100	100	100	0	0	0	0	0	0	0	0	0	0	100.00	44.45	10.00
28	100	100	100	100	100	100	100	100	100	0	0	0	0	0	0	0	0	0	0	100.00	3.03	8.94
30	100	100	100	100	100	100	100	100	100	0	0	0	0	0	0	0	0	0	0	100.00	40.59	9.90
32	100	100	100	100	100	100	100	100	100	0	0	0	0	0	0	0	0	0	0	100.00	17.50	9.32
34	100	100	100	100	100	100	100	100	100	0	0	0	0	0	0	0	0	0	0	100.00	16.28	9.29
36	100	100	100	100	100	100	100	100	100	0	0	0	0	0	0	0	0	0	0	100.00	15.05	9.26
38	100	100	100	100	100	100	100	100	100	0	0	0	0	0	0	0	0	0	0	100.00	11.67	9.17
40	100	100	100	100	100	100	100	100	100	0	0	0	0	0	0	0	0	0	0	100.00	11.13	9.16
42	100	100	100	100	100	100	100	100	100	0	0	0	0	0	0	0	0	0	0	100.00	3.07	8.94
44	100	100	100	100	100	100	100	100	100	0	0	0	0	0	0	0	0	0	0	100.00	17.59	9.33
46	100	100	100	100	100	100	100	100	100	0	0	0	0	0	0	0	0	0	0	100.00	1.40	8.86

Figure C.21: Best F evaluation for shell  $II_{C6}$ .

F	% Coverage per Latitude																		% Average	Distance min [km]	Rate	
	0°	5°	10°	15°	20°	25°	30°	35°	40°	45°	50°	55°	60°	65°	70°	75°	80°	85°				90°
1	100	98.3	94.3	100	100	100	100	100	100	0	0	0	0	0	0	0	0	0	0	99.18	2.11	8.80
3	100	93.7	99	100	99.7	95.7	100	100	100	0	0	0	0	0	0	0	0	0	0	98.68	25.23	9.10
5	100	86.3	100	99	95.3	100	100	100	100	0	0	0	0	0	0	0	0	0	0	97.84	20.42	8.96
7	100	84.7	100	84	100	100	96.3	100	100	0	0	0	0	0	0	0	0	0	0	96.11	57.79	9.31
9	100	88.3	100	99	100	98.3	100	100	90.3	0	0	0	0	0	0	0	0	0	0	97.32	31.07	9.06
11	100	94.7	95.3	100	86	100	83.7	100	77	0	0	0	0	0	0	0	0	0	0	92.97	5.61	8.32
13	100	98.7	81.7	100	100	82.3	100	92.7	70.3	0	0	0	0	0	0	0	0	0	0	91.74	2.11	8.15
15	100	100	89.7	89.3	100	100	86.7	100	67.7	0	0	0	0	0	0	0	0	0	0	92.60	19.14	8.48
17	100	100	100	91.3	85.3	100	100	100	74.3	0	0	0	0	0	0	0	0	0	0	94.54	12.98	8.57
19	100	100	100	100	100	100	97.7	100	84.7	0	0	0	0	0	0	0	0	0	0	98.04	35.21	9.18
21	100	100	100	100	100	100	100	100	98.7	0	0	0	0	0	0	0	0	0	0	99.86	7.28	8.96
23	100	100	100	98.7	95.7	91	100	100	100	0	0	0	0	0	0	0	0	0	0	98.38	5.61	8.80
25	100	100	96	91.7	100	100	100	100	100	0	0	0	0	0	0	0	0	0	0	98.63	2.11	8.76
27	100	100	92.7	99.7	100	100	100	100	100	0	0	0	0	0	0	0	0	0	0	99.16	7.26	8.90
29	100	97.7	97.7	100	100	100	100	100	100	0	0	0	0	0	0	0	0	0	0	99.49	9.47	8.96
31	100	95.3	100	100	100	100	100	100	100	0	0	0	0	0	0	0	0	0	0	99.48	66.96	9.73
33	100	96.7	100	100	100	100	100	100	100	0	0	0	0	0	0	0	0	0	0	99.63	3.39	8.88
35	100	99.3	100	100	100	100	100	100	100	0	0	0	0	0	0	0	0	0	0	99.92	5.61	8.94
37	100	100	100	100	100	100	100	100	100	0	0	0	0	0	0	0	0	0	0	100.00	2.11	8.88
39	100	100	100	100	100	100	100	100	100	0	0	0	0	0	0	0	0	0	0	100.00	15.67	9.09
41	100	100	100	100	100	100	100	100	100	0	0	0	0	0	0	0	0	0	0	100.00	31.07	9.30
43	100	100	100	100	100	100	100	100	100	0	0	0	0	0	0	0	0	0	0	100.00	84.07	10.00
45	100	100	98.3	97	100	100	100	100	100	0	0	0	0	0	0	0	0	0	0	99.48	7.28	8.93
47	100	100	94	99	100	100	100	100	100	0	0	0	0	0	0	0	0	0	0	99.22	5.61	8.88

Figure C.22: Best F evaluation for shell  $II_{C7}$ .

Alternative proposals

F	% Coverage per Latitude																		% Average	Distance min [km]	Rate	
	0°	5°	10°	15°	20°	25°	30°	35°	40°	45°	50°	55°	60°	65°	70°	75°	80°	85°				90°
0	100	93.3	90.7	99.3	100	100	100	100	100	0	0	0	0	0	0	0	0	0	0	98.14	12.29	9.38
2	100	96.7	92	88.7	100	96.7	100	100	100	0	0	0	0	0	0	0	0	0	0	97.12	19.84	9.57
4	100	98.7	98.7	90.7	91.3	100	100	100	100	0	0	0	0	0	0	0	0	0	0	97.71	12.29	9.34
6	100	100	100	100	96	95	100	100	100	0	0	0	0	0	0	0	0	0	0	99.00	10.43	9.39
8	100	100	99.3	99.7	100	100	100	100	100	0	0	0	0	0	0	0	0	0	0	99.89	12.29	9.54
10	100	99.7	91.3	85.7	87.7	99.3	100	100	100	0	0	0	0	0	0	0	0	0	0	95.97	24.24	9.63
12	100	92	74.3	71	80.7	82.7	87.7	100	100	0	0	0	0	0	0	0	0	0	0	87.60	5.61	8.16
14	100	83.7	68.3	90	100	100	100	100	99.7	0	0	0	0	0	0	0	0	0	0	93.52	28.48	9.57
16	100	75.7	80	100	88	71.7	70	100	87.7	0	0	0	0	0	0	0	0	0	0	85.90	12.29	8.27
18	100	67.7	92.3	88.7	67	96	100	100	72.3	0	0	0	0	0	0	0	0	0	0	87.11	1.40	7.92
20	100	62.7	100	63.7	96.3	86	67.7	83.3	60.7	0	0	0	0	0	0	0	0	0	0	80.04	12.29	7.73
22	99.7	65.3	96.3	74.3	91.7	76.7	100	71.3	50.7	0	0	0	0	0	0	0	0	0	0	80.67	0.49	7.21
24	100	72.7	80.7	97.3	62.7	100	71.7	100	54.7	0	0	0	0	0	0	0	0	0	0	82.20	12.29	7.93
26	100	80.7	66.7	98	91	64.3	99.3	100	60.3	0	0	0	0	0	0	0	0	0	0	84.48	30.24	8.82
28	100	88.7	64.3	79.7	99	100	86.3	100	76.7	0	0	0	0	0	0	0	0	0	0	88.30	12.29	8.48
30	100	95.7	81.3	70.3	71.7	89.7	100	100	90.7	0	0	0	0	0	0	0	0	0	0	88.82	3.55	8.19
32	100	100	96.7	93.3	90	92.7	100	100	100	0	0	0	0	0	0	0	0	0	0	96.97	12.29	9.27
34	100	100	100	100	100	100	100	100	100	0	0	0	0	0	0	0	0	0	0	100.00	24.24	10.00
36	100	99.3	99.3	97	88.3	82	100	100	100	0	0	0	0	0	0	0	0	0	0	96.21	12.29	9.20
38	100	97.3	92.3	80.7	94.3	100	100	100	100	0	0	0	0	0	0	0	0	0	0	96.07	10.43	9.12
40	100	95	85.3	94.3	100	100	100	100	100	0	0	0	0	0	0	0	0	0	0	97.18	12.29	9.29
42	100	91.7	88	99.7	99.7	99.3	100	100	100	0	0	0	0	0	0	0	0	0	0	97.60	11.67	9.31
44	100	88.3	96.7	100	98.3	100	100	100	100	0	0	0	0	0	0	0	0	0	0	98.14	12.29	9.38
46	99.7	89.3	97	98	100	100	100	100	99	0	0	0	0	0	0	0	0	0	0	98.11	3.23	9.01

Figure C.23: Best F evaluation for shell  $II_{C8}$ .

F	% Coverage per Latitude																		% Average	Distance min [km]	Rate	
	0°	5°	10°	15°	20°	25°	30°	35°	40°	45°	50°	55°	60°	65°	70°	75°	80°	85°				90°
1	82.7	87.3	90	82.3	79	79.7	96.7	100	98.7	0	0	0	0	0	0	0	0	0	0	88.49	22.21	9.45
3	79	85	75	76	80	85	89.7	100	99.3	0	0	0	0	0	0	0	0	0	0	85.44	20.65	9.12
5	77	77.7	76	71.3	92.3	83.3	96	100	81	0	0	0	0	0	0	0	0	0	0	83.84	86.29	9.87
7	76.7	68	83.3	80.3	75.7	93.3	99.7	99.7	67.7	0	0	0	0	0	0	0	0	0	0	82.71	29.83	8.96
9	77	60	77.3	80.7	93.7	96	100	100	77.3	0	0	0	0	0	0	0	0	0	0	84.67	22.21	9.06
11	79.7	60.7	69.3	86.3	81	91	100	100	97.3	0	0	0	0	0	0	0	0	0	0	85.03	32.09	9.23
13	83.3	71.3	63.3	90.7	80.7	96.3	97	100	99.3	0	0	0	0	0	0	0	0	0	0	86.88	67.46	9.92
15	87.3	79.7	62.3	66	99.3	73.3	100	100	97.7	0	0	0	0	0	0	0	0	0	0	85.07	50.17	9.49
17	90.3	86.3	73.3	61.3	71	99.7	88.7	100	100	0	0	0	0	0	0	0	0	0	0	85.62	22.21	9.16
19	90.3	92.3	86.7	80	66	67	100	100	100	0	0	0	0	0	0	0	0	0	0	86.92	20.65	9.27
21	89.7	89.3	90.3	94.3	95.3	82.3	63.7	100	99.3	0	0	0	0	0	0	0	0	0	0	89.36	33.64	9.70
23	85.7	83	76	70.7	71.7	80.7	100	100	90.3	0	0	0	0	0	0	0	0	0	0	84.23	92.97	10.00
25	82.7	74.7	59.3	47.7	52.7	59.3	55.3	100	70.7	0	0	0	0	0	0	0	0	0	0	66.93	22.21	7.23
27	79	66	44.7	61.3	80.3	85.3	86	95.7	57	0	0	0	0	0	0	0	0	0	0	72.81	69.98	8.50
29	77	58	52.7	78	69.3	46	50.7	60.3	41.7	0	0	0	0	0	0	0	0	0	0	59.30	33.52	6.59
31	76.7	50.7	66	74.3	40.7	73.3	76.3	53.7	34.3	0	0	0	0	0	0	0	0	0	0	60.67	13.82	6.46
33	77	43.3	78.3	52.7	72	66.7	60	85.7	39.3	0	0	0	0	0	0	0	0	0	0	63.89	22.21	6.91
35	79.7	43.7	80.3	49.7	80	59	75.3	100	53	0	0	0	0	0	0	0	0	0	0	68.97	9.08	7.25
37	83.3	52	72	75	50.7	90.7	76.7	100	69	0	0	0	0	0	0	0	0	0	0	74.38	15.93	7.91
39	87.3	61.3	59	89.7	72.7	53	79.3	100	84.7	0	0	0	0	0	0	0	0	0	0	76.33	53.45	8.63
41	90.3	71	52.3	71	95.3	94.7	97.3	100	99.7	0	0	0	0	0	0	0	0	0	0	85.73	22.21	9.17
43	90.3	81	63	59	68	80	85.7	100	100	0	0	0	0	0	0	0	0	0	0	80.78	35.04	8.84
45	89.7	86.7	79.7	74.7	75.3	86.7	100	100	100	0	0	0	0	0	0	0	0	0	0	88.09	28.25	9.50
47	85.7	88.3	93	95.3	100	99	89.3	100	97	0	0	0	0	0	0	0	0	0	0	94.18	9.61	9.86

Figure C.24: Best F evaluation for shell  $II_{C9}$ .

# Bibliography

- [1] Mark Handley. «Delay is Not an Option: Low Latency Routing in Space». In: *Proceedings of the 17th ACM Workshop on Hot Topics in Networks*. HotNets '18. Redmond, WA, USA, 2018, pp. 85–91 (cit. on pp. 1, 19, 34, 53).
- [2] Jon Brodtkin. «SpaceX hits two milestones in plan for low-latency satellite broadband». In: *Ars Technica* (2018) (cit. on pp. 3, 18).
- [3] *Starlink Official Website*. <https://www.starlink.com/> (cit. on pp. 3, 4).
- [4] «FCC: Application for modification of authorization for the spacex NGSO satellite system». In: *Federal Communications Commission* (2020) (cit. on p. 4).
- [5] George Gilder. «Light Speed Trap Ahead». In: *Forbes* (1997) (cit. on p. 5).
- [6] «Teledesic Plays Its Last Card, Leaves the Game». In: *Wayback Machine Space News* (2003) (cit. on p. 5).
- [7] Tim Fernholz. «Inside the race to create the next generation of satellite internet». In: *QUARTZ* (2015) (cit. on p. 5).
- [8] *SpaceX Seattle 2015*. <https://www.youtube.com/watch?v=AHeZHyOnsm4> (cit. on p. 5).
- [9] Caleb Henry. «SpaceX asks FCC to make exception for LEO constellations in Connect America Fund decisions». In: *SpaceNews* (2017) (cit. on p. 5).
- [10] Stephen Clark. «SpaceX launches more Starlink satellites, beta testing well underway». In: *Spaceflight Now* (2020) (cit. on p. 6).
- [11] Caleb Henry. «FCC OKs lower orbit for some Starlink satellites». In: *Space-News* (2019) (cit. on p. 6).
- [12] Stephen Clark. «SpaceX modifies Starlink network design as another 60 satellites gear up for launch». In: *Spaceflight Now* (2020) (cit. on p. 6).
- [13] «Space Station Applications Accepted for Filing». In: *Federal Communications Commission* (2021) (cit. on p. 6).
- [14] «SpaceX is manufacturing 120 Starlink Internet satellites per month». In: *CNBC* (2020) (cit. on p. 6).

- [15] Jon Porter. «SpaceX’s new Starlink Business tier promises up to 500Mbps for \$500 a month - The new antenna carries an upfront cost of \$2500». In: *The Verge* (2022) (cit. on p. 6).
- [16] «Starlink Press Kit». In: *spacex.com* (2019) (cit. on p. 8).
- [17] Elon Musk. «Starlink». In: *starlink.com* (2019) (cit. on p. 8).
- [18] Gunter Krebs. «Starlink Block v1.0». In: *starlink.com* (2020) (cit. on p. 9).
- [19] Eric Mack. «SpaceX launches first batch of Starlink satellites wearing sun visors». In: *starlink.com* (2022) (cit. on p. 9).
- [20] Arndt Garrity John; Husar. «Digital Connectivity and Low Earth Orbit Satellite Constellations: Opportunities for Asia and the Pacific». In: *think-asia.org* (2021) (cit. on p. 9).
- [21] Stephen Clark. «SpaceX to ramp up Vandenberg launch cadence with Starlink missions». In: *Spaceflight Now* (2021) (cit. on p. 9).
- [22] Eric Ralph. «SpaceX CEO Elon Musk reveals next-generation Starlink satellite details». In: *Teslarati* (2022) (cit. on p. 9).
- [23] *Starlink Official Website, Updates*. <https://www.spacex.com/updates/> (cit. on pp. 9–13).
- [24] «After SpaceX Starlink Launch, a Fear of Satellites That Outnumber All Visible Stars». In: *The Economist* (2019) (cit. on p. 12).
- [25] Alexandra Witze. «The unexpected brightness of new satellites could ruin the night sky». In: *Nature* (2019) (cit. on p. 12).
- [26] «SpaceX’s Starlink Could Change The Night Sky Forever, And Astronomers Are Not Happy». In: *Forbes* (2020) (cit. on p. 12).
- [27] «SpaceX to debut satellite-dimming sunshade on Starlink launch next month». In: *Spaceflight Now* (2020) (cit. on p. 13).
- [28] «New center to coordinate work to mitigate effect of satellite constellations on astronomy». In: *SpaceNews* (2022) (cit. on p. 14).
- [29] Alexandra Witze. «’Unsustainable’: how satellite swarms pose a rising threat to astronomy». In: *Nature* (2022) (cit. on p. 14).
- [30] «Petition of starlink services, LLC for designation as an eligible telecommunications carrier». In: (2021) (cit. on p. 15).
- [31] [https://en.wikipedia.org/wiki/Phased\\_array#/media/File:Phased\\_array\\_animation\\_with\\_arrow\\_10frames\\_371x400px\\_100ms.gif](https://en.wikipedia.org/wiki/Phased_array#/media/File:Phased_array_animation_with_arrow_10frames_371x400px_100ms.gif) (cit. on pp. 15, 16).
- [32] *Starlink Official Website, Customer Support*. <https://support.starlink.com/?topic=4badc520-cf8e-b3aa-dd49-b731686d5bf1> (cit. on p. 17).

- [33] «SpaceX to test Starlink terminals on ships». In: *advanced-television.com* (2020) (cit. on p. 17).
- [34] <https://starlink.sx/> (cit. on p. 18).
- [35] Halim Yanikomeroglu Aizaz U. Chaudhry. «Laser Inter-Satellite Links in a Starlink Constellation». In: (2019) (cit. on p. 19).
- [36] Caleb Henry. «Amazon planning 3,236-satellite constellation for internet connectivity». In: *SpaceNews* (2019) (cit. on p. 24).
- [37] Ashwini Sakharkar. «Amazon’s Project Kuiper to launch first two prototype internet satellites in 2022». In: *InceptiveMind* (2021) (cit. on p. 24).
- [38] Jeff Foust. «Amazon unveils flat-panel customer terminal for Kuiper constellation». In: *SpaceNews* (2020) (cit. on p. 24).
- [39] «Technical Appendix - Application of Kuiper Systems LLC for Authority to Launch and Operate a Non-Geostationary Satellite Orbit System in Ka-band Frequencies». In: *Federal Communications Commission* (2019e) (cit. on pp. 24, 26).
- [40] Joppe Bernd Born. «On the use of low earth orbit satellite constellations for offshore communication». In: *Technische Universiteit Delft, Fugro n.v. - ITOV department* (2020) (cit. on pp. 25, 30).
- [41] [https://en.wikipedia.org/wiki/OneWeb\\_satellite\\_constellation](https://en.wikipedia.org/wiki/OneWeb_satellite_constellation) (cit. on p. 27).
- [42] «OneWeb to resume satellite launches through agreement with SpaceX». In: *Oneweb official website* (2022) (cit. on p. 27).
- [43] «Petition for Declaratory Ruling to Grant Access to the U.S. Market for Telesat’s NGSO Constellation - Petition for Declaratory Ruling. Petition for Declaratory Ruling to Grant Access to the U.S. Market for Telesat’s NGSO Constellation». In: *Federal Communications Commission* (2016e) (cit. on pp. 27, 31).
- [44] «Attachment Schedule S Tech Report - Application to Modify Petition for Declaratory Ruling to Grant Access to the U.S. Market for Telesat NGSO Constellation». In: *Federal Communications Commission* (2020a) (cit. on p. 29).
- [45] «Computational resources provided by hpc@polito, which is a project of Academic Computing within the Department of Control and Computer Engineering at the Politecnico di Torino (<http://www.hpc.polito.it>)». In: () (cit. on p. 33).

- [46] Jintao Liang, Aizaz U. Chaudhry, and Halim Yanikomeroglu. «Phasing Parameter Analysis for Satellite Collision Avoidance in Starlink and Kuiper Constellations». In: *2021 IEEE 4th 5G World Forum (5GWF)*. 2021, pp. 493–498. DOI: 10.1109/5GWF52925.2021.00093 (cit. on pp. 36, 40).
- [47] John G Walker. «Satellite constellations». In: *Journal of the British Interplanetary Society* 37 (1984), p. 559 (cit. on p. 36).
- [48] Israel Leyva-Mayorga, Beatriz Soret, Bho Matthiesen, Maik Röper, Dirk Wübben, Armin Dekorsy, and Petar Popovski. *NGSO Constellation Design for Global Connectivity*. Mar. 2022 (cit. on p. 37).
- [49] [https://en.wikipedia.org/wiki/File:Mean\\_Anomaly.svg](https://en.wikipedia.org/wiki/File:Mean_Anomaly.svg) (cit. on p. 37).
- [50] Karel F. Wakker. «Fundamentals of Astrodynamics». In: *TU Delft* (2015) (cit. on p. 38).
- [51] Aizaz U. Chaudhry and Halim Yanikomeroglu. «Laser Inter-Satellite Links in a Starlink Constellation». In: *IEEE vehicular technology magazine* (2021) (cit. on p. 54).
- [52] <https://www.udacity.com/blog/2021/10/implementing-dijkstras-algorithm-in-python.html> (cit. on p. 55).
- [53] Alasdair Rae. «Mapped: The World’s Population Density by Latitude». In: *Visual capitalist* (2022) (cit. on p. 62).